

Electronic Thesis and Dissertation Repository

10-21-2022 10:30 AM

Herbicide Mediated Selection of Sulfonamide Resistant E. coli

Laura P. Muntz, *The University of Western Ontario*

Supervisor: Dr. Michael J Fruci, *Agriculture and Agri-Food Canada*

: Dr. Martin J McGavin, *The University of Western Ontario*

A thesis submitted in partial fulfillment of the requirements for the Master of Science degree in
Microbiology and Immunology

© Laura P. Muntz 2022

Follow this and additional works at: <https://ir.lib.uwo.ca/etd>



Part of the [Agricultural Science Commons](#), [Bacteria Commons](#), [Bacteriology Commons](#), and the
[Environmental Microbiology and Microbial Ecology Commons](#)

Recommended Citation

Muntz, Laura P., "Herbicide Mediated Selection of Sulfonamide Resistant E. coli" (2022). *Electronic Thesis and Dissertation Repository*. 8974.

<https://ir.lib.uwo.ca/etd/8974>

This Dissertation/Thesis is brought to you for free and open access by Scholarship@Western. It has been accepted for inclusion in Electronic Thesis and Dissertation Repository by an authorized administrator of Scholarship@Western. For more information, please contact wlsadmin@uwo.ca.

Abstract

Asulam is an herbicide that is structurally analogous to sulfonamide antibiotics (sulfas), with the potential to contribute to the global antibiotic resistance crisis by cross-selecting for sulfa-resistant bacteria. To determine if asulam can select for antibiotic resistant bacteria, isothermal titration calorimetry (ITC) was used to assess the binding affinity of asulam with the target protein of sulfas, dihydropteroate synthase (DHPS). ITC confirmed asulam interacts with DHPS, and *in vitro* directed evolution experiments showed that prolonged asulam exposure can select for sulfa-insensitive DHPS in *E. coli*. Since mobile *sul* genes also encode for sulfa-insensitive DHPS, the potential effect of asulam on the dissemination of the *sul* genes in a simulated bacterial community was assessed. These data suggested that asulam can promote sulfa-resistance by increasing the frequency of chromosomal *folP* mutations, and/or acquisition of *sul* genes in *E. coli*, and uniquely induce deletions of multiple genes at concentrations exceeding environmental relevance.

Keywords

Antibiotic resistance, *E. coli*, DHPS, Asulam, herbicides, Sulfonamides, One Health

Summary for the Lay Audience

Antibiotic resistant bacteria cause infections that do not respond to standard treatments and require more costly and intensive interventions. These types of infections have become increasingly common and reducing the prevalence of antibiotic resistance has become a healthcare priority. An effective strategy has been the reduction of usage of antibiotics, as the misuse and overuse of these drugs is known to contribute to the increased prevalence of these infections. However, other chemicals can also increase the frequency of antibiotic resistance in bacterial communities, including agrichemicals such as pesticides and herbicides. When bacteria that reside in crop soil are exposed to these agrichemicals, they can become resistant to antibiotics and have the potential to spread to humans via consumptions of food grown in contaminated soil. Therefore, determining how agrichemicals contribute to promoting antibiotic resistance to implement appropriate regulations regarding the usage of these chemicals is paramount for reducing the burden of antibiotic resistant bacterial infections on the healthcare system. In this study, the herbicide asulam is assessed for its ability to select for and promote the dissemination of sulfonamide antibiotic resistant bacteria due to the chemical similarities shared between this herbicide and this class of antibiotics.

Acknowledgements

I would like to thank my family: Darcy, Keji, and Juno. Even though none of you can read this, your continuous love and support were integral to the completion of this thesis. Thank you.

Co-Authorship Statement

Data for Figure 2 and Figure 3 were collected and analyzed with this assistance of Lee-Ann Biere in the Macromolecular Crystallography Facility & Biomolecular Interactions and Conformations Facility of the Biochemistry department of the University of Western Ontario.

Table of Contents

Abstract	i
Keywords.....	i
Summary for the Lay Audience	ii
Acknowledgements	iii
Co-Authorship Statement	iv
Table of Contents	v
List of Tables	x
Table of Figures.....	xi
Table of Appendices.....	xiii
List of Abbreviations	xiv
Chapter 1: Introduction	1
1.1 The Antibiotic Resistance Crisis	1
1.1.1 Origins and Trends of Antibiotic Resistance	1
1.1.2 Antibiotic Usage and Environmental Pollution.....	1
1.1.3 Relevance of One Health to the Antibiotic Resistance Crisis	3
1.1.4 The Role of Agriculture in The Antibiotic Resistance Crisis.	3
1.1.5. Antibiotics and Antibiotic Resistance.....	4
1.2 Sulfas and Associated Compounds.....	5
1.2.1 Sulfas: Development and Applications.....	5

1.2.2 Sulfa Mechanism of Action.....	6
1.2.3 Thymineless Death	8
1.2.4 Sulfa-Resistance Mechanisms	8
1.2.5 Asulam	10
1.3 Rationale and Significance	11
1.4 Hypothesis and Research Aims	11
Chapter 2: Material and Methods	13
2.1 Bacterial strains, plasmids, and growth conditions	13
2.2 Antibiotics, ASM, and Degradation products	18
2.3 DNA Methods	22
2.3.1 Agarose Gel Electrophoresis.....	22
2.3.2 Colony PCR amplification of <i>folP</i> from <i>E. coli</i>	22
2.3.3 Purification and Sequencing of PCR Products	23
2.3.4 Chromosomal DNA extraction and whole genome sequencing of <i>E. coli</i>	25
2.3.5 Whole Genome Sequence Analysis.....	25
2.3.6 Preparation of CaCl ₂ Competent <i>E. coli</i> cells	25
2.3.7 Plasmid Transformation: <i>E. coli</i> BL21(DE3) pLysS with pET28a	25
2.3.8 Plasmid Transformation of <i>E. coli</i> Δ <i>folP</i> with pDGP2	26
2.4 Antibiotic Susceptibility Testing	27

2.4.1 Two-Fold Broth Microdilution Method.....	27
2.4.2 Two-Fold Adapted Agar Microdilution Method	27
2.4.3 E-Test Co-Trimoxazole MIC test	28
2.5 Directed evolution Assays	29
2.5.1 Selection and Confirmation of SMX ^R Isolates	30
2.6 Conjugation Experiments	30
2.6.1 PCR amplification of the <i>sul</i> genes from bacterial DNA extracted from manure.....	32
2.7 <i>In vitro</i> Growth Assay	32
2.8 Purification of the Polyhistidine-Tagged <i>EcDHPS</i> Protein.....	33
2.9 Isothermal Titration Calorimetry (ITC)	35
2.9.1 Titrating SMX into <i>EcDHPS</i>	35
2.9.2 Titrating ASM into <i>EcDHPS</i>	35
2.10 Western immunoblotting.....	35
Chapter 3: Results.....	37
3.1 ASM Selects for Sulfamethoxazole-Resistant <i>E. coli</i>	37
3.1.1 ASM exerts antibiotic action against <i>E. coli</i>	37
3.1.2 ASM and ASMG target <i>EcDHPS</i>	39
3.2 Both SMX and ASM act as a ligand for <i>EcDHPS</i>	39
3.3 ASM, but not ASMG or SAN select for SMX resistant <i>E. coli in vitro</i>	45

3.3.1 Identification and Characterization of ASM-selected folP mutations in <i>E. coli</i>	50
3.3.2 ASM-selected SMX ^R isolates are pan-sulfa resistance	52
3.3.3 ASM and SMX select for additional chromosomal mutations in <i>E. coli</i>	55
3.3.4 Most SMX ^R isolates do not exhibit growth deficiency <i>in vitro</i>	59
3.4 ASM influences the transfer of the <i>sul</i> genes in a simulated microbial community at a comparable rate to SMX	63
Chapter 4 Discussion	65
4.1 ASM can exert antibiotic action against <i>E. coli</i> comparable to some sulfas	65
4.1.1 ASM likely exerts antibiotic action via DHPS inhibition	65
4.2 ASM selects for SMX ^R <i>E. coli</i> at concentrations exceeding environmental relevance.....	66
4.2.1 Soil microcosms for the improvement of recapitulating soil communities in directed evolution experiments.....	66
4.2.2. Concentrations of ASM that select for sulfa-resistance are not found in the environment	67
4.2.3 ASM selects for <i>folP</i> mutations known to confer sulfa resistance in <i>E. coli</i>	68
4.2.2 ASM- and SMX-selected SMX ^R <i>E. coli</i> harbor unique genomic changes	69
4.3 ASM does not increase the frequency of sulfa resistance conferred by mobilized <i>sul</i> genes in a simulated microbial community	73

4.4 Future Directions	75
4.5 Conclusion.....	76
Appendices.....	77
References	82
Curriculum Vitae	105

List of Tables

Table 1 Bacterial strains and plasmids used in this study	14
Table 2. Common identifiers, structure, and relevant qualities of the sulfonamide compounds used in this study	19
Table 3. Oglionucleotide sequences of primers designed for this study and synthesized by IDT	24
Table 4. ASM and its degradation products possess antibiotic activity against E. coli. Minimum inhibitory concentration (MIC) of <i>E. coli</i> strains lacking a DHPS enzyme ($\Delta folP$), harboring wild-type (WT) DHPS, or a sulfa-insensitive form of DHPS encoded by the indicated <i>sul</i> gene	38
Table 5. Emergence of SMX^R colonies in directed evolution experiments carried out at the indicated concentration. Compounds that yielded SMX ^R <i>E. coli</i> BW25113 on the indicated day of exposure and concentration are noted as positive for SMX ^R with (+), and compounds that did not are labelled as (-). ACE served as the vehicle control for SAN, and DMSO was used for all other compounds tested	46

Table of Figures

Figure 1. The bacterial <i>de novo</i> folate biosynthesis and utilization pathway with all enzymes circled in yellow and the step of the pathway they are involved in indicated by a line. The antifolate antibiotics sulfamethoxazole (SMX) and trimethoprim (TMP) are represented by labelled pills connected to their corresponding enzymatic target by dotted lines. Folic acid derivatives are circled in green, and the conversion of 5,10-methylenetetrahydrofolate to dihydrofolate via thymidylate synthase catalyzing the conversion of deoxyuridine monophosphate (dUMP) to deoxythymidine monophosphate (dTMP). Downstream products of this pathway are indicated by purple outlines, with the final products used in purine nucleotide synthesis and one-carbon metabolism.	7
Figure 2. Binding curves of each ITC experiment replicate performed with 25 injections of 100 mM SMX titrated into 5 μ M <i>EcDHPS</i> for two replicates (A and B respectively)	41
Figure 3. Binding curves of each ITC experiment performed with 25 injections of 200 μ M ASM titrated into 5 μ M <i>EcDHPS</i> for two replicates (A and B respectively)	44
Figure 4. Average resistance frequency of all treatments that yielded SMX^R <i>E. coli</i> in <i>in vitro</i> directed evolution experiments (N=2). Plotted by treatment applied (A) or by day of the experiment (B). Statistical significance as determined by an ordinary two-way ANOVA with Tukey's multiple comparisons test with single pooled variance is indicated by asterisks (**** P <0.0001), and no significance is noted as ns.	48
Figure 5. Pie charts of <i>folP</i> mutations observed on day 7 (A), and day 10 (B) of the directed evolution experiments, as well as mutations observed in treatments SMX 10 μ g/mL (C), SMX 100 μ g/mL (D), and ASM 100 μ g/mL (E).....	51

Figure 6. Genomic variance observed in the SMX^R (A) ASM-selected and (B) SMX-selected isolates collected from Day 7 or Day 10 as indicated above the bars. Each uniquely coloured bar above the isolate name identified on the x-axis represents a gene that was deleted or mutated compared to the wild-type as indicated in the legend, and the total number of genes is listed on the y-axis. Each gene included in the α or β gene sets as described in Appendix 4 is represented by a cyan or yellow bar as labelled..... 58

Figure 7. Growth curves for *E. coli* (A) $\Delta folP$ expressing *folP* mutations on the pDGP2 expression plasmid, (B) ASM-selected SMX^R isolates, and (C) SMX-selected isolates, with the *E. coli* BW25113 (WT) (A, B, C) for comparison. Data represents the mean OD₆₀₀ for every 4 hours of growth recorded from three independent experiments performed in technical triplicate for each strain tested. The optical densities of each strain at 600 nm were baseline-corrected by subtracting the OD₆₀₀ of uninoculated MHII media. Asterisks next strains listed in the legend represent the statistical significance determined by unpaired t-tests. 61

Figure 8. Conjugation frequency of CV601 as the recipients of the *sul* genes from native soil bacteria when exposed to SMX or ASM at the indicated concentrations compared to no drug. Symbols indicate the mean conjugation frequency of two independent experiments, with error bars representing SEM. . 64

Figure 9. DNA stability regulatory mechanisms dependent on folate derivatives 5,10 methylenetetrahydrofolate and 5 methyltetrahydrofolate adapted from Duthie *et al.*, 2002¹⁶⁰. X denotes the interruption of methyl group donation..... 71

Table of Appendices

Appendix 1. Production of DHPS protein in <i>E. coli</i> trans-complemented <i>folP</i> variants with a BioRad Dual Colour Precision Plus Protein Standard indicating the approximate protein size.....	77
Appendix 2. Chemical analysis of the swine manure sample sourced from a Southern Ontario swine farm used in the conjugation experiments.....	78
Appendix 3. Amino acid sequences of the Wild type (WT) EcDHPS, aligned to the following mutants: P64S, P64A, F28L, Δ E68; protein topology of DHPS is indicated above the aligned sequences, α -helices and p- helices are displayed as squiggles, β -strands are rendered as arrows, and strict β -turns as TT letters, with loop 1 and 2 of the DHPS enzyme indicated by a blue (loop 1) or green (loop 2) line above the relevant residues (image generated by EndScript ¹³³) (B) Mutations in the <i>folP</i> gene identified by sequence analysis of <i>E. coli</i> isolates exposed to ASM or SMX treatments at the indicated concentration ($\mu\text{g}/\text{mL}$), or by the day collected (7 or 10)	79
Appendix 4. Genes deleted in the designated α (chromosome position 812,270 – 1,686,588) and β (2,412,100 – 2,427,009) gene sets in select SMX ^R isolates collected from the directed evolution experiments.....	80
Appendix 5. Whole Genome Sequencing Statistics provided by the Microbial Genome Sequencing Center	81

List of Abbreviations

Abbreviation	Definition
μg	Microgram
μL	Microliter
μM	Micromolar
AASM	Acetyl asulam
ACE	Acetone
ARB	Antibiotic resistant bacteria
ARG	Antibiotic resistance gene
ASM	Asulam
ASMG	Asulam glucoside
DASM	Desamino asulam
DHPP	6- Hydroxymethyl-7,8-dihydropterin-pyrophosphate
DHPS	Dihydropteroate synthase
DMSO	Dimethyl sulfoxide
FASM	Formyl asulam
g	Gram
GFP	Green fluorescent protein
ha	Hectare
HPPK	6-Hydroxymethyl-7,8-dihydropterin pyrophosphokinase
K_a	Association constant
KAN	Kanamycin
K_d	Dissociation constant
kg	kilogram

Abbreviation	Definition
L	Liter
MASM	Malonyl asulam
mg	Milligram
MHII	Mueller Hinton II
MIC	Minimum inhibitory concentration
mL	Milliliter
mM	Millimolar
MSC	Minimum selection concentration
<i>p</i> ABA	<i>para</i> -aminobenzoic acid
PCR	Polymerase chain reaction
PEC	Predicted environmental concentration
RIF	Rifampicin
SAN	Sulfanilamide
SDZ	sulfadiazine
SMX	Sulfamethoxazole
SXT	Co-trimoxazole

Chapter 1: Introduction

1.1 The Antibiotic Resistance Crisis

1.1.1 Origins and Trends of Antibiotic Resistance

Antibiotic resistance is an ancient evolutionary strategy wherein bacteria become insensitive to chemical compounds released by other organisms in the shared environment that can inhibit or alter bacterial physiology¹². While the phenomenon of antibiotic resistance predates the introduction of antibiotics to modern medicine, the antibiotic resistance crisis the world faces today represents a new era of bacterial evolution influenced by the anthropogenic use of antibiotics^{13,14}. Antibiotic use is commonplace in current medical practices, from the treatment of acute infections to facilitating the revolution of surgical intervention through infection prevention; antibiotics have become an essential tool in modern medicine¹⁵. Unfortunately, the medical community quickly learned that these drugs came with a caveat, as the increase in the usage of these drugs has coincided with the increased prevalence of antibiotic resistant infections^{16,17}. The rapid emergence of resistance following the introduction of each new antibiotic eventually made pursuing antibiotic discovery research a futile pursuit, diverting the path of medical research away from developing novel antibiotics¹⁸. Without incentive to develop new antibiotics, maintaining the efficacy of the arsenal of antibiotics used in medicine today has become a priority^{19–21}

1.1.2 Antibiotic Usage and Environmental Pollution

Antibiotics are used as first-line therapeutics for treating infections caused by bacterial pathogens in humans, animals, and plants^{11,22–26}. These drugs are used extensively in veterinary applications, agriculture, horticulture, aquaculture, and clinical medicine; with many classes of antibiotics having applications across multiple industries (e.g., sulfas) are used to treat bacterial infections in human

patients and are also administered to livestock and companion animals in veterinary medicine)^{27–33}. The widespread use of antibiotics combined with their mass production and consumption has consequently resulted in the ubiquity of antibiotic residues as contaminants^{3,34,35}.

The quantity of antibiotics consumed globally is staggering, with over 73 billion doses of antibiotics were estimated to have been sold in retail and hospital settings worldwide in 2010³⁶. In Canada alone, the annual dispensing rate of antibiotic prescriptions by community pharmacies in 2019 was 627 prescriptions per 1000 individuals³⁷. Many antibiotics remain pharmacologically active post-excretion and are distributed into the environment in their active form through the disposal of wastewater from communities consuming antibiotics^{13,33,38,39}. Wastewater from the industrial production needed to meet the global demand of antibiotics also releases these drugs into waterways, contaminating adjacent bodies of water such as rivers, lakes, harbors, and streams with high concentrations of antibiotics^{40–44}. Water can also be contaminated through antibiotic use in aquaculture, which pollutes both freshwater and coastal ecosystems^{45–48}. Soil is another environmental compartment often contaminated by the anthropogenic use of antibiotics, with current practices in agriculture contributing significantly to the antibiotic pollution of soil environments^{39,49–51}. Antibiotic pollution in agricultural soils is typically the result of directly treating crops for bacterial diseases, and/or from the amendment of animal manure sourced from antibiotic-treated livestock into crop soil as fertilizer^{24,39,49–52}. Animal manure is often contaminated with antibiotics from routine use of these drugs in infection prevention and treatment of food-producing animals, and from the use of antibiotics as growth-promoters in animals destined for meat production^{29,30,47}. Since antibiotic contamination is so common in agriculture, produce grown in contaminated crop soils and meat from food-producing animals can also be laden with antibiotic residues, with potential impacts on human health if consumed^{10,39,53,54}.

1.1.3 Relevance of One Health to the Antibiotic Resistance Crisis

Environmental antibiotic pollution often coincides with an increase in antibiotic resistance genes within environmental microbial communities^{7,38,43,55–57}. Foodborne pathogens are often found in soil environments, and antibiotic resistant foodborne pathogens can be introduced to humans through contaminated food^{10,11,58}. Outbreaks caused by antibiotic resistant bacterial pathogens require more intensive treatment, increasing the cost to treat these infections^{2,35,59–61}. In Canada, 1 in 16 patients admitted to a hospital will develop a nosocomial infection from a multidrug-resistant organism, which has economic consequences³⁷. In 2018, the Canadian healthcare system spent \$1.4 billion CAD on costs associated with the treatment of antibiotic resistant infections^{62,63}. Therefore, preventing exacerbating the antibiotic resistance crisis is critical in sustaining our healthcare system, and all industries that use antibiotics must take responsibility in managing the crisis to effectively address it. The One Health approach frames antibiotic resistance within the context of global human, animal, and environmental health, and strives to emphasize how communication and collaboration across multiple sectors can effectively reduce the prevalence of resistant infections^{19,62,64,65}.

To implement the One Health approach, the Canadian government has emphasized the shared responsibility of the Public Health Agency of Canada, Health Canada, the Canadian Food Inspection Agency, the Canadian Institutes of Health Research, and Agriculture & Agri-Food Canada as a multisectoral and collaborative task force to address the antibiotic resistance crisis⁶². These government agencies monitor, and research antibiotic resistance across all relevant sectors to develop policies and education programs that effectively reduce the abundance of antibiotic resistant bacteria to ultimately maintain the efficacy and utility of antibiotics for the stakeholders that rely on them⁶².

1.1.4 The Role of Agriculture in The Antibiotic Resistance Crisis.

Plant and animal agriculture heavily rely on antibiotics for reliable food production^{28,47,66,67}. In fact, animal agriculture is the largest consumer of antibiotics

in Canada, with 82% of antibiotics sold in Canada in 2014 being distributed for use in animal agriculture^{37,68}. Antibiotics are used to treat bacterial infections and promote growth in animals raised for food, and there is significant overlap between antibiotic classes used for human and veterinary medicine (e.g., aminoglycosides, trimethoprim, sulfas, tetracyclines, macrolides, β -lactams, and fluoroquinolones)^{29,47,69}. While antibiotic use in horticultural agriculture is significantly less extensive compared to animal agriculture, there are still applications for antibiotics in combatting plant disease^{70,71}. Bacterial plant pathogens such *Erwinia amylovora* and *Xanthomonas arboricola* can infect important food crops like orchard fruits⁷¹⁻⁷³. To prevent crop losses, antibiotic intervention with antibiotics (e.g., the aminoglycoside, streptomycin, or the tetracycline antibiotic, oxytetracycline) is required, but the efficacy of these treatments is waning due to increased rates of resistance^{7,24,70,72-74}.

While agricultural activities are known to pollute the environment with antibiotics that promote the emergence of resistance, commonly used agrichemicals such as herbicides and pesticides have also demonstrated the potential to select for antibiotic resistant bacteria^{4,5,7,8,75}. Since antibiotics, pesticides, and herbicides often co-occur as contaminants in agricultural run-off, the environmental compartments contaminated with these agrichemicals can become enriched for antibiotic resistance genes (ARGs)^{7-9,66,75}. Recent research has shown that agrichemicals that are routinely applied in crops like glyphosate, dicamba, and glufosinate, can increase the abundance of ARGs in soil, and influence the susceptibility of some human pathogens to antibiotic killing^{4,5}.

1.1.5. Antibiotics and Antibiotic Resistance

Antibiotics can act against bacteria through bactericidal action, wherein the bacterial cell is killed, or by bacteriostatic action, which inhibits the growth and proliferation of bacteria⁷⁶. To circumvent the action of antibiotics, bacteria can employ a myriad of mechanisms that can be classified as either intrinsic or acquired resistance mechanisms⁷⁷⁻⁸¹. Intrinsically resistant bacteria demonstrate

an innate capacity to resist certain types of antibiotic action. Some bacteria, including *Pseudomonas spp.*, *Mycobacterium spp.*, and *Salmonella spp.*, possess multidrug efflux pumps that provide intrinsic resistance by exporting many types of chemicals, including antibiotics, out of the cell^{82–84}. In contrast, acquired resistance refers to when a susceptible bacterial population becomes resistant to a given antibiotic either through *de novo* chromosomal mutations, or the acquisition of a mobile genetic element (e.g., transposons, plasmids)^{22,23,85,86}

1.2 Sulfas and Associated Compounds

1.2.1 Sulfas: Development and Applications

Sulfonamides antibiotics (sulfas) are bacterial antifolates that exert antibiotic activity by binding to the bacterial dihydropteroate synthase enzyme (DHPS), inhibiting the folate pathway by forming a dead-end metabolic product^{87,88}. The *de novo* biosynthesis of folate is essential for bacterial growth; therefore, the inhibition of this pathway consequently prevents the proliferation of bacterial cells^{76,89,90}. Sulfas are broad spectrum acting antibiotics that were first synthesized in 1932 by the German pharmacologist Gerhard Domagk, who was awarded a Nobel prize for his discovery of the antimicrobial action of the prototypical sulfa drug, sulfanilamide^{4,66}. Dogmagk used his discovery to successfully treat his daughter's infection, and the drug was commercialized and sold as "Prontosil" by 1939^{15,91}. During the 1940s, sulfas were praised by military physicians during World War II for reducing morbidity and mortality in their patients, who were routinely prescribed sulfas for diseases and conditions ranging from infection prophylaxis, to treating systemic infections such as pneumonia and meningitis⁹¹. However, the widespread use of sulfas was followed by the observation of a sulfa-resistant human pathogen (*Staphylococcus aureus*) by 1943⁹². Sulfa-resistance and resistance to other prototypical antibiotics in bacterial human pathogens became more common over time, and the man who discovered sulfas, Gerhard Domagk, died of an antibiotic resistant infection himself in 1964¹⁵. The prevalence of sulfa resistance combined

with the discovery of more powerful antibiotics such as penicillin and streptomycin resulted in the obsolescence of sulfas in clinical medicine⁹¹.

Today, sulfas are administered in combination with trimethoprim, which targets dihydrofolate reductase (DHFR) as co-trimoxazole (SXT) to treat infections such as pneumonia, caused by the fungal pathogen *Pneumocystis jirovecii*, or urinary tract infections (UTIs) caused by bacterial pathogens such as *Escherichia coli*^{93,94}. While overall sulfa use has declined over time, SXT is still considered an essential medicine by the World Health Organization, and the potential of using a drug that is already approved for use in humans to treat multidrug-resistant *Staphylococcus aureus* (MRSA) has renewed interest in this class of antibiotics^{93,95,96}. Sulfas are used much more widely in other applications, notably in veterinary medicine, which is the largest consumer of sulfas, due to the heavy usage of these drugs in animals produced for food^{30,31,49,69}. Sulfas are administered as veterinary drugs (e.g., sulfachloropyridazine, sulfadiazine, sulfamethazine, and sulfamethoxazole) and are often excreted in their active form, ultimately polluting environments adjacent to livestock farms and manure-amended crop soils^{31,49,51,52,97,98}.

1.2.2 Sulfa Mechanism of Action

As mentioned above, sulfas inhibit bacterial growth by interfering with the *de novo* production of folate; a highly conserved and essential process in bacteria due to the inability of prokaryotes to acquire folate from the environment^{99,100}. Folate, bioavailable in the form of folic acid, is an essential metabolite that cells utilize for several one-carbon transfer reactions, representing intermediate steps in synthesis of purine and pyrimidine nucleotides, and amino acid synthesis^{101,102}. Encoded by the *folP* gene, DHPS catalyses the condensation of 6-hydroxymethyl-7, 8-dihydropterin pyrophosphate (DHPP) with *para*-aminobenzoic acid (*p*ABA) by DHPS, which ultimately leads to the formation of the vital co-enzyme, tetrahydrofolate (Figure 1)^{101,103}.

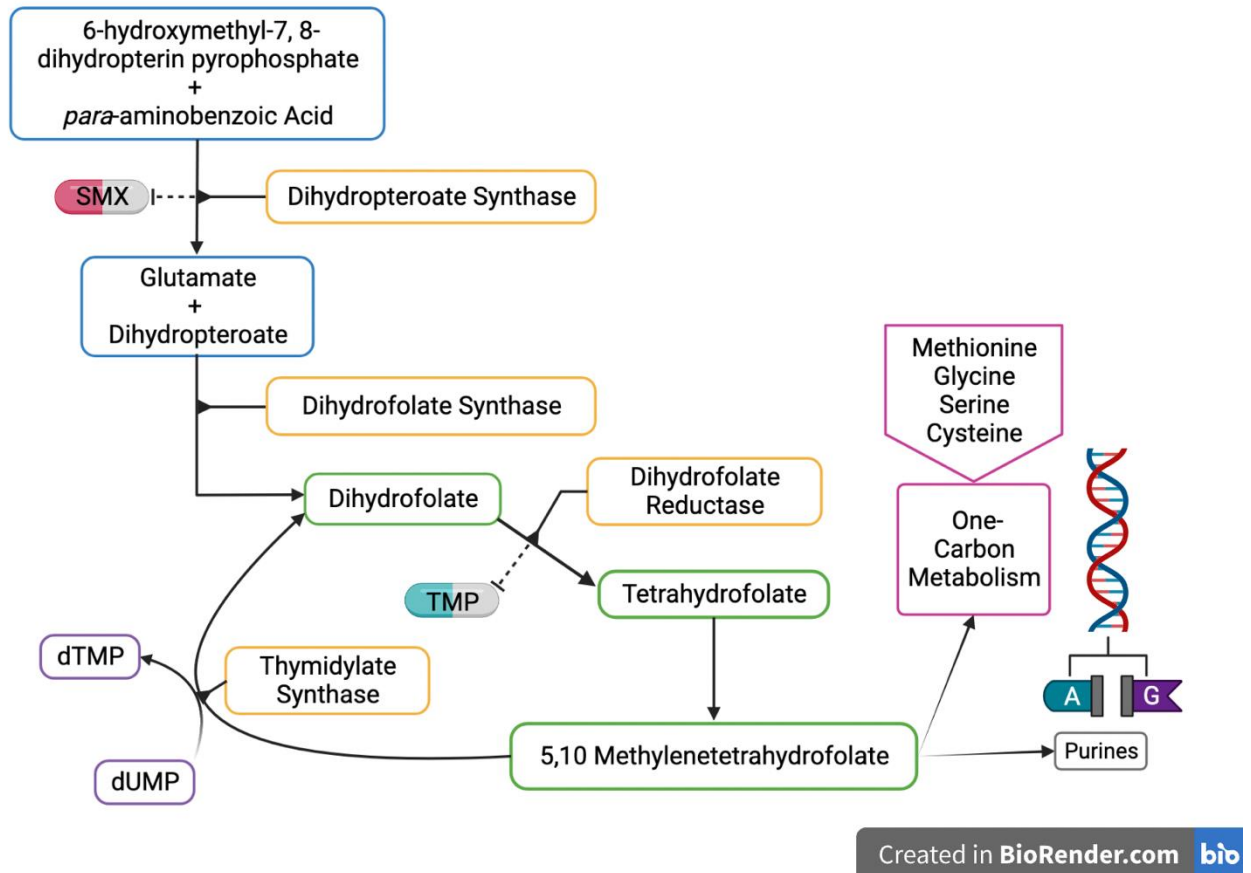


Figure 1. The bacterial *de novo* folate biosynthesis and utilization pathway with all enzymes circled in yellow and the step of the pathway they are involved in indicated by a line. The antifolate antibiotics sulfamethoxazole (SMX) and trimethoprim (TMP) are represented by labelled pills connected to their corresponding enzymatic target by dotted lines. Folic acid derivatives are circled in green, and the conversion of 5,10-methylenetetrahydrofolate to dihydrofolate via thymidylate synthase catalyzing the conversion of deoxyuridine monophosphate (dUMP) to deoxythymidine monophosphate (dTMP). Downstream products of this pathway are indicated by purple outlines, with the final products used in purine nucleotide synthesis and one-carbon metabolism.

Ultimately, without folate, DNA replication cannot continue due to the lack of available purine nucleotides, leading to both single- and double-strand DNA breaks, and the cells die due to thymineless death (TLD)^{104–106}

1.2.3 Thymineless Death

Thymineless death (TLD) is a phenomenon observed in bacterial, yeast, and mammalian cells characterized by a rapid loss in viability following thymine starvation^{103,107–109}. Despite over 60 years of research into the subject, the exact mechanism of TLD remains elusive¹⁰⁹. In bacteria, TLD was first observed in *E. coli*¹¹⁰ in 1954 in a thymine auxotrophic strain, and this phenomenon was later further characterized using *E. coli thyA* mutants that demonstrated the same thymidine auxotrophic phenotype^{109,110}. These *E. coli thyA* mutants are unable to synthesize thymidine monophosphate (dTMP), a precursor molecule to DNA, and lose viability in media lacking thymine^{111,112}. Several models have been proposed to explain TLD, with the current hypothesis suggesting that when cells are starved of thymine, DNA replication slows to a halt and chromosomal DNA loss occurs as DNA replication forks begin to break due to the lack of thymine available to form purine nucleotides and other components of cellular replication^{105,106,110,113}. Additionally, laboratory observations during TLD in bacterial cells include unbalanced growth due to the continuation of RNA and protein synthesis in the absence of active DNA replication, release of chromosomal fragments thought to be the result of thymine-starvation induced DNA damage, alterations to the cell envelope and cytoplasm, increased intracellular reactive oxygen species (ROS), and the activation of genes associated with DNA damage and repair mechanisms^{114–116}

1.2.4 Sulfa-Resistance Mechanisms

Since sulfas target the bacterial enzyme DHPS, many antibiotic bacterial isolates express a form of sulfa insensitive DHPS^{78,87,94,99,117}. Intrinsically sulfa-resistant bacteria typically either exhibit a chromosomally expressed sulfa-insensitive DHPS enzyme with a low affinity for sulfas preventing their action; and/or efflux pumps

which export the antibiotic from the cell^{78,118}. Acquired sulfa resistance can be conferred by *de novo* mutations in the chromosomal DHPS gene, *folP* in bacteria with single amino acid substitutions in the enzyme's active site conferring resistance without compromising the production of folate^{119–121}. Point mutations at Pro64 (P64) or Phe(F28) in *E. coli* DHPS enzymes are known to confer sulfa resistance, and have been identified in both lab and clinical isolates⁹⁶. The DHPS enzyme has a classic TIM (α/β)₈ barrel protein structure with eight loops, two of which (loop 1 and loop 2, respectively) have been implicated in sulfa resistance⁹⁹. Some amino acid substitutions can alter the structure of loop 1 or loop 2 of DHPS in a manner that permits *pABA* to maintain high binding affinity with the active site while abrogating the binding of sulfas^{119,122}. In *E. coli*, chromosomally encoded bacterial efflux pumps can provide intrinsic resistance to different types of chemical stress, including antibiotics^{84,118}. Efflux-mediated resistance mechanisms can be conferred by changes in regulatory genetic elements that activate or suppress efflux pump gene expression. For example, LeuO is a global gene regulator in *E. coli* that counteracts the H-NS global repressor protein, which facilitates efflux pump overexpression¹²³. When overexpressed, sulfa-specific sensitivity determinants like multidrug efflux pumps, such as those encoded by the *mdtNOP* operon that facilitate sulfa resistance¹²³

Although chromosomal mutations that confer sulfa resistance are common, the most prevalent mechanism of acquired resistance is attributed to the gene transfer of mobile genetic sulfa resistance determinants (e.g., plasmid or integrons)⁸⁶. The most reported group of mobile genetic elements that confer sulfa resistance are known as the *sul* genes⁸⁶. There are currently four known *sul* genes, *sul1*, *sul2*, *sul3*, and *sul4*; which are hypothesized to be mobilized *folP* variants derived from ancestral *Rhodobiaceae* and *Leptospiraceae spp.*^{86,117}. The sulfa-insensitive forms of DHPS encoded by the *sul* genes bind with *pABA*, and allow bacteria to produce *de novo* folate unimpeded by sulfas. The first two *sul* genes, *sul1* and *sul2*, were discovered in 1975 and 1980 on plasmids taken from resistant clinical isolates, and *sul3* was identified in 2003. The *sul3* gene was discovered and revealed to be extremely common in the pig population of Switzerland, where sulfas were

routinely administered with a subsequent increase in resistant infections¹²⁴. The most recent discovery was the *sul4* gene from bacterial DNA extracted from Indian river sediment samples in 2017 and has since been detected across Asia and Europe. The *sul* genes are often found in resistant isolates sourced from environmental samples, as well as nosocomial resistant infections, demonstrating the potential link between the environmental resistome and clinically relevant pathogens^{86,125,126}.

1.2.5 Asulam

Asulam (ASM) is a post-emergent herbicide currently applied to eliminate bracken, wild grasses, and other weeds in commercial agriculture and land management practices to control weeds and invasive species across the globe, with previous applications in Canada for controlling wild oats^{127,128}. Sold commercially as Asulox and formulated as a water-soluble sodium salt, ASM is applied by aerial spray or directly sprayed onto the target area at a standard rate of 2400 g/hectare¹²⁹. The chemical structure of ASM is analogous to sulfas and exerts its herbicidal action in a similar manner to how sulfas act against bacteria (Figure 2)^{130,131}. The herbicidal mechanism of action of ASM targets the folic acid biosynthesis pathway in plants, which is unique to ASM, and is the only herbicide with this mechanism of action on the market^{130,132}. Although higher eukaryotic organisms (i.e. animals) can obtain folate from external sources, lower eukaryotes, such as plants and some fungi rely on *de novo* tetrahydrofolate biosynthesis to produce DNA and amino acids¹³³. ASM exerts herbicidal activity by disrupting the binding of *p*ABA to the HPPK/DHPS (6-Hydroxymethyl-7,8-dihydropterin pyrophosphokinase/dihydropteroate synthase) a bifunctional enzyme in plants^{130,133}. After application, ASM induces a slow senescence that kills the plant through folate depletion, but ASM is also hypothesized to also have inhibitory effects on protein and RNA synthesis that contribute to plant death^{128,130–132,134}. After application, ASM degrades into several products, including the sulfa, sulfanilamide, and other compounds [(desamino asulam (DASM), acetyl asulam (AASM) formyl asulam, (FASM), asulam glucoside (ASMG), and malonyl asulam

(MASM)]¹²⁹. As evidenced by the presence of ASM and sulfanilamide in honey adjacent to ASM-treated crops, these compounds are known to contaminate the environment, and readily mobilize in groundwater^{129,135}. When applied at the standard rate, the predicted environmental concentration (PEC) of ASM in surface water can range from 0.5-62 µg/L, and from 0.3-9 µg/kg in sediment¹²⁹. Although ASM is not considered a high-risk herbicide with concern to its direct effects on either environmental or human health, nor are its degradation products, there is a knowledge/data gap regarding the long-term risk these compounds may have on soil microorganism communities and human health¹²⁹.

1.3 Rationale and Significance

Given the structural similarity of ASM and its degradation products (AASM, DASM, MASM, and ASMG) with sulfas, these compounds may have the capacity to exert antibiotic activity via the same mechanism of action as sulfas and/or select for sulfa-resistant bacteria. Using *E. coli* BW25113 as a surrogate for Gram-negative bacteria, the antibiotic action and selection potential of ASM and its environmentally relevant degradation products can be determined. Since there is renewed interest in expanding the use of ASM, assessing if it can select for drug-resistant bacteria will aid in developing policy frameworks to mitigate the spread of drug resistant pathogens, and thus preserve our current arsenal of antibiotics.

1.4 Hypothesis and Research Aims

Given the structural similarities between the herbicide ASM and its degradation products with sulfas, the hypothesis of this study is that ASM and its degradation products promote acquired sulfa resistance either via the selection of sulfa-resistant *E. coli* isolates that harbor *folP* mutations, or by increasing the dissemination plasmids carrying the *sul* genes to *E. coli*

Three research aims were designed to test this hypothesis: I) Assess if ASM and/or its degradation products exert antimicrobial activity via DHPS enzyme inhibition. II) Evaluate if ASM and/or its degradation products select for sulfamethoxazole-resistant *E. coli in vitro* III) Determine if ASM and/or its degradation products can promote the dissemination of plasmid-borne *sul* genes in a complex microbial community such as manure.

Chapter 2: Material and Methods

2.1 Bacterial strains, plasmids, and growth conditions

A list of the bacterial strains and plasmids used and/or constructed in this study are described in Table 1. *E. coli* strains were cultured in Luria broth (L-broth), (BD Difco, USA) and Luria agar (L-agar) (VWR Scientific, USA) or Mueller Hinton II broth (MHII-broth), (Sigma-Aldrich, USA) and Mueller Hinton II-agar (MHII-agar, Sigma-Aldrich) with antibiotics, or 200 µg/ml thymidine (Sigma-Aldrich) and 40 mM folinic acid (Alfa Aesar, USA) as necessary. The *E. coli* strain CV601 was a kind gift from Dr. Kornelia Smalla, and the *E. coli* K12 strains harbouring plasmids p77_{PW}, p54-1_{CH}, 12 p10_{CH}, p73-2_{CH}, and p27_{CH} were a kind gift from Dr. Magela Lavina (Table 1)^{86,136}. Unless otherwise stated, all cultures were grown at 37°C, and liquid cultures were incubated on a rotary shaker at 200 rpm. The plasmid pGDP2 was a kind gift from Dr. Gerry Wright¹³⁷. In *E. coli*, pGDP2 and its derivatives were maintained or selected with 25 µg/ml of kanamycin. Plasmid pLysS was maintained with 50 µg/ml chloramphenicol. Plasmid pET28a and its derivatives were maintained or selected with 50 µg/ml kanamycin. All bacterial strains were maintained as frozen stocks (-80°C) in 7.5% dimethyl sulfoxide (DMSO).

Table 1 Bacterial strains and plasmids used in this study

<i>E. coli</i> Strains	Relevant Characteristics	Source or Reference
DH10 β	F ⁻ <i>mcrA</i> Δ (<i>mrr-hsdRMS-mcrBC</i>) ϕ 80/ <i>lacZ</i> Δ M15 Δ <i>lacX74 recA1 endA1</i> <i>araD139</i> Δ (<i>ara-leu</i>)7697 <i>galU</i> <i>galK</i> λ - <i>rpsL</i> (Str ^R) <i>nupG</i>	New England Biolabs
K12 p10 _{CH}	<i>E. coli</i> K12 harboring plasmid p10 _{CH} containing resistance markers: Int1 ⁺ :: <i>sul1</i>	Poey <i>et al</i> ⁸⁴
K12 p27 _{CH}	<i>E. coli</i> K12 harboring plasmid p27 _{CH} containing resistance markers: Int1 ⁺ :: <i>sul2</i>	Poey <i>et al</i> ⁸⁴
K12 p73-2 _{CH}	<i>E. coli</i> K12 harboring plasmid p73-2 _{CH} containing resistance markers: Int1 ⁺ :: <i>sul3</i>	Poey <i>et al</i> ⁸⁴
BL21 (DE3)/pLysS	F ⁻ <i>ompT hsdSB</i> (<i>rB</i> ⁻ , <i>mB</i> ⁻) <i>gal dcm</i> (DE3)	Millipore
BW25113	<i>E. coli</i> K-12 BW25113 Δ (<i>araD-araB</i>)567 Δ <i>lacZ4787</i> (:: <i>rrnB-3</i>) <i>rph-1</i> Δ (<i>rhaD-rhaB</i>)568 <i>hsdR514</i>	Dharmacon
CV601	Conjugation Experiment Recipient Strain (SMX ^S , RIF ^R , KAN ^R , GFP ⁺)	Heuer <i>et al</i> ¹³⁴
Δ <i>folP</i>	BW25113 carrying an unmarked, in-frame <i>folP</i> gene deletion	Venkatesan <i>et al</i> ¹³⁶
Δ <i>folP</i> /pGDP2 :: <i>folP</i> _{Ec}	BW25113 carrying an unmarked, in-frame <i>folP</i> gene deletion harboring the pGDP2 plasmid expressing wild-type <i>folP</i> _{Ec} (KAN ^R)	This study
Δ <i>folP</i> pGDP2 :: <i>folP</i> _{P64S}	BW25113 carrying an unmarked, in-frame <i>folP</i> gene deletion harboring the pGDP2 plasmid expressing the <i>folP</i> _{P64S} mutation	This study
Δ <i>folP</i> pGDP2 :: <i>folP</i> _{P64A}	BW25113 carrying an unmarked, in-frame <i>folP</i> gene deletion harboring the pGDP2 plasmid expressing <i>folP</i> _{P64A} mutation	This study
Δ <i>folP</i> pGDP2 :: <i>folP</i> _{F28L}	BW25113 carrying an unmarked, in-frame <i>folP</i> gene deletion harboring the pGDP2 plasmid expressing <i>EcfolP</i> ^{F28L}	This study

<i>E. coli</i> Strains	Relevant Characteristics	Source or Reference
$\Delta folP$ pGDP2 :: <i>folP</i> $_{\Delta E68}$	BW25113 carrying an unmarked, in-frame <i>folP</i> gene deletion harboring the pGDP2 plasmid expressing <i>EcfolP</i> $_{\Delta E68}$	This study
$\Delta folP$ pGDP2 :: <i>sul1</i>	BW25113 carrying an unmarked, in-frame <i>folP</i> gene deletion harboring the pGDP2 plasmid expressing <i>sul1</i>	Venkatesan et al ¹³⁶
$\Delta folP$ pGDP2 :: <i>sul2</i>	BW25113 carrying an unmarked, in-frame <i>folP</i> gene deletion harboring the pGDP2 plasmid expressing <i>sul2</i>	Venkatesan et al ¹³⁶
$\Delta folP$ pGDP2 :: <i>sul3</i>	BW25113 carrying an unmarked, in-frame <i>folP</i> gene deletion harboring the pGDP2 plasmid expressing <i>sul2</i>	Venkatesan et al ¹³⁶
$\Delta folP$ pGDP2 :: <i>sul4</i>	BW25113 carrying an unmarked, in-frame <i>folP</i> gene deletion harboring the pGDP2 plasmid expressing <i>sul4</i>	Venkatesan et al ¹³⁶
ASM100 ⁷ -1	ASM-selected, SMX ^R <i>E. coli</i> Keio BW25113	This study
ASM100 ⁷ -2	ASM-selected, SMX ^R <i>E. coli</i> Keio BW25113	This study
ASM100 ⁷ -3	ASM-selected, SMX ^R <i>E. coli</i> Keio BW25113	This study
ASM100 ⁷ -4	ASM-selected, SMX ^R <i>E. coli</i> Keio BW25113	This study
ASM100 ⁷ -5	ASM-selected, SMX ^R <i>E. coli</i> Keio BW25113	This study
ASM100 ¹⁰ -1	ASM-selected, SMX ^R <i>E. coli</i> Keio BW25113	This study
ASM100 ¹⁰ -2	ASM-selected, SMX ^R <i>E. coli</i> Keio BW25113	This study
SMX100 ⁷ -1	ASM-selected, SMX ^R <i>E. coli</i> Keio BW25113	This study
SMX100 ⁷ -2	SMX-selected, SMX ^R <i>E. coli</i> Keio BW25113	This study
SMX100 ⁷ -3	SMX-selected, SMX ^R <i>E. coli</i> Keio BW25113	This study
SMX100 ¹⁰ -1	SMX-selected, SMX ^R <i>E. coli</i> Keio BW25113	This study
SMX100 ¹⁰ -2	SMX-selected, SMX ^R <i>E. coli</i> Keio BW25113	This study
SMX10 ⁷ -1	SMX-selected, SMX ^R <i>E. coli</i> Keio BW25113	This study

<i>E. coli</i> Strains	Relevant Characteristics	Source or Reference
SMX10 ⁷ -2	SMX-selected, SMX ^R <i>E. coli</i> Keio BW25113	This study
SMX10 ¹⁰ -1	SMX-selected, SMX ^R <i>E. coli</i> Keio BW25113	This study
SMX10 ¹⁰ -2	SMX-selected, SMX ^R <i>E. coli</i> Keio BW25113	This study
Plasmids		
pET28a	Protein expression vector with a 6XHis tag, a thrombin digestion site and a T7 tag	Novagen
pET28a:: <i>folP</i> _{Ec}	Protein expression vector with an N-terminal 6xHis tag, a N-terminal thrombin digestion site	This study
pGDP2	<i>E. coli</i> gene expression vector (KAN ^R)	Cox <i>et al</i> , 2017 ¹³⁵
pGDP2:: <i>folP</i> _{Ec}	pGDP2 :: <i>folP</i> _{Ec}	Rampton, M (Unpublished)
pGDP2:: <i>folP</i> _{P64S}	pGDP2:: <i>folP</i> _{P64S} -FLAG Tag	Rampton, M (Unpublished)
pGDP2:: <i>folP</i> _{P64A}	pGDP2:: <i>folP</i> _{P64A} -FLAG Tag	This study
pGDP2:: <i>folP</i> _{F28L}	pGDP2:: <i>folP</i> _{F28L} -FLAG Tag	Rampton M (Unpublished)
pGDP2:: <i>folP</i> _{ΔE68}	pGDP2:: <i>folP</i> _{ΔE68} -FLAG Tag	This study
pGDP2 :: <i>sul1</i>	<i>sul1</i>	Venkatesan <i>et al</i> ¹³⁶
pGDP2 :: <i>sul2</i>	<i>sul2</i>	Venkatesan <i>et al</i> ¹³⁶
pGDP2 :: <i>sul3</i>	<i>sul3</i>	Venkatesan <i>et al</i> ¹³⁶

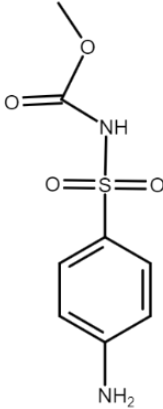
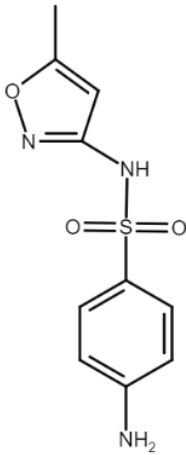
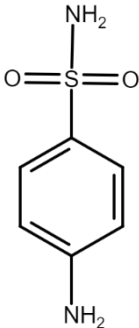
<i>E. coli</i> Strains	Relevant Characteristics	Source or Reference
pGDP2 :: <i>sul4</i>	<i>sul4</i>	Venkatesan et <i>al</i> ¹³⁶

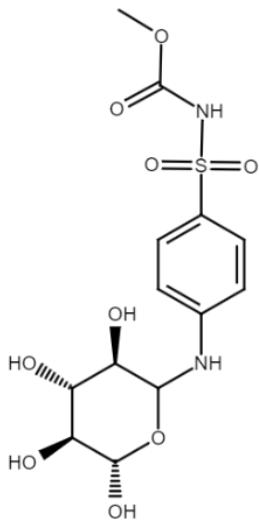
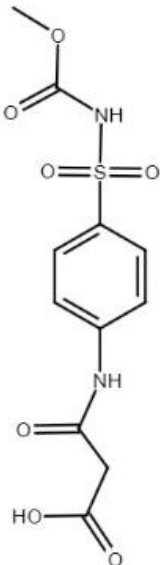
SMX^S, sulfamethoxazole susceptible; SMX^R, sulfamethoxazole resistance; KAN^R, kanamycin resistance; CAM^R, chloramphenicol resistance; GFP⁺, Green fluorescent protein, P_{64S}, Pro64→Ser *folP* gene mutation; P_{64A}, Pro64→Ala *folP* mutation; ΔE₆₈, Glu68del *folP* mutation; F_{28L}, Phe28→Leu *folP* mutation; FLAG-TAG for monitoring protein expression via immunoblotting

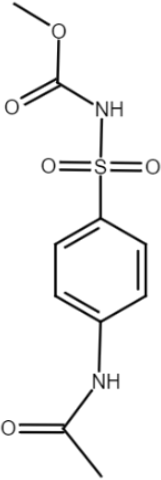
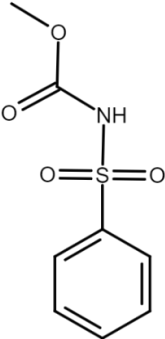
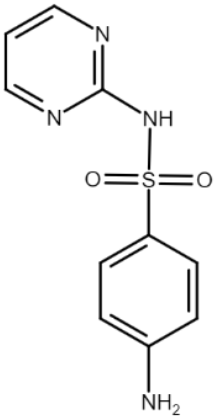
2.2 Antibiotics, ASM, and Degradation products

All sulfonamide compounds used in this study were prepared as stock solutions dissolved in a compatible solvent at 50 mg/mL and stored frozen at -20°C. A list of sulfonamide compounds used in this study and the solvents used are outlined in Table 2.

Table 2. Common identifiers, structure, and relevant qualities of the sulfonamide compounds used in this study

Compound	Structure	Solubility	Purity	Source
Asulam (ASM)		50 mg/mL in DMSO ^b	>99%	Toronto Research Chemicals
Sulfamethoxazole (SMX)		50 mg/mL in DMSO	>99%	Sigma- Aldrich
Sulfanilamide (SAN)		50 mg/mL in Acetone	>99%	Sigma- Aldrich

Compound	Structure	Solubility	Purity	Source
Asulam Glucoside (ASMG)		50 mg/mL in DMSO	95%	ChemSpace
Malonyl Asulam (MASM)		50 mg/mL in DMSO	95%	ChemSpace

Compound	Structure	Solubility	Purity	Source
Acetyl Asulam (AASM)		50 mg/mL in DMSO	95%	ChemSpace
Desamino Asulam (DASM)		50 mg/mL in DMSO	95%	ChemSpace
Sulfadiazine (SDZ)		50 mg/mL in Acetone		Sigma- Aldrich

a, International Union of Pure and Applied Chemistry; b, dimethyl sulfoxide. Structures were generated using ChemSpace Structure Search tool available at chem-space.com

2.3 DNA Methods

2.3.1 Agarose Gel Electrophoresis

Agarose gel electrophoresis was used to separate DNA fragments. Agarose gels (0.8% w/v) were prepared using 1X TAE (40 mM tris(hydroxymethyl) aminomethane, 20 mM acetic acid (Sigma-Aldrich), 1 mM ethylenediaminetetraacetic acid (ETDA)) buffer to dissolve agarose (0.8% w/v) with RedSafe nucleic acid staining solution (0.05% v/v) added to visualize DNA fragments. DNA samples were prepared for gel electrophoresis by diluting 2 μ L of DNA concentrated to a minimum of 10 ng/ μ L measured using a Nanodrop Spectrophotometer (Thermo Fisher Scientific) in 6 μ L of nuclease-free sterile water with 2 μ L of 6 X DNA loading dye (0.25% (w/v) bromophenol blue, 0.25% (w/v) xylene cyanol FF, and 15% (w/v) Ficoll 400 dissolved in deionized water), and all 10 μ L were loaded into a designated well of the gel. Once all samples were loaded, a 1Kb plus DNA ladder RTU (Froggabio, Canada) or 100bp DNA ladder RTU (Froggabio) depending on the size of the amplicon, was added to the first empty well of the gel, and electrophoresis was performed with a BioRad PowerPac set to 120V for 20-30 minutes. Gels were visualized using either a BioRad Chemidoc XRS Gel Imaging System or Cambridge imaging system (UVITEC, UK)

2.3.2 Colony PCR amplification of *folP* from *E. coli*

To amplify the *folP* gene from *E. coli* colonies, oligonucleotides were designed using the PrimerQuest tool by Integrated DNA Technologies (IDT) (Coralville, USA), synthesized by IDT, and resuspended in nuclease-free water (NF-Water) for colony PCR. For each *E. coli* strain used, template DNA was collected by selecting a single bacterial colony from an agar plate and suspended it in 30 μ L (NF-Water). The suspension was boiled for 5 minutes on a Life Tech Heating block (VWR Scientific), followed by centrifugation at 13 000 rpm for 3 minutes in a Sorvall Legend Micro 21R tabletop centrifuge (ThermoFisher Scientific). The template DNA was then placed on ice until added to the reaction mixture. PCR mixes were prepared to a final concentration of 42% (v/v) NF-Water, 5% (v/v) DMSO, 200 μ M

of dNTPs, 0.5 μ M of each forward and reverse primer, 0.02 U/ μ L of Phusion® High-Fidelity DNA Polymerase (New England Biolabs, Canada). PCR was carried out using a C1000 Touch™ Thermal Cycler (BioRad, USA) with the following thermal cycles: 30 sec at 98 °C for initial denaturation of DNA, followed by 30 cycles of 30 sec at 98 °C, 30 sec at 60 °C, and 72 °C for 30 seconds; with the final elongation completed at 72 °C for 7 min.

2.3.3 Purification and Sequencing of PCR Products

All *folP* amplicon PCR products were column purified or gel purified using the Wizard SV Gel and PCR Clean-Up System kit (Promega Corp., Canada). DNA was quantified and DNA quality was checked using a Nanodrop Spectrophotometer (Thermo Fisher Scientific). Nucleotide sequencing of PCR products was carried out by the London Regional Genomics Centre (Robarts Research Institute) using *folp_F* and *folp_R* as forward and reverse primers respectively (Table 3).

Table 3. Oglionucleotide sequences of primers designed for this study and synthesized by IDT

Oglionucleotide	Sequence (5' – 3')
<i>folP_F</i>	CGACGCACCGCAGATTGATGACCTG
<i>folP_R</i>	CCAGTGCTGACTCCAGCATATAGCC
<i>sul1_F</i>	GCCCATGAGATCAGACGTATTG
<i>sul1_R</i>	GTTGGAAGCTGTTCGATTGAAAC
<i>sul2_F</i>	GTGGTGTGGCCTATCTCAAT
<i>sul2_R</i>	GACGAGTTTGGCAGATGATTTC
<i>sul3_F</i>	GAACCGATGTGAAATCTCGTTTAG
<i>sul3_R</i>	CATCATGGGTGCGGAGATAA
<i>sul4_F</i>	GGCTGTGGACGTCGTTATTT
<i>sul4_R</i>	TAAGGCGATGTCGATGCTTTC

2.3.4 Chromosomal DNA extraction and whole genome sequencing of *E. coli*

Whole genome sequencing was performed at the Microbial Genome Sequencing Center (MiGS) (Pittsburgh, USA). Sample libraries were prepared using the Illumina DNA Prep kit and IDT 10bp UDI indices, and sequenced on an Illumina NextSeq 2000, producing 2x151bp reads. Demultiplexing, quality control and adapter trimming was performed with bcl-convert.

2.3.5 Whole Genome Sequence Analysis

All sequencing data was processed by the MiGS computational pipeline. Sequencing reads were mapped to the reference genome (NCBI accession #CP009273) by bowtie2 version 2.4.5 mapping software and SNP calling was conducted using the breseq version 0.36.1 single nucleotide polymorphism (SNP) caller¹³⁸. A minimum of 88% bp > Q30 was obtained for all isolates sequenced (Appendix 5). The reference-guided *de novo* genome assembly tool in Seqman NGen (DNASTar, USA) was used with the NCBI accession #CP009273 as the reference genome, and the variant calling accuracy workflow in Seqman NGen (DNASTAR, USA) was used to confirm the breseq detected SNPs.

2.3.6 Preparation of CaCl₂ Competent *E. coli* cells

Standard protocols were used for the preparation of chemically competent (CaCl₂) *E. coli* cells as described by Sambrook and Russell¹³⁹. Briefly, *E. coli* Δ *folP* cells were made competent by inoculating a 50 mL culture of broth with 500 μ L of prepared overnight culture supplemented with 200 mM thymidine (Sigma-Aldrich) and 50 μ M folinic acid (Alfa Aesar). This subculture was incubated at 37°C with shaking at 200 rpm until an optical density at 600 nm (OD₆₀₀) of 0.40 was reached. Cells were placed on ice for 20 minutes, and subsequently pelleted by centrifugation for 15 min at 8000 rpm and 4°C. Cells were resuspended in chilled 100 mM CaCl₂ and put on ice for 20 min. In 40 μ L aliquots, cells were dispensed into microfuge tubes and frozen at -80°C until ready for transformation.

2.3.7 Plasmid Transformation: *E. coli* BL21(DE3) pLysS with pET28a

Gene synthesis and cloning of the *folP* gene in pET28a was conducted by Gene Universal, USA. Plasmid pET28a DNA was prepared for transformation using the GeneJet Plasmid Miniprep kit (ThermoFisher Scientific) according to the protocol outlined by the manufacturer, and the DNA concentration was determined using a Nanodrop Spectrophotometer (ThermoFisher Scientific). Plasmids were transformed into *E. coli* by mixing 1 μ L of 50 ng/mL plasmid DNA with 50 μ L of BL21(DE3) pLysS competent *E. coli* cells, and heating the mixture in a waterbath set to 47°C for 30 sec. After heat shock, cells were placed on ice for 2 min, then mixed with soft media (SOC) and incubated for 45 min at 37 °C with end-over-end rotation. After incubation, the mixture was then serially diluted 1 in 10, and 1 in 100. Both dilutions and an undiluted sample were plated onto transformant-selective media (L-Broth supplemented with 50 μ g/mL kanamycin) and incubated overnight at 37°C. A single colony was selected and isolated to be cultured as a frozen stock.

2.3.8 Plasmid Transformation of *E. coli* Δ *folP* with pDGP2

The *E. coli folP* gene was synthesized and subcloned into pGDP2 by BioBasic, Canada. Plasmid DNA was prepared using the GeneJet Plasmid Miniprep kit (ThermoFisher Scientific) according to the protocol outlined by the manufacturer. The concentration of extracted plasmid DNA was determined using a Nanodrop Spectrophotometer (Thermofisher Scientific). Plasmids were transformed into *E. coli* by mixing 2 μ L of 50 ng/mL plasmid DNA with 40 μ L of chemically competent *E. coli* Δ *folP* cells, and incubating the mixture on ice for 20 min. After incubating on ice, the mixture was heat-shocked by heating the mixture in a waterbath set to 42°C for 1 min 30 sec. After heat shock, cells were placed on ice for 2 min, then mixed with 800 μ L L-broth and incubated for 1 hour at 37 °C with end over end rotation. After incubation, the mixture was then serially diluted 1 in 10 to 10⁻². Undiluted, 10⁻¹, and 10⁻² diluted samples were plated onto transformant-selective media (L-agar supplemented with 25 μ g/mL) and incubated overnight at 37°C. A single colony was selected and isolated to be cultured as a frozen stock.

2.4 Antibiotic Susceptibility Testing

2.4.1 Two-Fold Broth Microdilution Method

The broth dilution method was used to determine the minimum inhibitory concentration (MIC) of antibiotics compatible with this method. These assays were performed based on previously described methods¹⁴⁰. Briefly, the antibiotic to be tested was prepared by supplementing fresh, sterile MHII media with X2 the highest concentration of drug to be tested. The antibiotic-supplemented media was added to the first column of well of a Corning™ Costar™, U-bottom, 96-well plate in 100 µL aliquots. The remaining wells of the 96-well plate were filled with 50 µL fresh, sterile MHII broth, and 50 µL of antibiotic-supplemented media was pipetted from the first column of well, mixed into the second column of wells, then subsequently serially diluted in this 2-fold fashion until the final column of wells, and the remaining 50 µL was discarded. Each well was then inoculated using 50 µL of prepared cells, which were grown as an overnight culture, then diluted using two 1 in 20 dilutions in MHII media prior to inoculation. Plates were incubated overnight in static conditions at 37 °C. After incubation, MICs were recorded as the lowest concentration of drug that completely inhibited growth.

2.4.2 Two-Fold Adapted Agar Microdilution Method

Due to the limited availability of some of the compounds used in this study, the minimum inhibitory concentration (MIC) determinations were achieved by adapting the previously described agar and broth dilution method¹⁴⁰. This was achieved by using a Corning™ Costar™, U-bottom, 96-well plate format for agar dilutions in place of traditional square plates to minimize the amount of drug needed. The highest concentration of drug to be tested was added to 15 mL volume of sterilized, molten MHII agar cooled to 55 °C, and mixed by gentle inversion. Subsequently, 300 µL of the molten agar containing drug was loaded into the first column of wells of a Corning™ Costar™, U-bottom, 96-well plate pre-heated to 60 °C. To prevent cooling and thus, solidification of the agar in the wells, the Corning™ Costar™, U-bottom, 96-well plate was placed on an isotherm heating plate (ThermoFisher

Scientific) set to 80°C. The remaining wells were loaded with 150 µL of drug-free molten MHII agar. Next, 150 µL of drug-containing agar was taken from the first well and transferred into the 2nd column. The diluted drug-agar was mixed by pipetting, and 150 µL was removed and this serial dilution was repeated until the last column, which had no drug added to serve as a growth control. Once the agar was solidified in the wells, the plate was then dried to remove moisture by air-drying plates in a biological safety cabinet (BSC) for 10-15 minutes. To prepare the bacterial inoculum, 3-5 freshly streaked *E. coli* colonies were resuspended in 5mL sterile 0.85% NaCl saline solution, and the turbidity of the suspension was adjusted to that of a 0.5 McFarland Standard using a Sensititre Nephelometer (ThermoFisher Scientific) calibrated to a McFarland 0.5 BaSO₄ standard. Standardized *E. coli* suspensions were diluted 1 in 10 with 0.9% (v/v) saline, in a Corning™ Costar™, U-bottom, 96-well plate. A flame-sterilized 48-pin replicator with 1.5 mm pins was used to deliver the final inoculum of 1 µl (~10⁴ CFU/ml) onto the drug-agar plates. Inoculated plates were incubated at 37°C overnight. After incubation, MICs were recorded as the lowest concentration of drug that completely inhibited growth.

2.4.3 E-Test Co-Trimoxazole MIC test

To determine the co-trimoxazole MICs of *E. coli*, the E-test method was employed. Briefly, to prepare the inoculum, bacterial suspension standardized to a 0.5 MacFarland standard. The trimethoprim-sulfamethoxazole (1:19) E-test strips (Liofilchem, Italy) were then aseptically transferred a onto MHII agar freshly streaked with the standardized bacterial inoculum. The MIC was determined by assessing where the elliptical zone of inhibition intersected with the MIC scale on the test strip. In the case that the intersection was between two values, the higher value was counted as the MIC.

2.5 Directed evolution Assays

To assess the ability of ASM or ASMG to select for *folP* mutations, a 10-day directed evolution experiment was employed. Briefly, 100 μL of an overnight culture of *E. coli* Keio BW25113 grown at 37°C with shaking at 200 rpm was transferred into 10 mL of fresh MHII-broth containing either 0.01 $\mu\text{g/mL}$, 0.1 $\mu\text{g/mL}$, 1 $\mu\text{g/mL}$, 10 $\mu\text{g/mL}$, or 100 $\mu\text{g/mL}$ of ASM, ASMG, or sulfanilamide. Sulfamethoxazole was used as the positive control as it is known to select for sulfa-resistance, and the vehicle controls for these experiments were DMSO as it was used as a solvent for ASM, ASMG, and SMX; acetone (ACE) was used as a solvent for sulfanilamide and was therefore included as a vehicle control to ensure these compounds did not select for SMX-resistance. Flasks containing the same concentrations of SMX were also prepared to establish the resistance frequency when *E. coli* Keio BW25113 is exposed to a sulfa antibiotic known to select for sulfa-resistance. A 100 μL aliquot was taken daily from each flask to inoculate fresh media containing the corresponding concentration of drug for each group over a period of ten days. To monitor these cultures for emerging SMX-resistance, a 100 μL sample was taken on day one, seven, and ten, and screened for SMX-resistance. Each sample was serially diluted in MHII broth, and plated onto MHII agar containing no drug, as well as MHII agar containing 256 $\mu\text{g/mL}$ of SMX. Following an 18-hour incubation at 37 °C, colonies were enumerated, and the CFU/mL was calculated using the following equation:

$$\frac{\text{Colony Forming Units} \times \text{dilution factor plated}}{0.1 \text{ mL}}$$

The resistance frequency of each treatment per day was calculated using the following equation:

$$\frac{\text{Total Bacteria on MHII – agar } \left(\frac{\text{CFU}}{\text{mL}}\right)}{\text{Total bacteria on MHII – agar supplemented with SMX } \left(\frac{\text{CFU}}{\text{mL}}\right)}$$

From the directed evolution experiments, randomly selected SMX-resistant colonies were tested for significant and maintained resistance, with significant resistance defined as at least a 16-fold increase in MIC of SMX. This was achieved by selecting random colonies from the directed evolution experiments that grew on MHII agar supplemented with 256 µg/mL and patching them onto MHII agar containing 256 µg/mL and incubated for 48 hours to ensure any isolates that may have acquired a fitness loss at the cost of developing resistance could grow¹⁴¹. Isolates that maintained significant resistance were collected and cultured as frozen stocks for further characterization.

2.5.1 Selection and Confirmation of SMX^R Isolates

When colonies grew on the SMX-supplemented agar during the directed evolution assays, random colonies were selected and screened for maintained SMX-resistance by patching colonies onto MHII agar supplemented with 256 µg/mL, and significant resistance was tested by patching onto MHII agar supplemented with 512 µg/mL. When patched colonies grew on both 256 and 512 µg/mL SMX supplemented MHII plates, colonies were isolated and assigned an identifier based on the experimental condition the isolate was collected from. Each identified isolate was cultured as a frozen stock.

2.6 Conjugation Experiments

Raw swine manure used in these experiments was collected from a swine farm in Southwestern Ontario, Canada, with soil metadata included in Appendix 2. Samples were taken directly from the hauling tanker into 5-gallon pails. The pail was stirred prior to removing 2 x 1-liter grab samples to be stored in sterile

Polyethylene terephthalate (PET) jars. Swine manure was screened for the presence of the mobile *sul* genes by extracting the bacterial DNA fraction from 1 mL of manure using the QIAamp PowerFecal Pro DNA kit (Qiagen, USA). Bacterial DNA was used to conduct PCR using sequence-specific primers for the *sul1*, *sul2*, *sul3*, and *sul4* genes (Table 3). After screening for the *sul* genes, manure was aliquoted into 50 mL falcon tubes and mixed with 15% (v/v) glycerol to be stored at -80°C until experiments were performed. The protocol for the conjugation experiments was modified from Tran, T, et al¹⁴² as follows: Since the *sul* genes were detected in the swine manure samples (Appendix 2), The bacterial fraction of the swine manure samples was extracted and used as *sul* gene donor cells. To extract and prepare these donor cells, 1mL of manure was added to 9mL of MHII broth and incubated overnight under static condition at 30°C prior to mating. Particulate was removed by centrifugation at 300 × g for 5 min and the supernatant was collected. The bacterial fraction was extracted by a second centrifugation at 8000 × g for 15 min. The pellet was washed twice with a 10⁻¹ dilution L-broth. The final donor cell extraction was resuspended in 200µL 0.85% NaCl saline. To prepare recipients, the sulfa-sensitive, GFP-labelled *E. coli* CV601 (GFP^R, KAN^R, RIF^R) was incubated at 37°C in L-broth supplemented with rifampicin and kanamycin (50 µg/mL) overnight on a rotary shaker set to 200 rpm. After incubation, 1 mL of culture was centrifuged at 3100 × g for 5 min. The pellet was collected and washed twice with 1 in 10 diluted L-broth, and finally resuspended in 100µL saline. Matings were performed by mixing a 1:1 volume ratio of donor and recipient cells and plating 50 µL spots onto MHII agar supplemented with 100 µg/mL cyclohexamide to inhibit fungal growth. Manure and CV601 samples were also plated onto the same media in 25µL aliquots. After co-incubation at 30 °C for 12 hours in an incubating mini shaker (VWR Scientific) set to static conditions, mating spots were washed and resuspended in 2.5mL saline solution. Samples were then serially diluted and plated onto both MHII agar containing rifampicin and kanamycin (50 µg/mL) to select for all possible recipient cells. The MIC of SMX with *E. coli* CV601 was determined to be 32 µg/mL, so MHII agar plates containing 512 µg/mL SMX were used to select for sulfa-resistant transconjugants. To confirm

colonies that grew on this selective media were successful transconjugants harboring one of the known *sul* genes, colony PCR was performed using sequence-specific primers for the *sul* genes (Table 3) and the PCR products were separated using gel electrophoresis and visualized by imaging the DNA gel.

2.6.1 PCR amplification of the *sul* genes from bacterial DNA extracted from manure

To extract the DNA of the bacteria, present in the swine manure samples, 1 mL aliquots were transferred into 1.5 mL tubes and centrifuged at 16 000 × g. The supernatant was discarded, and the chromosomal DNA was isolated from the bacterial pellet using in a manner outlined by the manufacturer. The concentration of each DNA sample isolated was determined using a Nanodrop spectrophotometer. To detect if the known *sul* genes were present in these DNA samples, PCR amplification of the *sul* genes was performed using the extracted DNA as the template DNA, and forward and reverse primers designed with the PrimerQuest tool by IDT using *sul* gene sequences retrieved from the Comprehensive Antibiotic Resistance Database (CARD) (Table 3)¹²². PCR mixes were prepared to a final concentration of 42% (v/v) NF-Water, 5% (v/v, DMSO), 200 μM of dNTPs, 0.5 μM of each forward and reverse primer, 0.02 U/μL of Phusion ® High-Fidelity DNA Polymerase (New England Biolabs). PCR was carried out using a C1000 Touch™ Thermal Cycler (BioRad) with the following program: 98°C for 30 sec for initial denaturation of DNA, followed by 30 cycles of 30 sec at 98°C, 30 sec at 60°C, and 72°C for 15 seconds; with the final elongation completed at 72°C for 5 min.

2.7 In vitro Growth Assay

To assess if there is a fitness cost to acquired SMX resistance of the S^R isolates, an *in vitro* growth assay was employed. A 3mL overnight culture was prepared for each strain/isolate tested, which were then standardized to an OD₆₀₀ of 0.1 measured with a Nanodrop Spectrophotometer. Each well of a Corning™ Costar™ U-bottom, 96-well clear round bottom plate was filled with 100μL of MHII media

and 100 μ L of the standardized inoculum was added. Wells were also filled with 200 μ L fresh, sterile MHI broth as a negative control. The plate was incubated for 24 hours in a Thermo Scientific MULTISKAN GO set to heat at 37°C with continuous shaking, and the OD₆₀₀ of each well was read every 20 minutes using SKANIT 6.0.1 Software (ThermoFisher Scientific). Three independent experiments were performed each containing biological triplicates of each strain.

2.8 Purification of the Polyhistidine-Tagged *EcDHPS* Protein

To assess the binding kinetics of *EcDHPS* with SMX and ASM, *EcDHPS* protein was purified and prepared for isothermal titration calorimetry (ITC) based on previous drug-protein assays conducted with bacterial DHPS and sulfas^{87,99}. The *E. coli folP* gene (*folP_{Ec}*) was synthesized and cloned with an in-frame N-terminal polyhistidine tag into the expression vector pET28a by Gene Universal (USA), yielding plasmid pET28a::*folP_{Ec}*. Plasmid pET28a::*folP_{Ec}* was then transformed into chemically competent *E. coli* BL21(DE3) harbouring pLysS plasmids, and transformants were plated on L-agar containing 50 μ g/mL kanamycin for selection of pET28a, and 50 μ g/mL chloramphenicol for selection of pLysS. A single colony of *E. coli* BL21(DE3) containing pET28a::*folP_{Ec}* was used to inoculate a 10 mL overnight culture of L-broth supplemented with 50 μ g/mL of both kanamycin and chloramphenicol. The next day, the entire 10 mL of overnight culture was used to inoculate 1 L of L-broth, and cells were grown at 37°C with shaking at 200 rpm until the OD₆₀₀ read by a Nanodrop Spectrophotometer reached 0.6, at which point, expression of the his-tagged *EcDHPS* was induced by adding 1 mM IPTG. Induction was performed for 6 hours on a rotary shaker set to 200 rpm at 37 °C. Cells were then pelleted by centrifugation at 10 000 \times g for 10 min in a Sorvall UltraCentrifuge (ThermoFisher Scientific) at 4°C. The supernatant was discarded, and the cell pellets were stored at -20 °C until further purification. Cell pellets were thawed on ice and resuspended in 12 mL of lysis buffer (50 mM Tris pH 8, 0.5 M NaCl, Concentration Halt™ EDTA-free Protease Inhibitor Cocktail (Thermo Scientific)). Resuspensions were sonicated at 30% amp for 14 x 30 sec pulses (with 30 sec delay between pulses) on ice with a QSonica Q500 Sonicator

(Newtown, USA). The cell lysate was then centrifuged at 13 000 rpm for 60 min in a Sorvall Legend Micro 21R tabletop centrifuge (ThermoFisher Scientific) to remove cell debris, and the soluble cytoplasmic fraction containing the target protein was collected. *EcDHPS* was then purified by batch binding to Ni-NTA resin. The QIAGEN Ni-NTA resin was equilibrated by centrifuging 1 mL of resin mixed gently by inversion with 10 mL of elution buffer (50 mM Tris pH 8, 0.5 M NaCl). Once the Ni-NTA was equilibrated, the cell lysate was loaded onto the equilibrated Ni-NTA and incubated at room temperature with end over end rotation for 45 min to allow the his-tagged *EcDHPS* protein to bind to the resin. Once the protein was bound to the resin, the solution was centrifuged at 3000 × g in a (centrifuge) equipped with a swinging bucket rotor, and X2 1mL aliquots of the supernatant were collected. Next, the resin was washed three times by incubating the resin with 5 mL of wash buffer (50 mM Tris pH 8, 0.5 M NaCl, 5 mM imidazole) (Avantor Performance Materials, USA) for 10 min with end-over-end rotation at room temperature, and the aliquot collection procedure was repeated for each wash. Three washes were completed, followed by protein elution performed by incubating the resin mixed with elution buffer (50 mM Tris pH 8, 0.5 M NaCl, 25 mM imidazole) for 15 min with end-over-end rotation at room temperature. Protein elutions were collected by centrifugation at 3000 × g equipped with a swinging bucket rotor, and x2 1 mL aliquots of the supernatant were collected. After the first elution, this procedure was repeated four more times, with 50 mM, 100 mM, 150 mM, and 250 mM imidazole in the elution buffer. The collected lysate, wash, and protein aliquots were checked for purity and approximate quantity using sodium dodecyl-sulfate polyacrylamide gel electrophoresis (SDS-PAGE). Based on visual analysis of the SDS-PAGE gel, the protein samples collected from the 150- and 250-mM imidazole elutions were pooled and further purified and dialyzed with purification buffer (50 mM HEPES 4-(2-hydroxyethyl)-1-piperazineethanesulfonic acid) (Sigma-Aldrich), 5 mM MgCl₂ (Sigma-Aldrich) pH 7.6) using a next generation chromatography (NGC) system (Biorad) equipped with a SEC650 size exclusion column to perform fast protein liquid chromatography (FPLC). FPLC purified fractions were collected and concentrated with a Vivaspin 6 concentrator (GE Life

Sciences,) according to the manufacturer's instructions, and the final concentration of protein was determined using the Bradford BCA as outlined by the manufacturer (ThermoFisher Scientific).

2.9 Isothermal Titration Calorimetry (ITC)

2.9.1 Titrating SMX into *EcDHPS*

To assess binding affinity of ASM with purified *EcDHPS*, isothermal titration calorimetry (ITC) experiments were performed using a NanoITC (TA Instruments, USA) at the Schulich Medicine & Dentistry Biomolecular Interactions & Conformations Facility (London, Ontario). The reference cell was equilibrated with ITC buffer (50mM HEPES pH 7.6 5mM MgCl₂ 2.5% DMSO, 10 mM Na₄P₂O₇) and 5 μM of *EcDHPS* suspended in 500 μL ITC buffer was loaded into the sample cell of the NanoITC. For the ligand, 50 μL of 100 μM SMX suspended in ITC buffer was drawn up into the titrant syringe, which was screwed into place on the NanoITC. Experiments were carried out over 25 injections of 2μL each in 300 sec intervals with the temperature set to 25 °C. Raw data was processed using NanoAnalyze by TA Instruments using an independent one-site binding model. Baseline corrections were performed by running a mock experiment before every biological replicate experiment using only ITC buffer in both the titrant syringe and the sample cell to subtract the heat of dilution from the reaction for an accurate calculation of binding affinity.

2.9.2 Titrating ASM into *EcDHPS*

Titration that was performed with 100 mM SMX was repeated with 200 μM ASM under the same experimental conditions and the resulting data analysis as described above.

2.10 Western immunoblotting

To confirm expression of DHPS in the trans-complemented of the *folP* gene variants used as controls in this study, western immunoblotting was performed

using anti-FLAG antibodies. Overnight cultures of *E. coli* were prepared with appropriate antibiotics when necessary. The next day, 200 μ L of this culture was used to inoculate a 10 mL subculture grown until the optical density at 600 nm of 0.5 was reached. A 1.5 mL aliquot of this culture was then pelleted and resuspended in 200 μ L phosphate buffered saline (PBS) and standardized to an OD of 0.5. After 180 μ L of 2X redmix was added to the resuspended *E. coli*, the mixture was denatured by boiling for 5 minutes at 95°C and subsequently sonicated for 25 sec at 30% amplitude using a QSonica Q500 Sonicator (Newtown, USA). Samples were run on an SDS-PAGE gel at 120V for. The SDS-PAGE gel was transferred onto an activated polyvinylidene difluoride (PVDF) membrane (soaked in methanol for 1 minute), and the gel was stacked between this activated PVDF membrane and Whatman paper soaked in transfer buffer (25 mM tris, 192 mM, glycine, pH 8.3, 0.1% SDS) and transferred using BioRad Trans-Blot® Turbo™ Transfer System. After transfer, the membrane was blocked with 10% milk powder in PBST (1 x PBS, 0.1% TWEEN-20) overnight at 4°C on a rotating shaker. Milk was washed off the membrane using PBST, with two 5 min washes. The primary antibody (ANTIFLAG® M2 antibody (1:1000 dilution)) was added by diluting in 10 mL PBST (0.1% BSA) and pouring the antibody solution over the membrane with gentle rocking for 1 hour, and the membrane was subsequently washed with PBST twice before adding the secondary antibody (polyclonal goat anti-mouse Anti-Mouse IgG (H&L (HRP) antibody (1:500 dilution)), prepared and poured onto the membrane in the same manner as the first antibody in 10 mL , followed by two washes with PBST and exposed to SuperSignal™ West Pico PLUS Chemiluminescent Substrates. A 7 s exposure was imaged using a DNA Bio-Imaging Labs MicroChemi 4.2 imaging system with GelCapture acquisition software (n=2) (Appendix 1).

Chapter 3: Results

3.1 ASM Selects for Sulfamethoxazole-Resistant *E. coli*

3.1.1 ASM exerts antibiotic action against *E. coli*

The antibiotic action of sulfas is contingent upon the capacity of these drugs to mimic *pABA*, the natural substrate of bacterial DHPS. Therefore, the shared structural features of *pABA*, sulfas, ASM, and the degradation products of ASM infers that all these compounds could interact with bacterial DHPS, and potentially exert antibiotic action via the inhibition of this enzyme. To assess the potential of ASM and its degradation products (AASM, MASM, DASM, & ASMG) to exert antibiotic action against *E. coli*, the minimum inhibitory concentration (MIC) of each compound was determined (Table 4). To accommodate the limited quantity of these compounds, a modified 2-fold agar dilution assays were employed. Mueller-Hinton II media was chosen as the growth medium for these assays to avoid the antagonistic effect of thymine against sulfas,

Table 4. ASM and its degradation products possess antibiotic activity against *E. coli*. Minimum inhibitory concentration (MIC) of *E. coli* strains lacking a DHPS enzyme ($\Delta folP$), harboring wild-type (WT) DHPS, or a sulfa-insensitive form of DHPS encoded by the indicated *sul* gene

Strain	DHPS ^a	(MIC) ($\mu\text{g/mL}$)						
		SMX	SAN	ASM	ASMG	DASM	AASM	MASM
$\Delta folP$	N/A	NG	NG	NG	NG	NG	NG	NG
$\Delta folP/pGDP2$	N/A	NG	NG	NG	NG	NG	NG	NG
BW25113	WT	16	2048	256	2048	2048	4096	4096
$\Delta folP/pGDP2::sul1$	<i>sul1</i>	2048	-	2048	-	2048	4096	4096
$\Delta folP/pGDP2::sul2$	<i>sul2</i>	2048	-	2048	-	2048	4096	4096
$\Delta folP/pGDP2::sul3$	<i>sul3</i>	2048	-	2048	-	2048	4096	4096
$\Delta folP/pGDP2::sul4$	<i>sul4</i>	2048	-	2048	-	2048	4096	4096

^a Abbreviations: DHPS, dihydropterate synthase; WT, wild-type; SMX, sulfamethoxazole; SAN, sulfanilamide; ASM, asulam; ASMG, asulam glucoside; DASM, desamino asulam; AASM, acetyl asulam; MASM, malonyl asulam; NG, no growth.

Amongst the strains tested, the two *E. coli* isolates lacking a DHPS enzyme ($\Delta folP$, $\Delta folP/pGDP2$), were known to be thymine auxotrophs¹⁴³. As expected, the $\Delta folP$ and $\Delta folP/pGDP2$ strains were unable to form colonies on MHII-agar, a thymine limited medium (Table 4). The parent strain, *E. coli* BW25113, had a SMX MIC of 16 $\mu\text{g/mL}$, whereas the MIC for ASM was 256 $\mu\text{g/mL}$ (Table 4). Conversely, ASM was more potent than sulfanilamide (SAN), which had an MIC 8-fold higher than ASM, and 128-fold higher than that of SMX with *E. coli* Keio BW25113 (Table 4). Therefore, ASM and its degradation product ASMG, which share structural similarity with the *pABA* and sulfa family of antibiotics, also exhibit antimicrobial activity, likely by targeting DHPS.

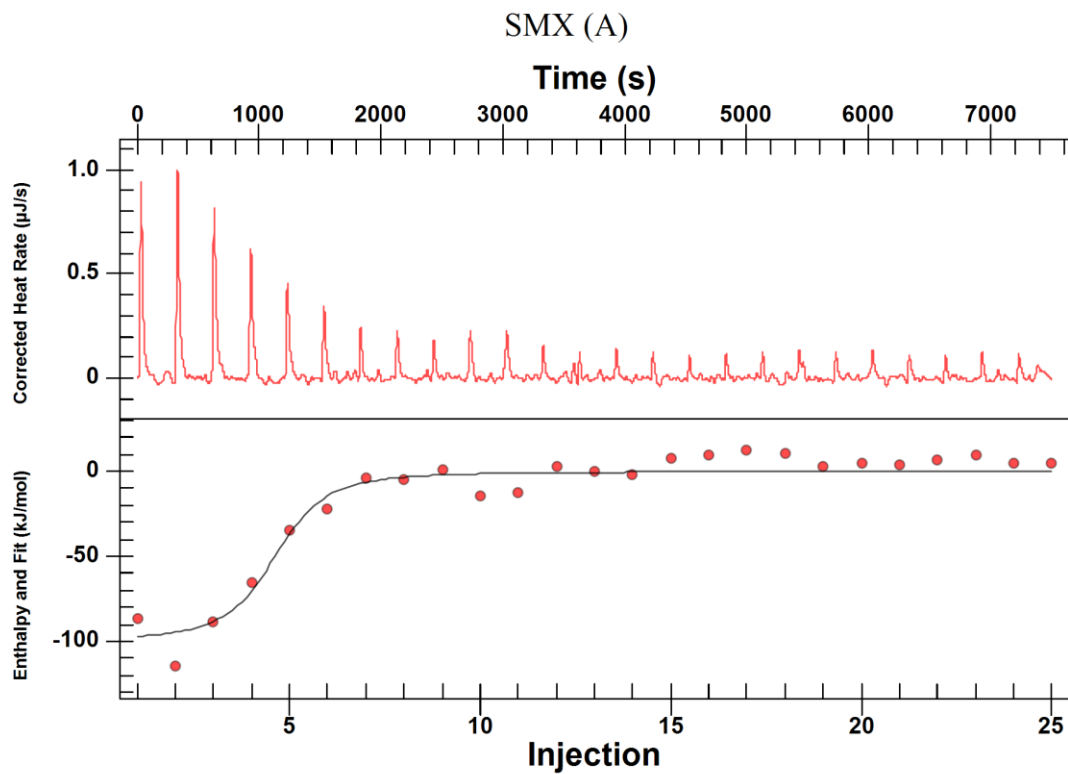
3.1.2 ASM and ASMG target *EcDHPS*

After establishing that ASM and its degradation products exhibit antibiotic activity, and that different forms of DHPS influence the susceptibility of *E. coli* to ASM and several ASM degradation products, the interaction between ASM and DHPS was investigated further. To elucidate if ASM mimics the interaction of sulfas with *EcDHPS*, the binding kinetics of *EcDHPS* with the clinically relevant sulfa gold standard, SMX, was first assessed using isothermal titration calorimetry (ITC).

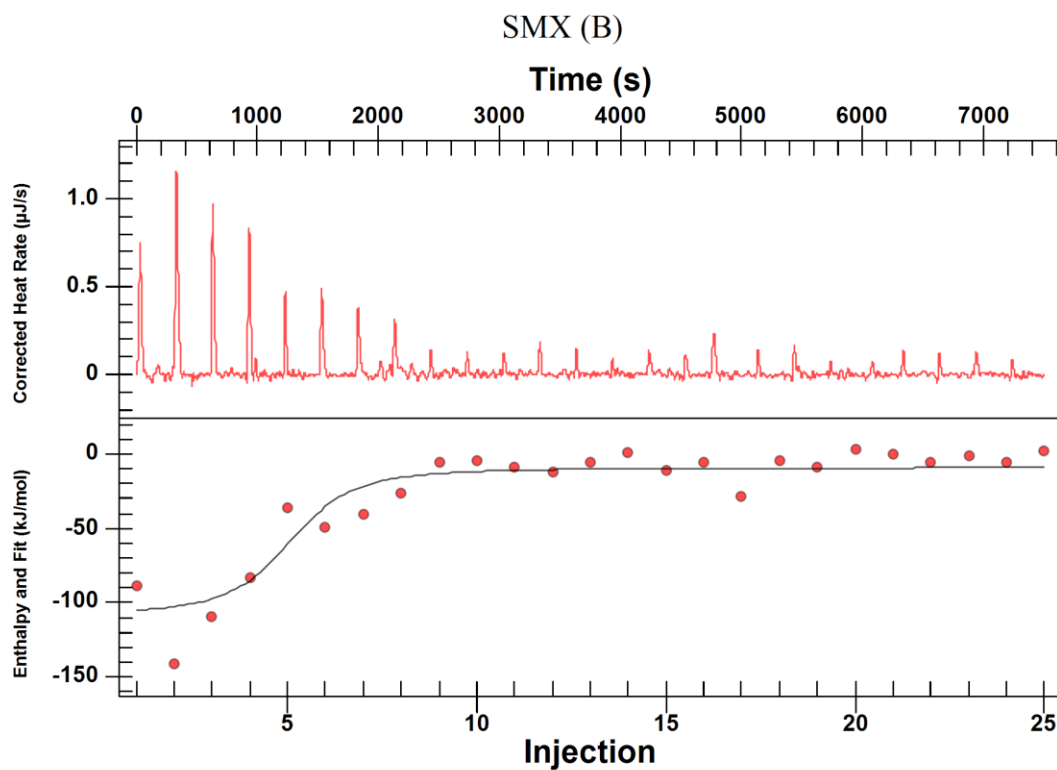
3.2 Both SMX and ASM act as a ligand for *EcDHPS*

ITC experiments were used to evaluate if ASM interacts with *EcDHPS*. As a positive control the binding affinity of *EcDHPS* and SMX was determined. These experiments were executed using purified *EcDHPS* protein and SMX, both prepared with 10 mM pyrophosphate to mimic the presence of DHPP and facilitate binding⁸⁷. The association constant (K_a) and dissociation constant (K_d) were determined to characterize the binding affinity of SMX and *EcDHPS*¹⁴⁴ (Figure 2).

(A)



Variable	Value	CI (95%)
K_d (M)	1.265E-7	$\pm 1.138E-7$
ΔH	-100	± 8.265
K_a (M^{-1})	7.90E6	

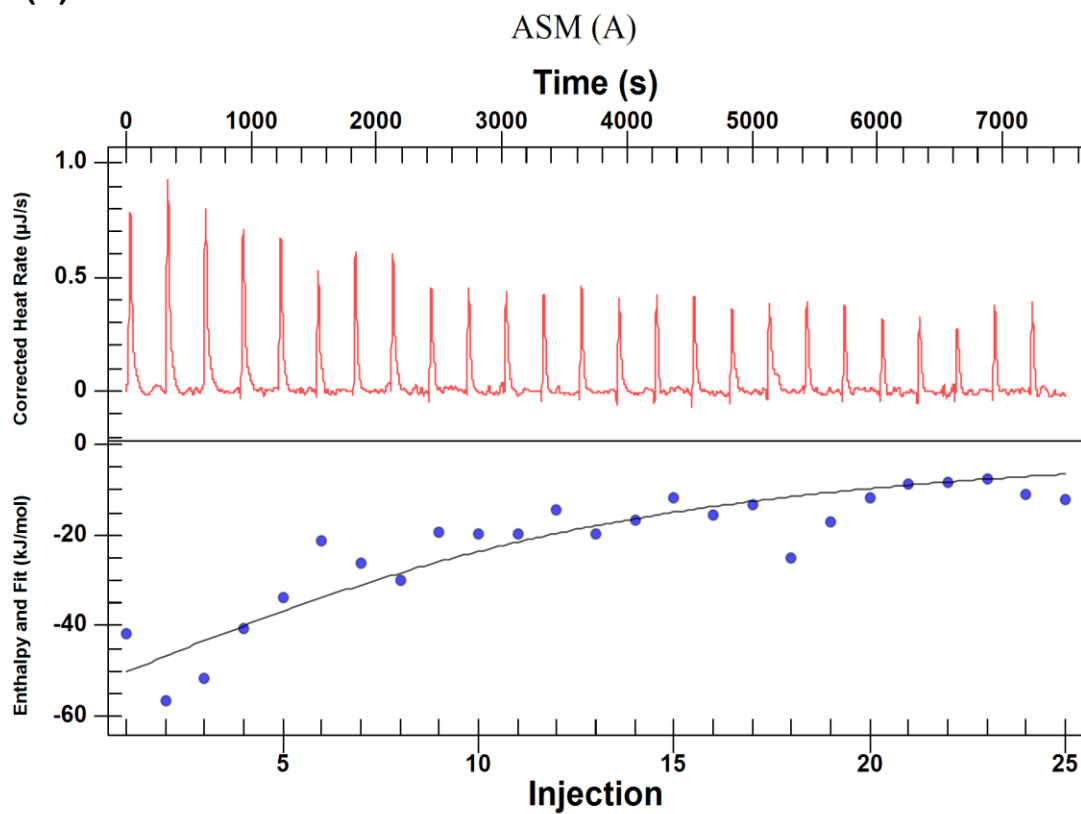
(B)

Variable	Value	CI (95%)
K_d (M)	1.89E-7	$\pm 3.074E-7$
ΔH	-100	± 19.50
K_a (M^{-1})	5.279E6	

Figure 2. Binding curves of each ITC experiment replicate performed with 25 injections of 100 mM SMX titrated into 5 μ M *EcDHPS* for two replicates (A and B respectively)

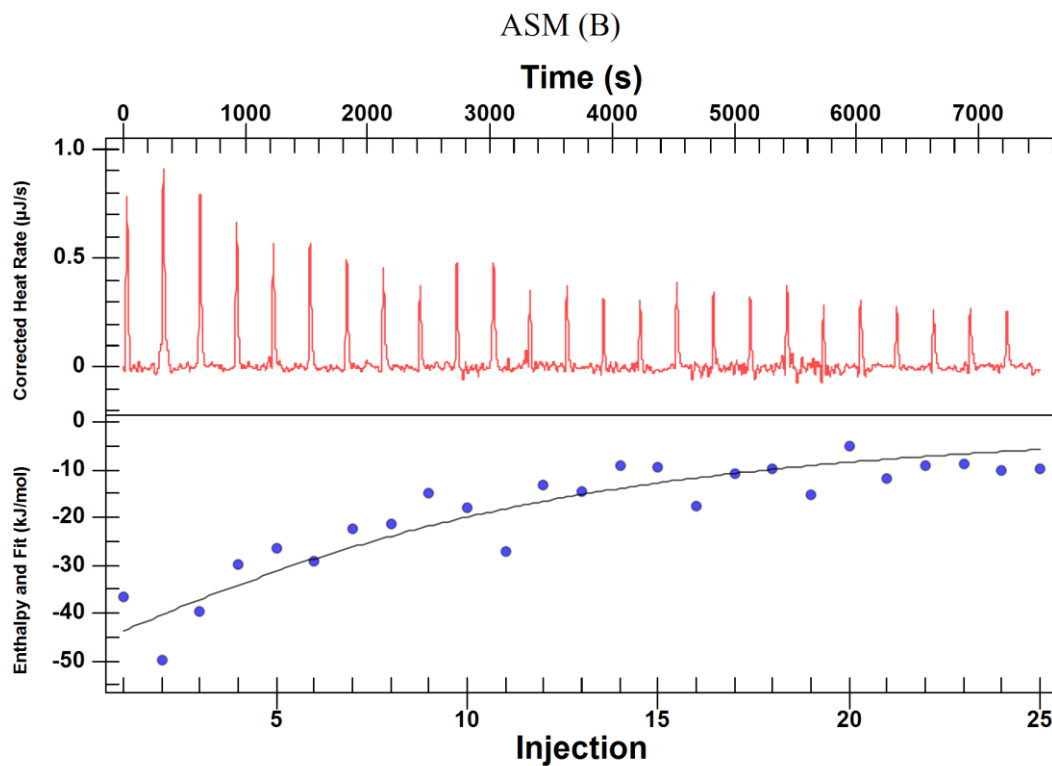
Consistent with previous studies, inorganic pyrophosphate was required to generate the *p*ABA/sulfa drug binding pocket, as SMX binding to DHPS was not observed in the absence of pyrophosphate. Binding affinity was also concentration dependent, as SMX binding with *Ec*DHPS occurred spontaneously at 100 μ M, but ASM at an equivalent concentration did not bind with *Ec*DHPS. Therefore, increasing concentrations of ASM were titrated into 5 mM *Ec*DHPS until binding was observed at 200 μ M ASM (Figure 3).

(A)



Variable	Value	CI (95%)
K_d (M)	2.00E-5	$\pm 1.248E-5$
ΔH (kJ/mol)	-100	± 36.41
K_a (M ⁻¹)	4.999E4	

(B)



Variable	Value	CI (95%)
K_d (M)	2.299E-5	$\pm 1.560\text{E-}5$
ΔH	-100	± 39.57
K_a (M^{-1})	4.349E4	

Figure 3. Binding curves of each ITC experiment performed with 25 injections of $200\mu\text{M}$ ASM titrated into $5\mu\text{M}$ *EcDHPS* for two replicates (A and B respectively)

These data suggest that ASM binds with *EcDHPS* in a similar manner to SMX, but the lower K_a of ASM and *EcDHPS* indicates this enzyme as compared to SMX.

3.3 ASM, but not ASMG or SAN select for SMX resistant *E. coli* in vitro

The ITC experiments confirmed that ASM interacts with *EcDHPS*, and ASM, ASMG, and SAN all demonstrated antibiotic activity contingent upon the DHPS status of *E. coli*. Together, these data suggest that ASM, ASMG, and SAN have potential to select for sulfa insensitive DHPS-variants in *E. coli*. To assess this, directed evolution experiments were executed by monitoring cultures of the sulfa-sensitive *E. coli* BW25113 strain in the presence of a range of sub-MIC levels of ASM, ASMG, or SAN, for emerging resistance over a 10-day exposure period. The lowest concentrations of drug tested (0.01 and 0.1 $\mu\text{g}/\text{mL}$) were selected to reflect the predicted range of concentration of ASM as a contaminant in surface water determined by the European Food Safety Authority, while the 1, 10, and 100 $\mu\text{g}/\text{mL}$ treatments provided a large window to determine the minimum selective concentration (MSC) of each compound tested^{129,145}. As a positive control, directed evolution experiments were carried out with SMX at the same concentrations, since they are within the range of concentrations of SMX known to select for sulfa resistance in experimental, clinical, and environmental settings^{125,126,146,147}.

Table 5. Emergence of SMX^R colonies in directed evolution experiments carried out at the indicated concentration. Compounds that yielded SMX^R *E. coli* BW25113 on the indicated day of exposure and concentration are noted as positive for SMX^R with (+), and compounds that did not are labelled as (-). ACE served as the vehicle control for SAN, and DMSO was used for all other compounds tested

Treatment	Concentration	SMX ^a Resistance (+/-) ^b		
		Day 1	Day 7	Day 10
Control				
No Drug	N/A	-	-	-
DMSO	% (v/v)	-	-	-
ACE	% (v/v)	-	-	-
Compound				
ASM	0.01 µg/mL	-	-	-
	0.1 µg/mL	-	-	-
	1 µg/mL	-	-	-
	10 µg/mL	-	-	-
	100 µg/mL	-	+	+
SMX	0.01 µg/mL	-	-	-
	0.1 µg/mL	-	-	-
	1 µg/mL	-	-	-
	10 µg/mL	-	+	+
	100 µg/mL	-	+	+
SAN	0.01 µg/mL	-	-	-
	0.1 µg/mL	-	-	-
	1 µg/mL	-	-	-
	10 µg/mL	-	-	-
	100 µg/mL	-	-	-
ASMG	0.01 µg/mL	-	-	-
	0.1 µg/mL	-	-	-
	1 µg/mL	-	-	-
	10 µg/mL	-	-	-
	100 µg/mL	-	-	-

^aAbbreviations: SMX, sulfamethoxazole; DMSO, dimethyl sulfoxide; ASM, asulam; SAN, sulfanilamide; ASMG, asulam glucoside.

ASM did select for SMX^R *E. coli in vitro*, but the environmentally relevant concentrations of ASM tested (0.01, 0.1 µg/mL) did not select for SMX^R *E. coli*, nor did the same concentrations of SMX (Table 5). As expected, *E. coli* exposed to 100 or 10 µg/mL SMX yielded SMX^R and interestingly, SMX^R colonies were also observed in ASM 100 µg/mL exposed *E. coli* (Table 5). These observations were time dependent, with the first SMX^R colonies detected on day 7 in the SMX 10, SMX 100, and ASM 100 µg/mL treatments, and these same treatments yielded SMX^R colonies on day 10 as well (Table 5).

The resistance frequency of each treatment was determined by enumerating the SMX^R bacteria (CFU/mL) in technical duplicates on media supplemented with 256 µg/mL SMX and dividing each value by the total number of bacteria present (CFU/mL), which was enumerated in technical duplicates from the same culture using a non-SMX^R selective media (Figure 4). Resistance frequency calculations can thus be summarized by the following equation:

$$\text{SMX Resistance Frequency} = \frac{\text{SMX Resistant Bacteria CFU per mL}}{\text{Total Bacteria CFU per mL}}$$

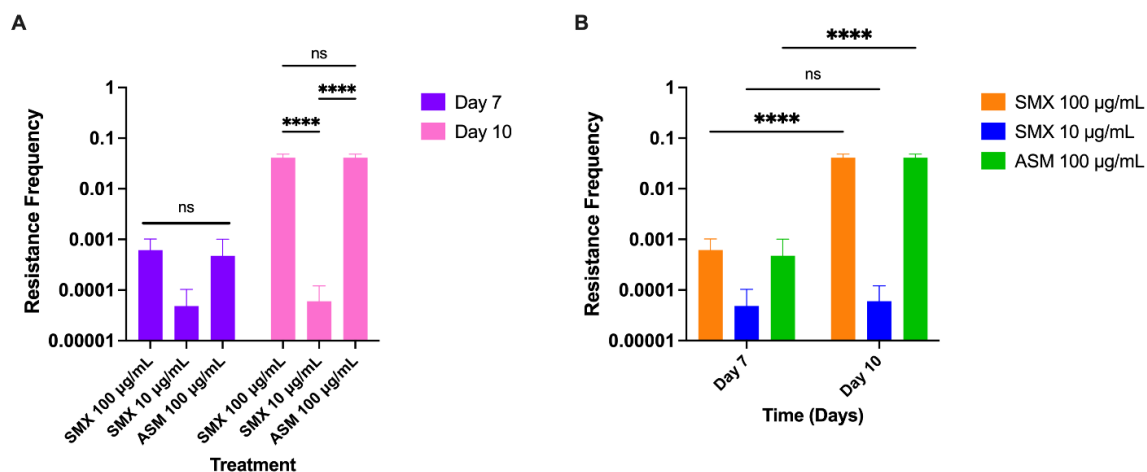


Figure 4. Average resistance frequency of all treatments that yielded SMX^R *E. coli* in *in vitro* directed evolution experiments (N=2). Plotted by treatment applied (A) or by day of the experiment (B). Statistical significance as determined by an ordinary two-way ANOVA with Tukey's multiple comparisons test with single pooled variance is indicated by asterisks (**** P < 0.0001), and no significance is noted as ns.

When SMX^R was first observed on day 7, there was no significant difference in the average resistance frequency amongst all treatments that yielded SMX^R *E. coli*, but by day 10, both ASM and SMX 100 µg/mL treatments had significantly higher resistance frequencies compared to SMX 10 µg/mL ($P < 0.0001$) (Figure 4). Both ASM and SMX 100 µg/mL treatments also demonstrated a significant increase in resistance frequency between day 7 and day 10 of each respective treatment ($P < 0.0001$), suggesting that the frequency of resistance increases in a time-dependent manner at these concentrations (Figure 4). Taken together, these data indicate that environmentally relevant concentrations of ASM, ASMG, SAN, and SMX, do not select for sulfa-resistant *E. coli*, and that only SMX and ASM at concentrations exceeding the predicted environmental concentrations can select for SMX^R *E. coli in vitro*¹²⁹.

3.3.1 Identification and Characterization of ASM-selected *folP* mutations in *E. coli*

Sulfa-resistance in clinical, experimental, and environmental bacterial isolates is often mediated by mutations in the chromosomally encoded *folP* gene, which encodes a structurally altered DHPS enzyme^{94,117,148}. Therefore, a subset of SMX^R isolates were randomly selected and screened for chromosomal *folP* mutations by PCR amplifying and sequencing the entire *folP* gene, including the upstream of this gene's promoter region. The resulting sequences were analyzed for single nucleotide polymorphisms (SNPs), which were detected by aligning the sequenced *folP* genes of the SMX^R isolates with the reference sequence for the parent strain, *E. coli* BW25113. A total of 105 isolates were selected and screened for *folP* mutations, and 103 of them were found to have acquired mutations or deletions when compared to the wild type (Figure 5).

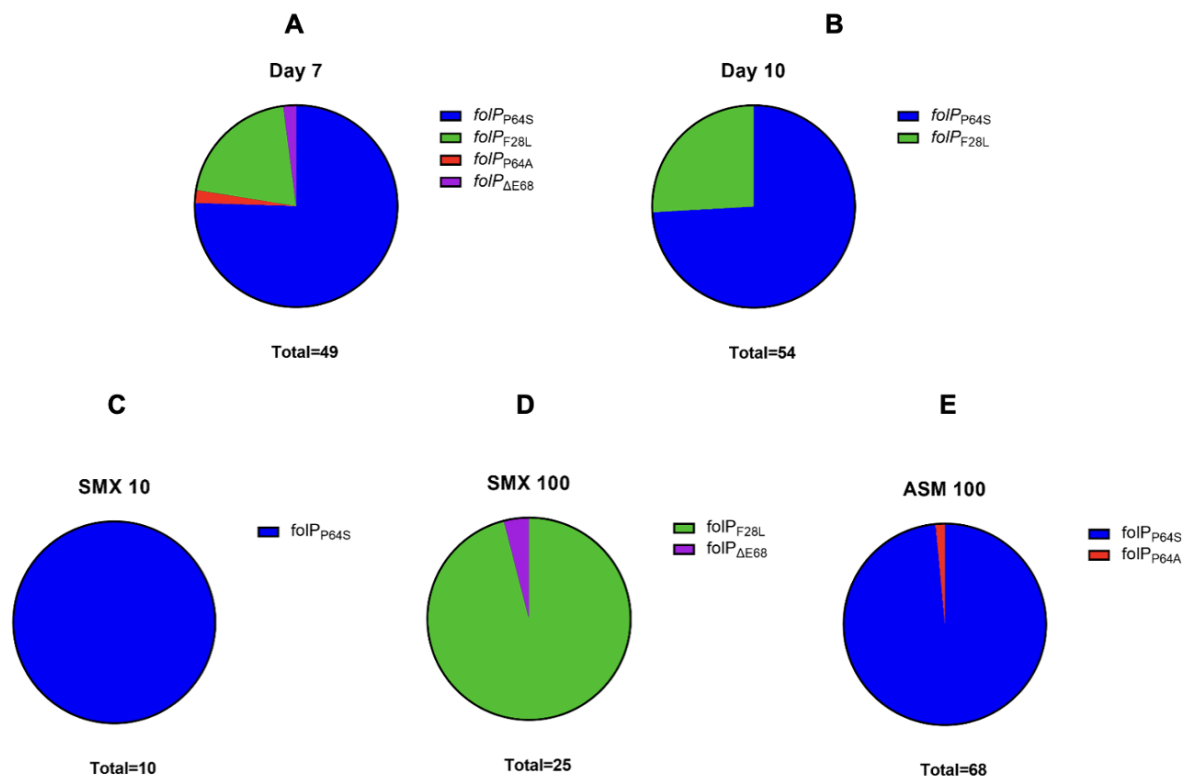


Figure 5. Pie charts of *folP* mutations observed on day 7 (A), and day 10 (B) of the directed evolution experiments, as well as mutations observed in treatments SMX 10 $\mu\text{g}/\text{mL}$ (C), SMX 100 $\mu\text{g}/\text{mL}$ (D), and ASM 100 $\mu\text{g}/\text{mL}$ (E).

On day 7, four distinct *folP* mutations were observed: P64S, P64A, F28L, and Δ E68, but on day 10, only P64S and F28L mutations were observed in *folP* (Figure 5). Of note, all mutations observed across all treatments are located within either of loop 1 or 2 of the DHPS enzyme; regions that are both reported in the literature to confer SMX^R when harboring mutations (Appendix 3)^{94,148}. The most common mutations were at position P64, where mutations emerged at least once in every treatment group, as well as on both day 7 and 10 (Figure 5). The second most common *folP* mutation observed, F28L, was identified in 24 of the SMX 100 μ g/mL exposed isolates; 10 of which were from day 7, and the remaining 14 were from day 10. Another mutation uniquely observed in the SMX 100 μ g/mL treatment group was Δ E68, occurring within loop 2 of the DHPS enzyme (Appendix 3). Intriguingly, no *folP* mutations were observed in two isolates recovered from the ASM 100 μ g/mL treatment group on day 7, indicating that chromosomal mutations in genes aside from *folP* may be contributing to sulfa resistance in these isolates. Importantly, no mutations were found in the promoter region upstream of the *folP* open reading frame, which is consistent with there being no previous implication of differential *folP* expression in association with sulfa resistance.

3.3.2 ASM-selected SMX^R isolates are *pan*-sulfa resistance

To assess if ASM and SMX select for pan-sulfa-resistant *E. coli*, a subset of SMX-resistant colonies (14 isolates in total) were subjected to MIC determination using ASM, SMX, SAN, SDZ and the clinically important drug, co-trimoxazole (SXT). To confirm that the resistance observed is conferred by the *folP* mutations observed in these isolates, an *E. coli folP* deletion strain was trans complemented with WT or one of the four *folP* variants that emerged during the *in vitro* selection experiments (P64S, P64A, F28L and Δ E68)¹⁴³. The MICs of these constructs were determined with the same compounds as the ASM- and SMX-selected isolates and compared.

Table 6. Heat map of minimum inhibitory concentration (MIC) determinations for wild-type *E. coli* BW25113, $\Delta folP/pGDP2::folP$, and ASM- or SMX-selected *E. coli*. The form of DHPS enzyme present in each strain is indicated by WT or by the mutation present in the *folP* gene. All strains were tested with sulfamethoxazole (SMX), asulam (ASM), sulfanilamide (SAN), sulfadiazine (SDZ), and co-trimoxazole (SXT) with concentrations tested using the adapted agar dilution method ranging from 2 to 4096 $\mu\text{g/mL}$ for SMX, ASM, SAN, and SDZ. Sensitivity to SXT was assessed with an E-test strip.

<i>E. coli</i> Strain	MIC ($\mu\text{g/mL}$)				
	SMX	ASM	SAN	SDZ	SXT
BW25113	16	256	2048	32	0.064
$\Delta folP$ pGDP2:: <i>folP</i> _{Ec}	16	512	4096	32	0.094
$\Delta folP$ pGDP2:: <i>folP</i> _{P64S}	512	512	4096	64	0.094
$\Delta folP$ pGDP2:: <i>folP</i> _{P64A}	512	2048	4096	128	0.094
$\Delta folP$ pGDP2:: <i>folP</i> _{F28L}	512	1024	4096	128	0.190
$\Delta folP$ pGDP2:: <i>folP</i> _{$\Delta E68$}	1024	1024	4096	128	0.094
ASM100 ⁷ -1	1024	2048	4096	4096	0.125
ASM100 ⁷ -2	1024	2048	4096	512	0.125
ASM100 ⁷ -3	1024	1024	4096	1024	0.125
ASM100 ⁷ -4	1024	2048	4096	256	0.064
ASM100 ⁷ -5	1024	2048	4096	256	0.064
ASM100 ¹⁰ -1	1024	2048	4096	512	0.125
ASM100 ¹⁰ -2	1024	2048	4096	4096	0.190
SMX100 ⁷ -1	1024	1024	4096	128	0.064
SMX100 ⁷ -2	1024	1024	2048	128	0.094
SMX100 ⁷ -3	1024	1024	2048	128	0.094
SMX100 ¹⁰ -1	1024	2048	4096	256	0.094
SMX100 ¹⁰ -2	512	2048	4096	256	0.064
SMX10 ⁷ -1	1024	2048	4096	256	0.190
SMX10 ⁷ -2	1024	2048	4096	512	0.125
SMX10 ¹⁰ -1	1024	2048	4096	512	0.125
SMX10 ¹⁰ -2	1024	2048	4096	512	0.094

The MICs of *E. coli* varied across both strains and compounds tested. As expected, $\Delta folP$ strains harboring individual *folP* mutations (with a c-terminal FLAG-tag to monitor expression) encoding for divergent forms of *EcDHPS* on the low-copy number *E. coli* expression vector pGDP2 had higher MICs for all sulfa drugs tested compared to the wild-type, *E. coli* BW25113 (Table 6) (FLAG-tag expression of the trans complemented *folP* genes was confirmed by the western blot found in Appendix 1). Some of these *folP* mutations are known to encode sulfa-insensitive forms of DHPS (P64S, P64A, F28L), and notably, these strains also had increased an MIC for ASM, suggesting these SNPs may confer cross-resistance to ASM in addition to sulfa resistance (Table 6). The novel *folP* mutation $\Delta E68$ also demonstrated pan-sulfa resistance, but both SMX100⁷⁻³ and the trans-complemented $\Delta folP$ construct harboring the $\Delta E68$ mutation more susceptible compared to the other *folP* variants (Table 6). Of note, SMX- and ASM-selected *E. coli* isolates demonstrated higher MICs for both SMX and ASM compared to the parent strain of these isolates, *E. coli* BW25113 (Table 6). In fact, the SMX- and ASM-selected isolates were generally more resistant to all compounds tested compared to BW25113, but the variation in the MICs within this group was unexpected (Table 6). Amongst isolates collected on day 7 of ASM or SMX exposure at a concentration of 100 $\mu\text{g}/\text{mL}$, ASM-selected isolates demonstrated higher ASM and SMX resistance than SMX-selected isolates (Table 6). However, by day 10 both ASM and SMX-selected isolates had similar MICs for all drugs tested, suggesting resistance to SMX and ASM induced by SMX exposure increases over time, while ASM exposure yields higher resistance that emerges earlier compared to SMX-exposed *E. coli*, and this resistance was maintained over time in ASM-exposed *E. coli* (Table 6). The MICs for SDZ and SXT varied more than those of SMX, ASM, and SAN, with most ASM and SMX-selected isolates yielding higher resistance for these drugs compared to BW35113, with some notable exceptions. Two of the ASM-selected, SMX^R isolates were as susceptible to SXT as BW25113, and these isolates harbored wild-type DHPS enzymes (ASM100⁷⁻⁴, ASM100⁷⁻⁵).

3.3.3 ASM and SMX select for additional chromosomal mutations in *E. coli*

Plasmid-mediated expression of each *folP* variant in $\Delta folP$ conferred sulfa resistance, but the ASM- and SMX-selected SMX^R isolates demonstrated higher resistance levels (Table 6). The discrepancy in resistance observed amongst the SMX^R isolates and the trans-complemented *folP* mutants suggested the presence of other resistance determinants that could be found in the chromosome, prompting further investigation. Whole genome sequencing (WGS) was used to identify undetected genomic differences between the SMX^R isolates and the parent strain.

The total number of reads for each isolate and base quality scores are listed in Appendix 5. As a control measure, the chromosome of the in-house BW25113 strain was also sequenced and aligned with the reference genome in biological duplicate to ensure no unknown mutations were present in this strain. Intriguingly, it was revealed that several chromosomal differences were found in many of the ASM- and SMX-selected isolates (Table 7) (Figure 6). These include single nucleotide substitutions that promote amino acid substitutions in gene products, small insertions and deletions that promote frame-shift mutations (pseudogenes), as well as repeated occurrence of larger deletions in two distinct regions of the genome designated as either α or β , depending on their location on the chromosome.

Table 7. Unique genomic features observed in the ASM- and SMX-selected isolates. Single nucleotide polymorphisms (SNPs), deletions, and other mutations observed in each SMX^R isolate. Int indicates an affected intergenic region, nt indicates nucleotides, and genes encompassed in the α and β genesets are described in Appendix 4.

Strain ID	Classification of Genomic Feature				
	SNPs		Deletions		Other Mutations
	Gene	Nucleotide	Size of deletion (bp)	Gene/Geneset (α or β)	
ASM100 ⁷ -1	<i>folP</i>	G→A	14,885	β	Int(<i>ygbI</i>)T→C(<i>ygbJ</i>)
ASM100 ⁷ -2	<i>folP</i>	G→A	174	<i>deoC</i>	N/A
	<i>folM</i>	T→A			
ASM100 ⁷ -3	<i>folP</i>	C→G	N/A	N/A	Int(<i>ppc</i>)C→T(<i>argE</i>)
	<i>rpoC</i>	T→C			
	<i>rpoC</i>	G→C			
ASM100 ⁷ -4	<i>asnS</i>	(C→T)	27,697	α	N/A
	<i>icd</i>	(C→T) ^s			
	<i>icd</i>	(C→T) ^s			
ASM100 ⁷ -5	N/A	N/A	29,374	α	N/A
			174	<i>deoC</i>	
ASM100 ¹⁰ -1	<i>folP</i>	G→A	14,855	β	N/A
ASM100 ¹⁰ -2	<i>folP</i>	G→A	14,855	β	N/A
SMX100 ⁷ -1	<i>rhIE</i>	A→C	806	<i>deoB-deoD</i>	<i>folP</i> : Coding 202-204/849 nt
					Pseudogene
SMX100 ⁷ -2	<i>folP</i>	T→G	N/A	N/A	<i>deoB</i> : Coding 804/1224 nt
SMX100 ⁷ -3	<i>folP</i>	T→G	N/A	N/A	<i>deoB</i> : Coding 804/1224 nt
SMX100 ¹⁰ -1	<i>folP</i>	T→G	15,091	α	<i>deoB</i> : Coding 804/1224 nt
SMX100 ¹⁰ -2	<i>folp</i>	T→G	15,091	α	<i>deoB</i> : Coding 804/1224 nt
SMX10 ⁷ -1	<i>folP</i>	C→T	N/A	N/A	N/A
	<i>purT</i>	T→G			
SMX10 ⁷ -2	<i>folP</i>	C→T	N/A	N/A	N/A
	<i>spoT</i>	T→C			
SMX10 ¹⁰ -1	<i>folP</i>	C→T	N/A	N/A	N/A
	<i>rplF</i>	A→G			
	<i>spoT</i>	A→G			
SMX10 ¹⁰ -2	<i>folP</i>	C→T	N/A	N/A	N/A
	<i>gyrA</i>	G→T			

^s denotes a synonymous mutation

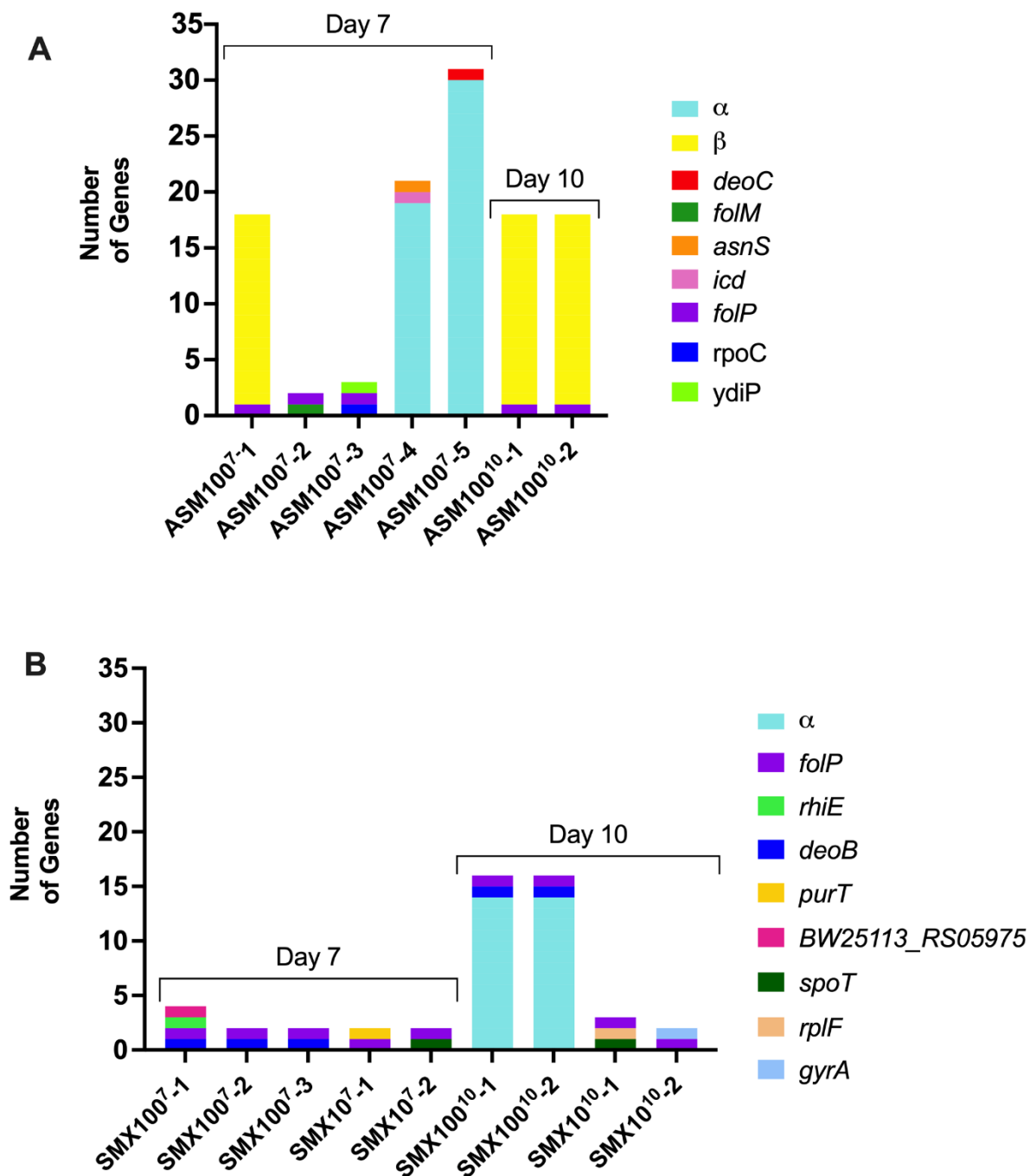


Figure 6. Genomic variance observed in the SMX^R (A) ASM-selected and (B) SMX-selected isolates collected from Day 7 or Day 10 as indicated above the bars. Each uniquely coloured bar above the isolate name identified on the x-axis represents a gene that was deleted or mutated compared to the wild-type as indicated in the legend, and the total number of genes is listed on the y-axis. Each gene included in the α or β gene sets as described in Appendix 4 is represented by a cyan or yellow bar as labelled.

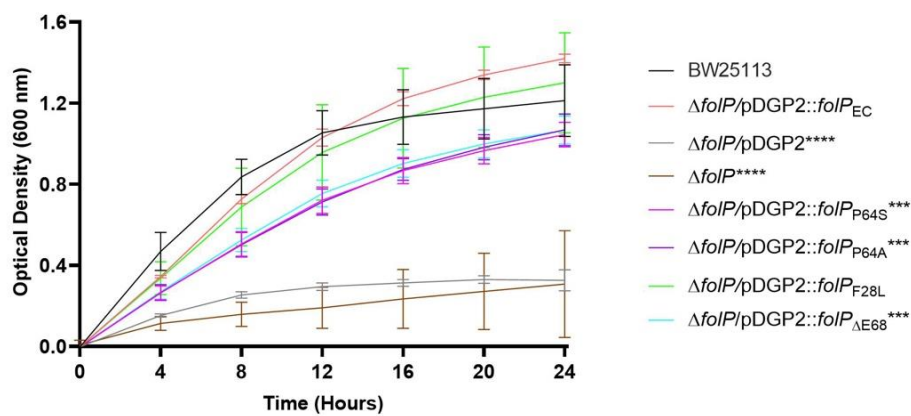
The whole-genome sequencing confirmed the presence of the *folP* mutations previously identified by Sanger sequencing, but many other genes, intergenic regions, and pseudogenes in the SMX^R isolates were also found to have acquired mutations and deletions compared to the wild type. Among the SMX 10 µg/mL exposed isolates, many SNPs occurred in genes involved in DNA and/or RNA related processes such as *spoT*, *gyrA*, *purT*, *rhlE*, and *rpIF* were present (Table 7). These genes were not mutated in any of the SMX 100 µg/mL exposed SMX^R isolates, but mutations in the deo operon (*deoC*, *deoB*, *deoD*) involved in nucleotide salvage were observed in many isolates in this group. Aside from *folP*, there was little overlap concerning the mutated genes of ASM- and SMX-selected isolates, however trends emerged with large deletions of the α or β genes (Table 7, Figure 6)

The most notable mutations observed in the ASM- and SMX-selected isolates were large deletions of genes encompassing 14,855 – 29,374 bp of either α or β gene set (Appendix 4). Deletions in the α gene set were observed in two ASM-selected isolates (ASM100⁷-4 and ASM100⁷-5), and in two SMX-selected isolates (SMX100¹⁰-1 and SMX100¹⁰-2) (Figure 7). ASM exposure was executed at a sublethal concentration of 100 µg/mL, and while no SMX^R isolates with α or β deletions were found in isolates exposed to a sublethal concentration of SMX (10 µg/mL), SMX exposure at 100 µg/mL did, which is substantially higher than the MIC of the parent strain (16 µg/mL).

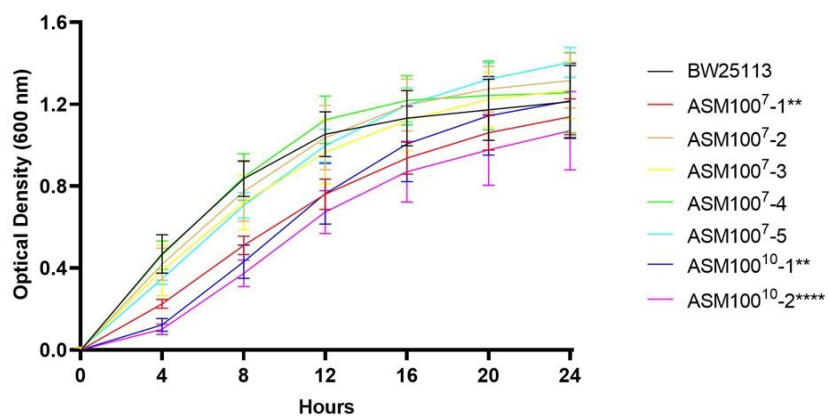
3.3.4 Most SMX^R isolates do not exhibit growth deficiency *in vitro*

To assess if mutations observed in the ASM- or SMX-selected SMX^R isolates, the growth rate of each selected isolate was assessed in MHII, media lacking any sulfa-antagonists (e.g., thymidine or folinic acid)

A



B



C

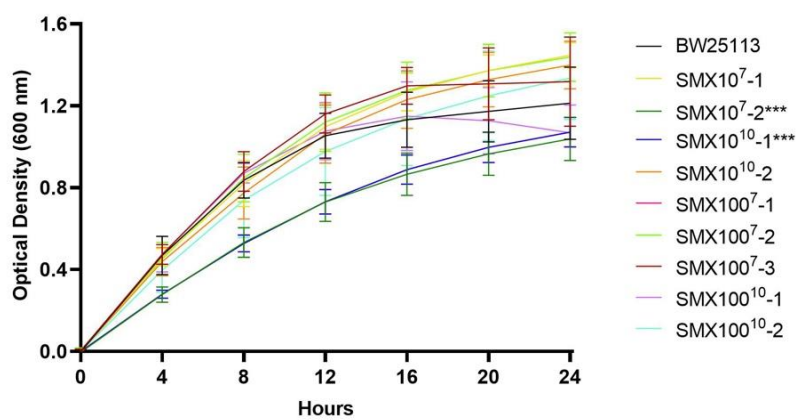


Figure 7. Growth curves for *E. coli* (A) $\Delta folP$ expressing *folP* mutations on the pDGP2 expression plasmid, (B) ASM-selected SMX^R isolates, and (C) SMX-selected isolates, with the *E. coli* BW25113 (WT) (A, B, C) for comparison. Data represents the mean OD₆₀₀ for every 4 hours of growth recorded from three independent experiments performed in technical triplicate for each strain tested. The optical densities of each strain at 600 nm were baseline-corrected by subtracting the OD₆₀₀ of uninoculated MHII media. Asterisks next strains listed in the legend represent the statistical significance determined by unpaired t-tests.

Out of the four subcloned *folP* mutants, three (P64S, P64A, and $\Delta E68$) demonstrated significantly lower growth rates compared to $\Delta folP/pDGP2 :: folP_{Ec}$ (unpaired t-test, $P= 0.0002$, 0.0002 and 0.0006 , respectively) (Figure 7). The growth of $\Delta folP/pDGP2::folP_{Ec}$ was not significantly different from that of the parent strain of the SMX^R subcloned mutants, *E. coli* BW25113 (Figure 7), confirming the subcloned *folP*_{Ec} did not confer a fitness cost compared to chromosomally expressed *folP* in wild type *E. coli* BW25113. Since $\Delta folP$ and $\Delta folP/pDGP2$ harboring the empty pDGP2 expression plasmid are thymine auxotrophic, it was unsurprising that these strains demonstrated significantly reduced growth compared to the wild type in MHII-broth, a thymine-limited medium ($P= <0.0001$ for both strains) (Figure 7)¹⁴³.

Amongst the ASM-selected isolates, only one isolate from day 7 of ASM exposure, ASM100⁷-1, had significantly reduced growth, ($P=0.0016$) (Figure 7). Both isolates from day 10 of ASM exposure had significantly reduced growth (ASM100¹⁰-1, $P=0.0008$); and ASM100¹⁰-2 ($p=<0.0001$)), suggesting long-term ASM exposure has fitness consequences for bacterial growth. SMX-selected isolates SMX100⁷-1 ($P=<0.0001$), SMX10⁷-1 ($P=<0.0001$), SMX10⁷-2 ($P=<0.0001$) also demonstrated reduced growth compared to wild type (Figure 8). While SMX100⁷-1 was less fit than the wild-type, the growth of this strain with its corresponding $\Delta folP$ mutant strain, $\Delta folP/pGDP2::folP_{\Delta E68}$ growth was consistent with SMX100⁷-1 (Figure 7). Of the isolates that were identified as harboring a large deletion in the chromosome, those with deletions in the β gene set had impeded growth compared to the wild type. Therefore, deletions observed in the β gene set appear to have a fitness cost.

3.4 ASM influences the transfer of the *sul* genes in a simulated microbial community at a comparable rate to SMX

Since the *sul* genes conferred resistance to ASM and SMX, and these compounds selected for SMX^R *E. coli in vitro*, the potential of these compounds to promote the dissemination of the *sul* genes in a simulated microbial soil community was assessed using conjugation experiments with a GFP-tagged *E. coli* strain and bacteria isolated from swine manure. Neither SMX nor ASM had a significant effect on the transfer of the *sul* genes from native soil microbes to *E. coli* CV601. Treatments from 1-100 mg/mL of SMX or ASM did not increase the emergence of SMX-resistant *E. coli* CV601 compared to the resistance frequency observed in the no drug treatment control (Figure 8)

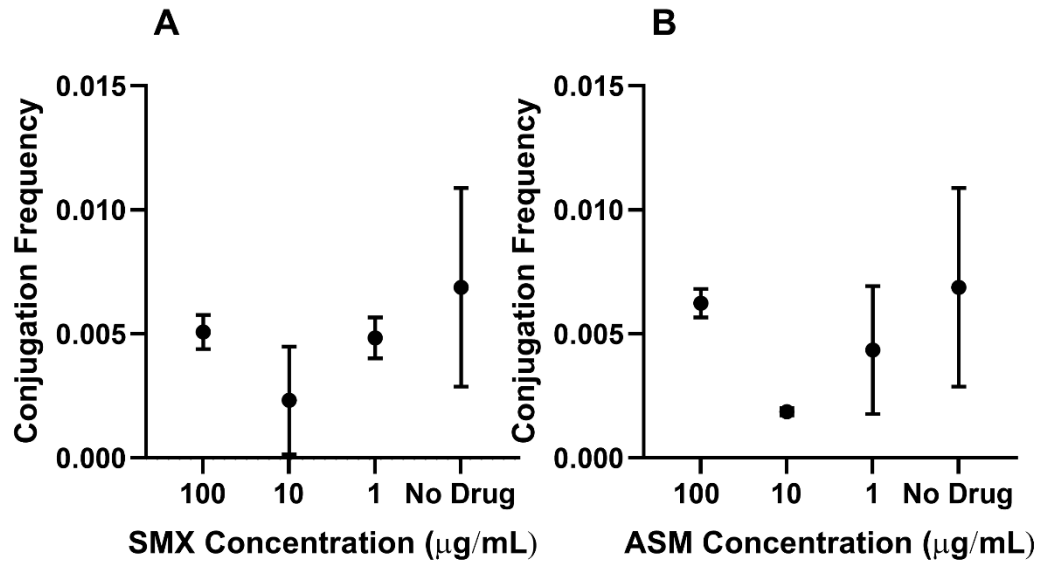


Figure 8. Conjugation frequency of CV601 as the recipients of the *sul* genes from native soil bacteria when exposed to SMX or ASM at the indicated concentrations compared to no drug. Symbols indicate the mean conjugation frequency of two independent experiments, with error bars representing SEM.

Chapter 4 Discussion

4.1 ASM can exert antibiotic action against *E. coli* comparable to some sulfas

The unknown long-term effects of ASM on environmental soil communities was cited as a concern in the risk assessment conducted by the European food safety authority for ASM use in commercial crops¹²⁹. The most alarming consequence of ASM entering the food chain is the threat to human health if ASM can promote the emergence of antibiotic resistant bacteria.^{10,11,149} Many agrichemicals used as biocontrol agents (e.g., pesticides and herbicides) such as glyphosate, dicamba, metolachlor, linuron, atrazine, can promote antibiotic resistance and influence the susceptibility of bacteria to some antibiotics^{5-9,75,150,151}. In this study, it was revealed that the herbicide ASM inhibited the growth of *E. coli* more effectively than the prototypical sulfa drug, SAN, but was a less potent than SMX. SMX and SAN contamination can enrich environments for ARGs and increases the prevalence of antibiotic resistant bacteria in the environment^{125,152-155}. Sulfa-selected bacteria often harbor sulfa-insensitive DHPS enzymes, and the herbicidal action of ASM is attributed to the inhibition of HPPK/DHPS in plants^{50,120,133}. Therefore, it was inferred that if ASM's antibiotic action is the result of bacterial DHPS enzyme inhibition as observed in sulfas, ASM may have the potential to similarly select for sulfa insensitive DHPS enzymes in bacteria.

4.1.1 ASM likely exerts antibiotic action via DHPS inhibition

After MIC determinations demonstrated that ASM susceptibility of *E. coli* was contingent on the DHPS status of each strain tested, ITC experiments confirmed that ASM binds with *Ec*DHPS. ASM exhibited a lower binding affinity (K_a) with *Ec*DHPS compared to SMX, which is reflected in the potency of these drugs. Of note, the ASM degradation product ASMG also demonstrated a higher MICs amongst *E. coli* strains harboring sulfa insensitive DHPS enzymes but was not tested using ITC due to the scarcity of this compound.

4.2 ASM selects for SMX^R *E. coli* at concentrations exceeding environmental relevance

The knowledge gap in information regarding ASM's effect on microbial communities stated by the European Food Safety Authority exposes many unknowns regarding the consequences of ASM to the long-term health of organisms. The mobilization of ARB to humans by the food supply chain is a concern for human health if these ARB can exploit a pathogenic lifestyle in humans^{10,39}. If soil is enriched for ARB by an agrichemical like ASM, it increases the likelihood that antibiotic resistance determinants will be found amongst the bacteria that reside in soil^{4,44,75}. With more ARB in soil, the risk that antibiotic resistant pathogen amongst these bacteria may reach the human population is subsequently increased^{10,39}. Therefore, elucidating if herbicides like ASM are contributing to an increase in ARB and appropriately managing their use can help preserve the effectiveness of current antibiotics by preventing enriching for ARB in crop soils. The results of this study have shown that ASM exerts antibiotic action but does not select for ARB at environmentally relevant concentrations. These results suggest that of bacterial communities in crop soil are unlikely to be enriched for ARB by standard ASM application. Therefore, it is improbable that ASM use in food crops will significantly exacerbate the prevalence of ARB human pathogens.
10,156

4.2.1 Soil microcosms for the improvement of recapitulating soil communities in directed evolution experiments

A major obstacle in researching environmental bacterial communities is that accurately recapitulating the conditions found in the environment in the laboratory that supports the growth of all native microbes has proven to be a challenging obstacle for environmental microbiologists^{157,158}. Therefore, directed evolution experiments were executed in liquid media for a range-finding experiment to determine what, if any, concentration of ASM could select for SMX^R *E. coli*. These experiments determined that among the range of concentrations tested, 100 µg/mL, the highest concentration tested, was the only ASM treatment that selected

for SMX^R *E. coli*. This observation is consistent with a previous study that demonstrated the minimum concentration of ASM required to inhibit growth in pea plants was 50 µg/mL¹³⁴. A follow-up study repeating the directed evolution experiments with concentrations of ASM from 50 – 100 µg/mL could elucidate the minimum selection concentration of ASM on *E. coli in vitro*¹³⁴. Additionally, repeating directed evolution experiments in soil microcosms would more accurately recapitulate the typical conditions in which ASM is applied¹⁵⁹. Soil microcosms may also provide more information on how ASM disseminates throughout the soil, and how microbes residing at different soil depths may be exposed to different concentrations of ASM. The complex matrix of soil has many more variables that influence microbial growth and depending on the rate of ASM degradation in soil, the conditions in which the soil is maintained (i.e., moisture level, type of soil used, presence of plants, exposure to sunlight, temperature of incubation, etc.) can all have consequences for microbes¹⁵⁹. Soil microcosms can provide a more holistic view of how environmental conditions can alter how bacterial communities respond to stressors like ASM exposure, and thus respond differently than the bacteria grown in this study, which were grown in a shaking culture in consistent conditions (37°C, grown in MHII)^{4,159}.

4.2.2. Concentrations of ASM that select for sulfa-resistance are not found in the environment

The emergence of both ASM- and SMX-selected SMX^R isolates was not only concentration dependent, but also time dependent. No SMX^R colonies were observed until day 7 of ASM or SMX exposure, and both treatments had an increase in resistance frequency observed by day 10. Although these results are intriguing, the concentration of ASM that yielded SMX^R is well above the predicted environmental concentrations (PEC) for ASM in both surface water and sediment. The experimental concentration of ASM that selected for SMX^R was 100 µg/mL, which is equivalent to 100 000 µg/L, which is significantly higher than the maximum PEC of ASM when applied at a standard rate of 2400 g/ha (795 µg/L). If ASM is

appropriately applied, it is unlikely a concentration of ASM that can select for SMX^R bacteria will accumulate in the environment. ¹²⁹..

One discrepancy with the directed evolution assays is that there was no quantification of ASM over the course of the experiment or assessment, nor was the rate of ASM degradation determined. If this experiment were to be repeated, the degradation of ASM into its degradation products could be assessed over the progression of the directed evolution experiments using liquid chromatography mass-spectrometry¹³⁵. This would confirm that ASM is maintaining a concentration consistent with what is assumed to be present during the directed evolution assays.

4.2.3 ASM selects for *folP* mutations known to confer sulfa resistance in *E. coli*

Sulfa resistance has been attributed to *folP* mutations in many bacterial species such as *Streptococcus mutans*, *Neisseria meningitidis*, and *E. coli*^{120–122}. To determine if ASM and its action on the *EcDHPS* enzyme resulted in *folP* mutations in *E. coli*, the *folP* gene of ASM-selected was sequenced and screened for mutations. In ASM-selected isolates, all *folP* mutations observed (P64S, P64A) have been previously reported as sulfa-resistance determinants¹²². All *folP* mutations found in the SMX-selected isolates were previously reported in the literature as well, except for $\Delta E68$, which likely confers resistance by altering the binding site in loop 2 of the DHPS enzyme (Appendix 3).

To confirm that the DHPS variants observed confer ASM and SMX resistance, ITC studies could be performed using purified variant *EcDHPS* proteins. The ITC studies demonstrated that SMX had a higher K_d compared to previous investigations with *Bacillus anthracis* DHPS, which is consistent with SMX acting as a competitive inhibitor of *pABA*⁸⁷. In contrast, ASM had a lower K_d compared to these same observations with *pABA*, consistent with this compound being a less

effective antibiotic⁸⁷. By using the established binding affinities of ASM and SMX, a control with *pABA* could be employed to further support the observations in this study. While additional ITC studies could support the findings here and potentially offer additional insight into the action of the degradation products, and variant DHPS enzymes, a barrier to pursuing further ITC studies with *EcDHPS* is the formation of a white powdered substance in the ITC equipment following experiments. This substance remained insoluble despite cleaning with water and methanol, which impedes the usage of this equipment. The formation of the precipitate was observed to exclusively occur when DMSO was added to the final protein sample, so if different solvents could be employed, this issue could possibly be resolved. Alternatively, the examination of DHPS inhibition by ASM could be assessed by employing the continuous spectrophotometric assay developed by Valderas *et al.*, which monitors the depletion of reduced nicotinamide adenine dinucleotide phosphate (NADPH) as it is utilized in enzyme binding to determine DHPS inhibition⁷⁸.

Interestingly, the level of pan-sulfa resistance conferred by each *folP* mutation in the ASM- and SMX-selected SMX^R was not consistent with the same *folP* mutations trans-complemented on a plasmid expression vector. In addition, two ASM-selected SMX^R isolates had no *folP* mutations present. These results suggested that other determinants of resistance may be present in the genome and triggered an investigation into genomic changes outside the *folP* gene that could influence resistance using whole genome sequencing (WGS).

4.2.2 ASM- and SMX-selected SMX^R *E. coli* harbor unique genomic changes

The resulting genome sequencing data from the SMX^R isolates revealed that both ASM and SMX-selected SMX^R isolates had undergone genomic changes outside of the *folP* gene, with large deletions of genes up to nearly 30 000 bp in size being most notable (genes deleted and their chromosomal positions are described in

Appendix 4). Two types of deletion (α and β) were found in ASM-selected isolates, while only α deletions were observed in some SMX-selected isolates, and only emerged on day 10. In growth curve assays, isolates with β deletions exhibited significantly slower growth rates compared to the parent strain, BW25113. Conversely, isolates with α deletions did not exhibit the same growth constraint despite the larger size of the α deletions. Amongst the SMX^R isolates harboring large deletions, all isolates with β deletions also had *folP*_{P64S} mutations as well, as did the isolates with α deletions from the SMX day 10. The two SMX^R isolates that did not have *folP* mutations were uniquely from day 7 of ASM treatment indicating this may not be a stable evolutionary strategy for *E. coli* to maintain in the long-term. None of the genes observed in the large deletions have been shown to be directly implicated in sulfa-resistance, but a knockout library could be created by constructing individual deletion strains for each gene from the α and β gene region, which can be MIC tested for sulfa-resistance. If any one of these deletion strains demonstrates resistance, those genes can be further investigated for their involvement in conferring sulfa-resistance. One possible explanation for the large deletions is that bacteria can circumvent antibiotic killing via metabolic changes. Slower metabolism results in fewer opportunities for antibiotics to exert their action by reducing abundance of antibiotic targets in the cell and minimizing the utilization of targeted pathways⁵³. Sustaining the normal DNA replication rate in bacteria is dependent on functioning folate metabolism. Therefore, a deficit of tetrahydrofolate in the cell due to ASM/SMX interference in the *de novo* folate pathway may create an environment wherein a slower replication rate is advantageous. Cellular replication relies on DNA stability, which is mediated by folate derivatives via two mechanisms (Figure 9).

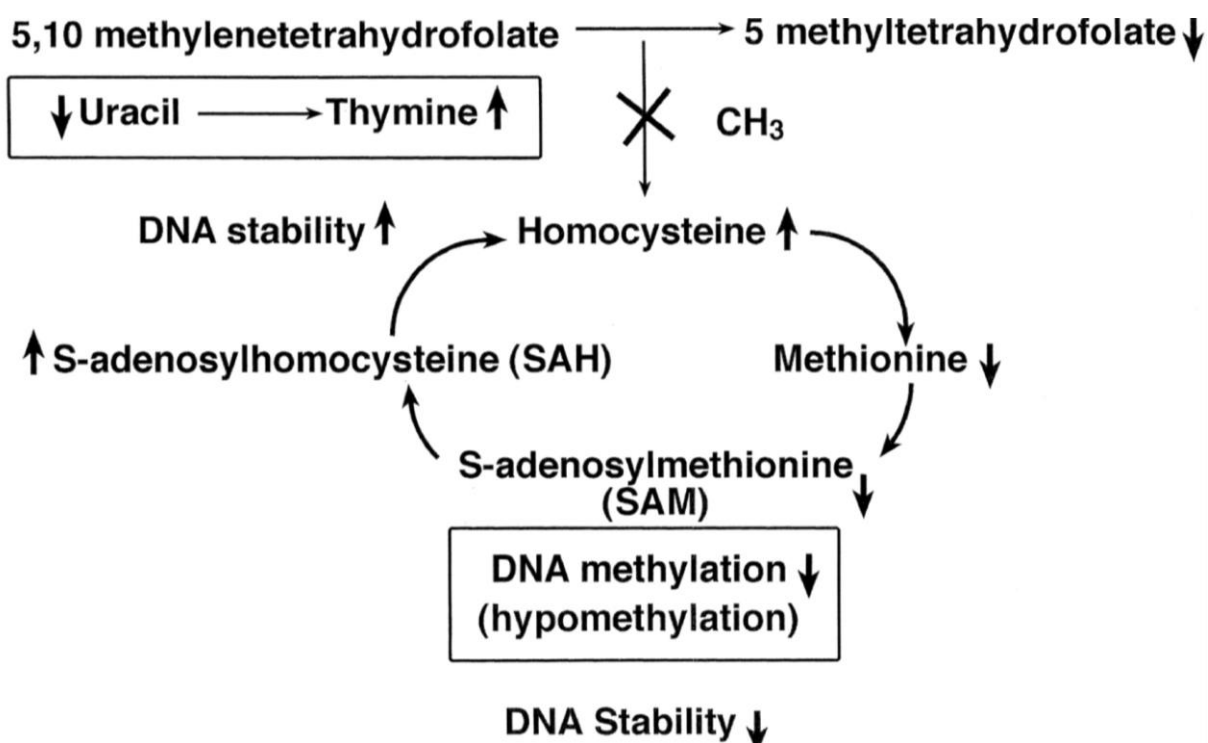


Figure 9. DNA stability regulatory mechanisms dependent on folate derivatives 5,10 methylenetetrahydrofolate and 5 methyltetrahydrofolate adapted from Duthie *et al.*, 2002¹⁶⁰. X denotes the interruption of methyl group donation

One of these mechanisms is the regulation of cytosine in gene transcription in DNA, which is controlled by S-adenosylmethionine (SAM) methylation^{160,161}. SAM production is mediated by homocysteine remethylating methionine, with 5-methyltetrahydrofolate acting as the methyl donor^{160,161}. If folate is depleted, intracellular SAM is also depleted, resulting in hypomethylation of DNA and disruptions in tRNA and rRNA methylation¹⁶⁰⁻¹⁶². Another folate-dependent DNA regulation mechanism is the donation of a methyl group to uracil by 5,10-Methylenetetrahydrofolate, which converts uracil to thymine¹⁶⁰. The thymine produced through this mechanism is essential for DNA synthesis and repair, but without folate to convert uracil, this can result in uracil misincorporation into DNA^{160,162}. If DNA repair is initiated to excise the mis incorporated uracil from the DNA molecule, and there is a deficit of deoxynucleotide triphosphates available due to an ongoing folate deficiency, a catastrophic and futile break and repair cycle can occur, which is a hallmark of TLD^{160,163}. Genomic instability caused by uracil misincorporation may lead to chromosomal damage like the large deletions observed in this study. Sublethal concentrations of SMX did not induce the formation of large deletions, however ASM at a sublethal concentration did, suggesting ASM may be more effective in disrupting bacterial DNA and/or RNA synthesis and/or metabolism than SMX. There are several limitations to making conclusions regarding the exact cause of the α and β deletions, including the lack of sequencing data from the no drug and drug vehicle controls tested in the directed evolution experiments. Since no SMX^R isolates were observed, no isolates were collected for sequencing, and therefore it cannot be confirmed that no mutations were observed in the no drug or vehicle control groups. If there are no mutations in these groups, the large deletions can be attributed to drug exposure. This phenomenon of large deletions could be also further investigated using bisulphite genomic sequencing to quantify DNA methylation in these isolates, and transcriptome sequencing (RNA-seq) to elucidate how the RNA and protein synthesis is affected by SMX and ASM, or if the large deletions in the DNA have downstream consequences for RNA and protein synthesis^{164,165}.

Other trends in genomic changes were observed in the ASM- and SMX-selected SMX^R isolates. Many of the mutations observed in the SMX^R isolates were in genes associated with function of DNA and RNA, such as *spoT*, *gyrA*, *purT*, *rpoC*, and *rhIE*^{166–173}. These results support the notion that sulfa resistance may be mediated by alterations to DNA/RNA associated processes. Deletions from 1-806 bp were observed in *deoB*, *deoC*, and *deoD* in both SMX- and ASM-selected isolates. The *thyA* gene and *deo* operon function is highly intertwined, and previous studies have shown *E. coli* lacking *deoB*, *thyA*, and *deoC* can survive on low levels of thymine compared to WT, further suggesting metabolic adaptations to impaired folate synthesis and usage are likely contributing to ASM/SMX resistance^{112,174,175}. The growth curve assays demonstrated that trans complementation of the *E. coli* Δ *folP* mutations can have a fitness cost, but most SMX^R isolates with *folP* mutations did not exhibit impeded growth. This indicates that the additional mutations observed in SMX^R isolates are likely compensatory adaptations to the fitness cost produced by *folP* mutations.

4.3 ASM does not increase the frequency of sulfa resistance conferred by mobilized *sul* genes in a simulated microbial community

Horticultural researchers have successfully developed ASM-resistant transgenic plants using *Enterobacteriaceae* R plasmids encoding for a *sul* gene in several species, including Arabidopsis, potatoes, and peas^{133,176–178}. These transgenic plants were developed after it was revealed that the *sul* gene confers ASM resistance, and therefore, ASM can be applied as a foliar selection method for transgenic plants.^{176,178} Since *sul* confers ASM resistance in plants, it was hypothesized that bacteria in a simulated community would disseminate the *sul* gene via conjugation more readily and rapidly under ASM exposure. As mentioned, recapitulating environmental conditions in the laboratory is a task that continues to challenge environmental microbiologists^{157,158,179}. Due to the complexity of designing an experiment that controls all variables found in the natural

environment, the conjugation experiments were simplified to avoid confounding variables. These experiments could be improved by using soil microcosms for similar reasons described above for making the directed evolution experiments more relevant to environmental conditions¹⁵⁹. Although successful matings did occur with *E. coli* CV601 acquiring plasmid-borne *sul* genes in the presence of ASM, the presence of up to 100 µg/mL of ASM did not result in a higher frequency of SMX^R *E. coli* compared to the no drug control. The frequency of SMX^R *E. coli* CV601 was similar in the presence or absence of ASM, as was the case for SMX. A major limitation to this study is the lack of quantification of donor cells present. The number of donors could be quantified using quantitative PCR (qPCR) with sequence specific primers for the *sul* genes to quantify the number of copies of each *sul* gene that could be mobilized to the recipient cells.

In bacterial communities, competition for limited resources can drive evolution^{180,181}. Soil bacteria are the source of many antibacterial products, with the potential function to eliminate competing species co-existing in the same environment^{182,183}. However, sulfa compounds are rarely produced by organisms, and sulfas are considered a synthetic contaminant in the environment, meaning it is unlikely that the SMX resistance in the no drug control can be attributed to sulfa production by the bacteria collected from the manure sample^{184,185}. A much more likely scenario is that under when co-incubated with other species, *E. coli* adapts as observed in other studies to a higher cell density via metabolic changes that can result in acquired antibiotic tolerance^{186–191}. The growth rate of these isolates was not measured, but growth curves could be employed to determine if these bacteria are less metabolically active¹⁹². There may also be other determinants of resistance present as observed in the SMX^R isolates collected from the *in vitro* selection experiments. The MICs of these collected isolates could be determined and compared to an *E. coli* CV601 construct harboring a *sul* gene to assess the level of resistance as was conducted in this study for the SMX^R isolates from the directed evolution experiments. If there are discrepancies in the level of resistance between the transconjugants and an *E. coli* CV601 construct harboring a *sul* gene,

WGS could detect other possible genomic determinants of resistance, and elucidate if the SMX-resistance in the no drug control isolates with no *sul* gene is conferred by a genomic change. Although the conjugation assays performed in this study are preliminary, they revealed that SMX resistance can be induced in the absence of drug by co-incubating *E. coli* with environmental bacteria. If SMX-resistance can be induced in the absence of a drug selection pressure.

4.4 Future Directions

This study demonstrated that ASM can influence bacteria in unexpected ways, further emphasizing the need to assess the long-term consequences to microorganisms residing in environmental compartments contaminated with ASM¹²⁹. For all experiments performed in this study, repetition with a representative Gram-positive bacterial species (e.g., *Bacillus subtilis* or *Staphylococcus aureus*) would provide insight into how Gram-positive pathogens that occupy environmental compartments may respond to ASM exposure.

Follow-up studies into the large deletions can be performed using many tools, including bisulfite whole genome sequencing to assess if DNA methylation is occurring. Transcriptomics, proteomics, and metabolomics can further characterize these isolates and provide more insight into mechanisms of resistance by further defining how ASM interferes with genetic replication. Another limitation that could be addressed in future studies would be the confirmation of folate starvation contributing to resistance by adding a control treatment with folic acid or *pABA* supplementation. Supplementation with either folic acid or *pABA* to carrot cultures treated with ASM can reverse ASM-induced growth inhibition¹⁹³. Therefore, repeating experiments with a *pABA* or folic acid supplemented control group could demonstrate the reversal of ASM killing in bacteria, which would further confirm that ASM's antibiotic action lies in inhibiting bacterial DHPS.

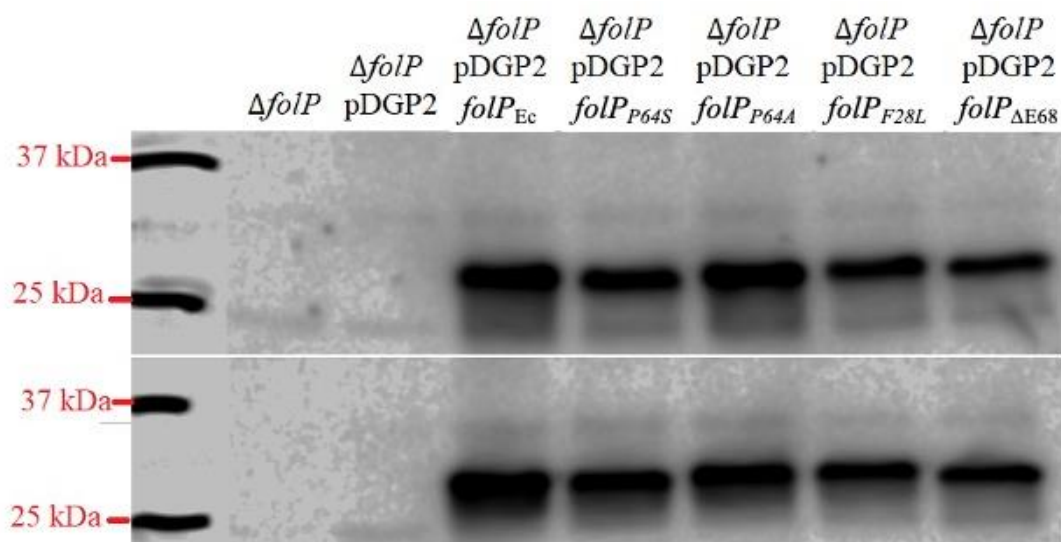
Another approach that could improve the relevancy of the experiments performed in this study would be to develop soil-based systems of growth to better reflect the natural conditions these microbial communities typically grow in. Soil microcosms are a viable tool for repeating the directed evolution experiments and conjugation experiments to improve the relevance of these experiments to agricultural systems.

If ITC experiments could be repeated, isolating DHPS protein from *folP* variants or *sul* genes would provide more insight into how ASM is interacting with variant forms of DHPS and confirm if the bacterial mechanism of ASM resistance. Other compounds such as ASM's degradation products could also be tested if these compounds were able to be synthesized in large enough amounts to execute these experiments.

4.5 Conclusion

In conclusion, it was determined that ASM, along with its degradation products SAN and ASMG exert antimicrobial activity, with drug/protein binding kinetic evidence that this action is at least partially attributed to DHPS enzyme inhibition. It was also determined that ASM, but not its degradation products, can select for SMX^R *E. coli in vitro* at concentrations exceeding the PEC of ASM. The ability of ASM to promote the dissemination of *sul* gene mediated SMX^R in a simulated microbial community could not be fully elucidated as the control group demonstrated SMX^R without the presence of the *sul* gene. However, preliminary results suggest that the *sul* genes were disseminated amongst the recipient bacteria under ASM-exposure. Overall, the data in this study are insufficient to make recommendations regarding the use of ASM but suggests that ASM has negligible effects on the promotion of ARB at environmentally relevant concentrations under laboratory conditions.

Appendices

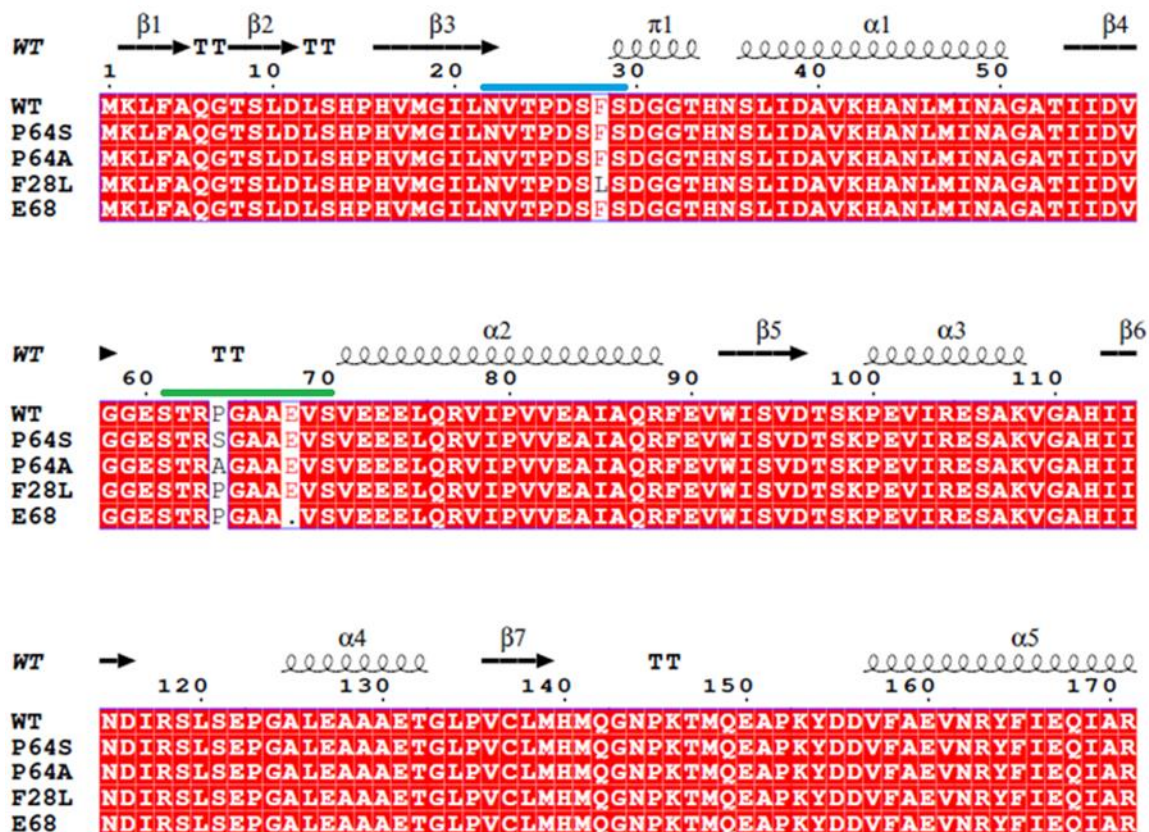


Appendix 1. Production of DHPS protein in *E. coli* trans-complemented *folP* variants with a BioRad Dual Colour Precision Plus Protein Standard indicating the approximate protein size

Appendix 2. Chemical analysis of the swine manure sample sourced from a Southern Ontario swine farm used in the conjugation experiments

Chemical Analysis of Swine Manure Sample 33363

Sulfur	785.1	ppm
Dry Matter	6.3	%
Total N	0.616	%
NH ₄ -N	3998	ppm
Total P	0.2457	%
Phosphate (P ₂ O ₅)	0.5651	%
Total K	0.3651	%
Potash (K as K ₂ O)	0.4381	%
Organic Matter	4.3	%
C:N Ratio	4:01	
Sodium	0.14	%
Aluminum	33.2	ppm
Boron	2.5	ppm
Calcium	0.1954	%
Copper	84.9	ppm
Iron	160.9	ppm
Magnesium	0.1562	ppm
Manganese	42.1	ppm
Zinc	103.5	ppm
pH	7.76	



Appendix 3. Amino acid sequences of the Wild type (WT) EcDHPS, aligned to the following mutants: P64S, P64A, F28L, Δ E68; protein topology of DHPS is indicated above the aligned sequences, α -helices and β -helices are displayed as squiggles, β -strands are rendered as arrows, and strict β -turns as TT letters, with loop 1 and 2 of the DHPS enzyme indicated by a blue (loop 1) or green (loop 2) line above the relevant residues (image generated by EndScript¹³³) **(B)** Mutations in the *folP* gene identified by sequence analysis of *E. coli* isolates exposed to ASM or SMX treatments at the indicated concentration ($\mu\text{g}/\text{mL}$), or by the day collected (7 or 10)

Appendix 4. Genes deleted in the designated α (chromosome position 812,270 – 1,686,588) and β (2,412,100 – 2,427,009) gene sets in select SMX^R isolates collected from the directed evolution experiments

Gene Set Identified in ASM- or SMX-selected SMX^R <i>E. coli</i>	
α	β
Genes Deleted	
Genes Deleted	Genes Deleted
<p><i>rstA, ydgC, folM, ydgl, ydgH, tqsa, mdtJ, mdtI, ydgD, asr, ynfM, ynfL, mlc, clcB, ynfF, ynfE, ynfD, ynfC, speG, ynfB, ynfA, rspA, rspB, rstB, tus, pntB, pntA, fumC, dmsB, bioD</i></p>	<p><i>yfbU, ackA, yfbV, pta, yfcC, yfcD, yfcE, yfcF, yfcG, folX, yfcH, rpnB, hisP, hisM, hisQ, argT</i></p>

Appendix 5. Whole Genome Sequencing Statistics provided by the Microbial Genome Sequencing Center

Isolate Name	Total Read Pairs	Total Reads	Total bp > Q30	% bp > Q30
ASM100 ⁷ -1	1734020	3468040	480491348	93.444
ASM100 ⁷ -2	1326260	2652520	367034861	93.236
ASM100 ⁷ -3	1404330	2808660	387830871	93.138
ASM100 ⁷ -4	1753182	3506364	485359658	93.23
ASM100 ⁷ -5	1376198	2752396	3.8E+08	93.008
ASM100 ¹⁰ -1	1460488	2920976	4E+08	93.088
ASM100 ¹⁰ -2	798347	1596694	2.2E+08	92.753
SMX100 ⁷ -1	1674745	3349490	450442993	93.194
SMX100 ⁷ -2	1768808	3537616	490168681	93.251
SMX100 ⁷ -3	1622043	3244086	449308642	93.287
SMX100 ¹⁰ -1	1329634	2659268	367119246	93.054
SMX100 ¹⁰ -2	1454719	2909438	403341730	93.183
SMX10 ⁷ -1	1415887	2831774	389878806	92.853
SMX10 ⁷ -2	1135550	2271100	301573883	88.871
SMX10 ¹⁰ -1	1331983	2663966	366672364	93.382
SMX10 ¹⁰ -2	1451931	2903862	401520531	93.02

References

1. Chang Id, Y. *et al.* Clinical pattern of antibiotic overuse and misuse in primary healthcare hospitals in the southwest of China. (2019) doi:10.1371/journal.pone.0214779.
2. Mauldin, P. D., Salgado, C. D., Hansen, I. S., Durup, D. T. & Bosso, J. A. Attributable hospital cost and length of stay associated with health care-associated infections caused by antibiotic-resistant gram-negative bacteria. *Antimicrobial Agents and Chemotherapy* **54**, 109–115 (2010).
3. Sabuncu, E. *et al.* Significant Reduction of Antibiotic Use in the Community after a Nationwide Campaign in France, 2002-2007. doi:10.1371/journal.pmed.1000084.
4. Liao, H. *et al.* Herbicide Selection Promotes Antibiotic Resistance in Soil Microbiomes. doi:10.1093/molbev/msab029.
5. Kurenbach, B. *et al.* *Herbicide ingredients change Salmonella enterica sv. Typhimurium and Escherichia coli antibiotic tolerances.*
6. Barbosa da Costa, N. *et al.* A Glyphosate-Based Herbicide Cross-Selects for Antibiotic Resistance Genes in Bacterioplankton Communities. *mSystems* **7**, (2022).
7. Xing, Y., Wu, S. & Men, Y. Exposure to Environmental Levels of Pesticides Stimulates and Diversifies Evolution in *Escherichia coli* toward Higher Antibiotic Resistance. *Cite This: Environ. Sci. Technol* **54**, (2020).
8. Curutiu, C., Lazar, V. & Chifiriuc, M. C. Pesticides and antimicrobial resistance: from environmental compartments to animal and human infections. *New Pesticides and Soil Sensors* 373–392 (2017) doi:10.1016/B978-0-12-804299-1.00011-4.

9. Kirubakaran, R., Murugan, A., Shameem, N. & Parray, J. A. Pesticide Residues in the Soil Cause Cross-Resistance Among Soil Bacteria. 205–218 (2019) doi:10.1007/978-981-13-6536-2_11.
10. Blau, K. *et al.* The transferable resistome of produce. *mBio* **9**, 1–15 (2018).
11. Forsberg, K. J. *et al.* The shared antibiotic resistome of soil bacteria and human pathogens. *Science* **337**, 1107 (2012).
12. D'costa, V. M. *et al.* Antibiotic resistance is ancient. *Nature* **477**, (2011).
13. Voigt, A. M. *et al.* Association between antibiotic residues, antibiotic resistant bacteria and antibiotic resistance genes in anthropogenic wastewater – An evaluation of clinical influences. *Chemosphere* **241**, 125032 (2020).
14. Larsen, J. *et al.* Emergence of methicillin resistance predates the clinical use of antibiotics. & Anders R. Larsen **602**, 56 (2022).
15. Sherman, I. W. *Drugs That Changed the World*. (CRC Press, 2016). doi:10.1201/9781315366739.
16. Zaffiri, L., Gardner, J. & Toledo-Pereyra, L. H. History of Antibiotics. From Salvarsan to Cephalosporins. *Journal of Investigative Surgery* **25**, 67–77 (2012).
17. Walsh, C. & Wencewicz, T. *Antibiotics: challenges, mechanisms, opportunities*. (American Society for Microbiology (ASM), 2016).
18. Lee Ventola, C. *The Antibiotic Resistance Crisis Part 1: Causes and Threats*. vol. 40 (2015).
19. Talebi, A., Abadi, B., Rizvanov, A. A., Haertlé, T. & Blatt, N. L. World Health Organization Report: Current Crisis of Antibiotic Resistance. doi:10.1007/s12668-019-00658-4.

20. Outterson, K., Powers, J. H., Seoane-Vazquez, E., Rodriguez-Monguio, R. & Kesselheim, A. S. Approval and withdrawal of new antibiotics and other anti-infectives in the U.S., 1980-2009. *Journal of Law, Medicine and Ethics* **41**, 688–696 (2013).
21. Laxminarayan, R. Antibiotic effectiveness: Balancing conservation against innovation. *Science* (1979) **345**, 1299–1301 (2014).
22. Chiou, C.-S. The Analysis of Plasmid-Mediated Streptomycin Resistance in *Erwinia amylovora*. *Phytopathology* **81**, 710 (1991).
23. Schnabel, E. L. & Jones, A. L. Distribution of tetracycline resistance genes and transposons among phylloplane bacteria in Michigan apple orchards. *Applied and Environmental Microbiology* **65**, 4898–4907 (1999).
24. Böszörményi, E. *et al.* Isolation and activity of Xenorhabdus antimicrobial compounds against the plant pathogens *Erwinia amylovora* and *Phytophthora nicotianae*. *Journal of Applied Microbiology* **107**, 746–759 (2009).
25. de Oliveira, D. M. P. *et al.* Rescuing Tetracycline Class Antibiotics for the Treatment of Multidrug-Resistant *Acinetobacter baumannii* Pulmonary Infection. *mBio* **13**, (2022).
26. Lillehaug, A., Lunestad, B. T. & Grave, K. Epidemiology of bacterial diseases in Norwegian aquaculture—a description based on antibiotic prescription data for the ten-year period 1991 to 2000. *Diseases of Aquatic Organisms* **53**, 115–125 (2003).
27. Keskitalo, M. *et al.* Control of Bacteria and Alteration of Plant Growth in Tissue Cultures of Tansy (*Tanacetum vulgare* L.) Treated with Antibiotics. *HortScience* **31**, 631e–6631 (1996).
28. CABI Agric Biosci, R., Taylor, P. & Reeder, R. Antibiotic use on crops in low and middle-income countries based on recommendations made by

- agricultural advisors. *CABI Agriculture and Bioscience 2020 1:1* **1**, 1–14 (2020).
29. Lin, J., Hunkapiller, A. A., Layton, A. C., Chang, Y. J. & Robbins, K. R. Response of Intestinal Microbiota to Antibiotic Growth Promoters in Chickens. <https://home.liebertpub.com/fpd> **10**, 331–337 (2013).
 30. Monahan, C., Harris, S., Morris, D. & Cummins, E. A comparative risk ranking of antibiotic pollution from human and veterinary antibiotic usage – An Irish case study. *Science of The Total Environment* **826**, 154008 (2022).
 31. Dinh, Q. T. *et al.* Analysis of sulfonamides, fluoroquinolones, tetracyclines, triphenylmethane dyes and other veterinary drug residues in cultured and wild seafood sold in Montreal, Canada. *Journal of Food Composition and Analysis* **94**, 103630 (2020).
 32. The First Miracle Drugs: How the Sulfa Drugs Transformed Medicine - ProQuest. <https://www.proquest.com/docview/233166464>.
 33. Straub, J. O., Hoffmann-, F. & Roche, L. Aquatic environmental risk assessment for human use of the old antibiotic sulfamethoxazole in Europe; Aquatic environmental risk assessment for human use of the old antibiotic sulfamethoxazole in Europe. doi:10.1002/etc.2945.
 34. Klein, E. Y. *et al.* Assessment of WHO antibiotic consumption and access targets in 76 countries, 2000–15: an analysis of pharmaceutical sales data. *The Lancet Infectious Diseases* **21**, 107–115 (2021).
 35. Murray, C. J. *et al.* Global burden of bacterial antimicrobial resistance in 2019: a systematic analysis. *The Lancet* **399**, 629–655 (2022).
 36. van Boeckel, T. P. *et al.* Global antibiotic consumption 2000 to 2010: An analysis of national pharmaceutical sales data. *The Lancet Infectious Diseases* **14**, 742–750 (2014).

37. Michael Crosby *et al.* Interprovincial variation in antibiotic use in Canada, 2019: a retrospective cross-sectional study. *Canadian Medical Association Journal* **10**, 262–268 (2022).
38. Karkman, A., Pärnänen, K. & Larsson, & D. G. J. Fecal pollution can explain antibiotic resistance gene abundances in anthropogenically impacted environments. doi:10.1038/s41467-018-07992-3.
39. Pan, M. & Chu, L. M. Transfer of antibiotics from wastewater or animal manure to soil and edible crops. *Environmental Pollution* **231**, 829–836 (2017).
40. Thai, P. K. *et al.* Occurrence of antibiotic residues and antibiotic-resistant bacteria in effluents of pharmaceutical manufacturers and other sources around Hanoi, Vietnam. *Science of The Total Environment* **645**, 393–400 (2018).
41. Graham, D. W. *et al.* Antibiotic resistance gene abundances associated with waste discharges to the Almendares river near Havana, Cuba. *Environmental Science and Technology* **45**, 418–424 (2011).
42. Huang, R., Ding, P., Huang, D. & Yang, F. Antibiotic pollution threatens public health in China. *The Lancet* **385**, 773–774 (2015).
43. Lübbert, C. *et al.* Environmental pollution with antimicrobial agents from bulk drug manufacturing industries in Hyderabad, South India, is associated with dissemination of extended-spectrum beta-lactamase and carbapenemase-producing pathogens. *Infection* **45**, 479–491 (2017).
44. Bengtsson-Palme, J. *et al.* Industrial wastewater treatment plant enriches antibiotic resistance genes and alters the structure of microbial communities. *Water Research* **162**, 437–445 (2019).
45. Lalonde, B. A., Ernst, W. & Greenwood, L. Measurement of oxytetracycline and emamectin benzoate in freshwater sediments downstream of land

- based aquaculture facilities in the Atlantic Region of Canada. *Bulletin of Environmental Contamination and Toxicology* **89**, 547–550 (2012).
46. Zou, S. *et al.* Occurrence and distribution of antibiotics in coastal water of the Bohai Bay, China: Impacts of river discharge and aquaculture activities. *Environmental Pollution* **159**, 2913–2920 (2011).
 47. Cvm, F. 2016 Summary Report on Antimicrobials Sold or Distributed for Use in Food-Producing Animals. (2017).
 48. Pouliquen, H. *et al.* Comparison of water, sediment, and plants for the monitoring of antibiotics: A case study on a river dedicated to fish farming. *Environmental Toxicology and Chemistry* **28**, 496–502 (2009).
 49. Albero, B., Tadeo, J. L., Escario, M., Miguel, E. & Pérez, R. A. Persistence and availability of veterinary antibiotics in soil and soil-manure systems. *Science of The Total Environment* **643**, 1562–1570 (2018).
 50. Hammesfahr, U., Heuer, H., Manzke, B., Smalla, K. & Thiele-Bruhn, S. Impact of the antibiotic sulfadiazine and pig manure on the microbial community structure in agricultural soils. *Soil Biology and Biochemistry* **40**, 1583–1591 (2008).
 51. Chen, C. *et al.* Antibiotics and Antibiotic Resistance Genes in Bulk and Rhizosphere Soils Subject to Manure Amendment and Vegetable Cultivation. doi:10.2134/jeq2018.02.0078.
 52. Xu, M. *et al.* Composting increased persistence of manure-borne antibiotic resistance genes in soils with different fertilization history. *Science of The Total Environment* **689**, 1172–1180 (2019).
 53. Martins, M. *et al.* Evidence of metabolic switching and implications for food safety from the phenome(s) of *Salmonella enterica* serovar Typhimurium DT104 cultured at selected points across the pork production food chain. *Appl Environ Microbiol* **79**, 5437–5449 (2013).

54. Oniciuc, E. A. *et al.* Food processing as a risk factor for antimicrobial resistance spread along the food chain. *Current Opinion in Food Science* **30**, 21–26 (2019).
55. Heuer, H. *et al.* *Gentamicin resistance genes in environmental bacteria: prevalence and transfer.* www.fems-microbiology.org doi:10.1111/j.1574-6941.2002.tb01019.x.
56. Haenni, M. *et al.* Environmental contamination in a high-income country (France) by antibiotics, antibiotic-resistant bacteria, and antibiotic resistance genes: Status and possible causes. *Environment International* **159**, 107047 (2022).
57. Su, H. C. *et al.* Class 1 and 2 integrons, *sul* resistance genes and antibiotic resistance in *Escherichia coli* isolated from Dongjiang River, South China. *Environmental Pollution* **169**, 42–49 (2012).
58. D'Costa, V. M., McGrann, K. M., Hughes, D. W. & Wright, G. D. Sampling the Antibiotic Resistome. *Science (1979)* **311**, 374–377 (2006).
59. The Cost of Antibiotic Resistance: Effect of Resistance Among *Staphylococcus aureus*, *Klebsiella pneumoniae*, *Acinetobacter baumannii*, and *Pseudomonas aeruginosa* on Length of Hospital Stay. *Infection Control & Hospital Epidemiology* **23**, 106–108 (2002).
60. Nadi, Z. R. *et al.* Evaluation of antibiotic resistance and prevalence of common *Salmonella enterica* serovars isolated from foodborne outbreaks. *Microchemical Journal* **155**, 104660 (2020).
61. Johler, S., Layer, F. & Stephan, R. Comparison of Virulence and Antibiotic Resistance Genes of Food Poisoning Outbreak Isolates of *Staphylococcus aureus* with Isolates Obtained from Bovine Mastitis Milk and Pig Carcasses. *Journal of Food Protection* **74**, 1852–1859 (2011).

62. Canada, P. H. A. of. Antimicrobial Resistance and One Health: Pan-Canadian framework for action on antimicrobial resistance and antimicrobial use. *Canada Communicable Disease Report* **43**, 217 (2017).
63. Academies, C. of C. *When Antibiotics Fail : The Expert Panel on the Potential Socio-Economic Impacts of Antimicrobial Resistance in Canada*. Council of Canadian Academies (2019).
64. Cabrera-Pardo, J. R. *et al.* A One Health – One World initiative to control antibiotic resistance: A Chile - Sweden collaboration. *One Health* **8**, 100100 (2019).
65. WHO. Antimicrobial resistance. Global report on surveillance. *World Health Organization* **61**, 12–28 (2014).
66. Kumar, K., C. Gupta, S., Chander, Y. & Singh, A. K. Antibiotic Use in Agriculture and Its Impact on the Terrestrial Environment. *Advances in Agronomy* **87**, 1–54 (2005).
67. Rodríguez, C. *et al.* Lettuce for human consumption collected in Costa Rica contains complex communities of culturable oxytetracycline- and gentamicin-resistant bacteria. *Applied and Environmental Microbiology* **72**, 5870–5876 (2006).
68. Pan-Canadian framework for action on antimicrobial resistance and antimicrobial use. *Canada communicable disease report = Relevé des maladies transmissibles au Canada* **43**, 217–219 (2017).
69. Moulin, G. *et al.* A comparison of antimicrobial usage in human and veterinary medicine in France from 1999 to 2005. *J Antimicrob Chemother* **62**, 617–625 (2008).
70. El-Hendawy, H. H., Zeid, I. M. & Mohamed, Z. K. The biological control of soft rot disease in melon caused by *Erwinia carotovora* subsp. *carotovora*

using *Pseudomonas fluorescens*. *Microbiological Research* **153**, 55–60 (1998).

71. Chanvatik, S. *et al.* Antibiotic use in mandarin production (*Citrus reticulata* Blanco) in major mandarin-producing areas in Thailand: A survey assessment. *PLOS ONE* **14**, e0225172 (2019).
72. Herbert, A. *et al.* Oxytetracycline and Streptomycin Resistance Genes in *Xanthomonas arboricola* pv. *pruni*, the Causal Agent of Bacterial Spot in Peach. *Frontiers in Microbiology* **13**, 228 (2022).
73. Tancos, K. A. *et al.* Prevalence of streptomycin-resistant *Erwinia amylovora* in New York apple orchards. *Plant Disease* **100**, 802–809 (2016).
74. Chiou, C. S. & Jones, A. L. Expression and identification of the *strA-strB* gene pair from streptomycin-resistant *Erwinia amylovora*. *Gene* **152**, 47–51 (1995).
75. Kurenbach, B., Hill, A. M., Godsoe, W., van Hamelsveld, S. & Heinemann, J. A. Agrichemicals and antibiotics in combination increase antibiotic resistance evolution. *PeerJ* **6**, e5801 (2018).
76. Nemeth, J., Oesch, G. & Kuster, S. P. Bacteriostatic versus bactericidal antibiotics for patients with serious bacterial infections: systematic review and meta-analysis. *Journal of Antimicrobial Chemotherapy* **70**, 382–395 (2015).
77. Macnair, C. R. & Brown, E. D. Outer Membrane Disruption Overcomes Intrinsic, Acquired, and Spontaneous Antibiotic Resistance. (2020) doi:10.1128/mBio.01615-20.
78. Valderas, M. W., Andi, B., Barrow, W. W. & Cook, P. F. Examination of intrinsic sulfonamide resistance in *Bacillus anthracis*: A novel assay for dihydropteroate synthase. *Biochimica et Biophysica Acta (BBA) - General Subjects* **1780**, 848–853 (2008).

79. Ammor, M. S. *et al.* Molecular Characterization of Intrinsic and Acquired Antibiotic Resistance in Lactic Acid Bacteria and Bifidobacteria. *Microbial Physiology* **14**, 6–15 (2008).
80. Pawlowski, A. C., Westman, E. L., Koteva, K., Waglechner, N. & Wright, G. D. The complex resistomes of Paenibacillaceae reflect diverse antibiotic chemical ecologies. *The ISME Journal* **2018** 12:3 **12**, 885–897 (2017).
81. Sandner-Miranda, L., Vinuesa, P., Cravioto, A. & Morales-Espinosa, R. The genomic basis of intrinsic and acquired antibiotic resistance in the genus *Serratia*. *Frontiers in Microbiology* **9**, 828 (2018).
82. Yamasaki, S., Nagasawa, S., Fukushima, A., Hayashi-nishino, M. & Nishino, K. Cooperation of the multidrug efflux pump and lipopolysaccharides in the intrinsic antibiotic resistance of *Salmonella enterica* serovar Typhimurium. *Journal of Antimicrobial Chemotherapy* **68**, 1066–1070 (2013).
83. Li, X. Z., Zhang, L. & Nikaido, H. Efflux pump-mediated intrinsic drug resistance in *Mycobacterium smegmatis*. *Antimicrobial Agents and Chemotherapy* **48**, 2415–2423 (2004).
84. Zgurskaya, H. I. Molecular analysis of efflux pump-based antibiotic resistance. *International Journal of Medical Microbiology* **292**, 95–105 (2002).
85. van Meervenne, E. *et al.* Strain-Specific Transfer of Antibiotic Resistance from an Environmental Plasmid to Foodborne Pathogens. *Journal of Biomedicine and Biotechnology* **2012**, (2012).
86. Poey, M. E., Azpiroz, M. F. & Laviña, M. On sulfonamide resistance, *sul* genes, class 1 integrons and their horizontal transfer in *Escherichia coli*. *Microbial Pathogenesis* **135**, 103611 (2019).
87. Hevener, K. E. *et al.* Structural Studies of Pterin-Based Inhibitors of Dihydropteroate Synthase †. *J. Med. Chem* **53**, 166–177 (2010).

88. Capasso, C. & Supuran, C. T. Dihydropteroate Synthase (Sulfonamides) and Dihydrofolate Reductase Inhibitors. in *Bacterial Resistance to Antibiotics: From Molecules to Man* (eds. Bonev, B. B. & Supuran, C. T.) 163–172 (John Wiley & Sons, Ltd, 2019). doi:10.1002/9781119593522.CH7.
89. Sangurdekar, D. P., Zhang, Z. & Khodursky, A. B. *The association of DNA damage response and nucleotide level modulation with the antibacterial mechanism of the anti-folate drug Trimethoprim.* <http://www.biomedcentral.com/1471-2164/12/583> (2011) doi:10.1186/1471-2164-12-583.
90. Soriano-Correa, C., Esquivel, R. O. & Sagar, R. P. Physicochemical and structural properties of bacteriostatic sulfonamides: Theoretical study. *International Journal of Quantum Chemistry* **94**, 165–172 (2003).
91. Lesch, J. E. *The first miracle drugs: how the sulfa drugs transformed medicine.* Oxford University Press (2007).
92. Landy, M., Larkum, N. W., Oswald, E. J. & Streightoff, F. Increased Synthesis of p-Aminobenzoic Acid Associated with the Development of Sulfonamide Resistance in *Staphylococcus aureus*. *Science* (1979) **97**, 265–267 (1943).
93. Co-trimoxazole and sudden death in patients receiving inhibitors of renin-angiotensin system: population based study. doi:10.1136/bmj.g6196.
94. Iliades, P., Meshnick, S. R. & Macreadie, I. G. Mutations in the *Pneumocystis jirovecii* DHPS gene confer cross-resistance to sulfa drugs. *Antimicrobial Agents and Chemotherapy* **49**, 741–748 (2005).
95. Hyun, D. Y., Mason, E. O., Forbes, A. & Kaplan, S. L. Trimethoprim-sulfamethoxazole or clindamycin for treatment of community-acquired methicillin-resistant *Staphylococcus aureus* skin and soft tissue infections. *Pediatr Infect Dis J* **28**, 57–59 (2009).

96. Stolk, P., Willemsen, M. J. C. & Leufkens, H. G. M. Rare essentials: drugs for rare diseases as essential medicines. *Bull World Health Organ* **84**, 745–751 (2006).
97. McKinney, C. W., Loftin, K. A., Meyer, M. T., Davis, J. G. & Pruden, A. Tet and *sul* antibiotic resistance genes in livestock lagoons of various operation type, configuration, and antibiotic occurrence. *Environmental Science and Technology* **44**, 6102–6109 (2010).
98. Boxall, A. B. A., Blackwell, P., Cavallo, R., Kay, P. & Tolls, J. The sorption and transport of a sulphonamide antibiotic in soil systems. *Toxicology Letters* **131**, 19–28 (2002).
99. Babaoglu, K., Qi, J., Lee, R. E. & White, S. W. Crystal Structure of 7,8-Dihydropteroate Synthase from *Bacillus anthracis*: Mechanism and Novel Inhibitor Design. *Structure* **12**, 1705–1717 (2004).
100. de Giori, G. S. & LeBlanc, J. G. Folate production by lactic acid bacteria. in *Polyphenols: Prevention and Treatment of Human Disease* (eds. Ronald Ross Watson, Victor R. Preedy & Sherma Zibadi) vol. 1 15–29 (Elsevier, 2018).
101. Chakraborty, S., Gruber, T., Barry, C. E., Boshoff, H. I. & Rhee, K. Y. Para-aminosalicylic acid acts as an alternative substrate of folate metabolism in *Mycobacterium tuberculosis*. *Science (1979)* **339**, 88–91 (2013).
102. Kim, P. B., Nelson, J. W. & Breaker, R. R. An Ancient Riboswitch Class in Bacteria Regulates Purine Biosynthesis and One-Carbon Metabolism. *Molecular Cell* **57**, 317–328 (2015).
103. Macreadie, I., Simpson, J., Swarbrick, J., Iliades, P. & Simpson, J. S. Folate biosynthesis-reappraisal of old and novel targets in the search for new antimicrobials. *The Open Enzyme Inhibition Journal* **1**, 12–33 (2008).

104. Hong, Y., Li, L., Luan, G., Drlica, K. & Zhao, X. Contribution of reactive oxygen species to thymineless death in *Escherichia coli*. *Nature Microbiology* (2017) doi:10.1038/s41564-017-0037-y.
105. Kuong, K. J. & Kuzminov, A. Stalled replication fork repair and misrepair during thymineless death in *Escherichia coli*. doi:10.1111/j.1365-2443.2010.01405.x.
106. Sangurdekar, D. P. *et al.* Thymineless death is associated with loss of essential genetic information from the replication origin *mi_7072* 1455..1467. (2010) doi:10.1111/j.1365-2958.2010.07072.x.
107. Bermingham, A. & Derrick, J. P. The folic acid biosynthesis pathway in bacteria: Evaluation of potential for antibacterial drug discovery. *BioEssays* **24**, 637–648 (2002).
108. Guzzo, M. B. *et al.* Methylfolate Trap Promotes Bacterial Thymineless Death by Sulfa Drugs. *PLOS Pathogens* **12**, e1005949 (2016).
109. BARNER, H. D. & COHEN, S. S. The induction of thymine synthesis by T2 infection of a thymine requiring mutant of *Escherichia coli*. *J Bacteriol* **68**, 80–88 (1954).
110. Fonville, N. C., Vaksman, Z., Denapoli, J., Hastings, P. J. & Rosenberg, S. M. Pathways of Resistance to Thymineless Death in *Escherichia coli* and the Function of UvrD. (2011) doi:10.1534/genetics.111.130161.
111. Khan, S. R. & Kuzminova, A. Thymineless death in *Escherichia coli* is unaffected by chromosomal replication complexity. *Journal of Bacteriology* **201**, (2019).
112. Khan, S. R. & Kuzminov, A. Thymine-starvation-induced chromosomal fragmentation is not required for thymineless death in *Escherichia coli*. *Mol Microbiol* **117**, 1138–1155 (2022).

113. Blundred, R., Myers, K., Helleday, T., Goldman, A. S. H. & Bryant, H. E. Human RECQL5 overcomes thymidine-induced replication stress. *DNA Repair* **9**, 964–975 (2010).
114. OKAGAKI, H., TSUBOTA, Y. & SIBATANI, A. Unbalanced growth and bacterial death in thymine-deficient and ultraviolet irradiated *Escherichia coli*. *J Bacteriol* **80**, 762–771 (1960).
115. Freifelder, D. & Katz, G. Persistence of small fragments of newly synthesized DNA in bacteria following thymidine starvation. *Journal of Molecular Biology* **57**, 351–354 (1971).
116. Hastings, P. J. & Rosenberg, S. M. A radical way to die. (2017) doi:10.1038/s41564-017-0074-6.
117. Poirel, L. *et al.* Origin of the Mobile Di-Hydro-Pterate Synthase Gene Determining Sulfonamide Resistance in Clinical Isolates Origin of Clinical Sulfonamide Resistance. (2019) doi:10.3389/fmicb.2018.03332.
118. Perreten, V. & Boerlin, P. A new sulfonamide resistance gene (*su3*) in *Escherichia coli* is widespread in the pig population of Switzerland. *Antimicrob Agents Chemother* **47**, 1169–1172 (2003).
119. Zhang, Y. *et al.* Characterization of microbial community and antibiotic resistance genes in activated sludge under tetracycline and sulfamethoxazole selection pressure. *Science of The Total Environment* **571**, 479–486 (2016).
120. Morpeth, S. C. *et al.* Effect of Trimethoprim-Sulfamethoxazole Prophylaxis on Antimicrobial Resistance of Fecal *Escherichia coli* in HIV-Infected Patients in Tanzania. doi:10.1097/QAI.0b013e31816856db.
121. Sharma, M. P. *et al.* EFFECTS OF POST-EMERGENCE WILD OAT HERBICIDES ON THE TRANSPIRATION OF WILD OATS. <https://doi.org/10.4141/cjps77-019> **57**, 127–132 (2011).

122. Ae, G. B. S., Ae, A. S. P. & Tyler, C. The Effectiveness of Asulam for Bracken (*Pteridium aquilinum*) Control in the United Kingdom: A Meta-Analysis. doi:10.1007/s00267-006-0128-7.
123. Food Safety Authority, E. *et al.* Updated peer review of the pesticide risk assessment of the active substance asulam (variant evaluated asulam-sodium). *Journal* **19**, 6921 (2021).
124. Pallett, K. E. Herbicides, Asulam. *Encyclopedia of Agrochemicals* (2003) doi:10.1002/047126363X.AGR025.
125. HEWERTSON, N. A. & COLLIN, H. A. Mechanism of action of asulam in celery tissue cultures. *Weed Research* **24**, 79–83 (1984).
126. Kirkwood, R. C., Veerasekaran, P. & Fletcher, W. W. Studies on the mode of action of asulam in bracken (*Pteridium aquilinum* L. Kuhn). *Proceedings of the Royal Society of Edinburgh, Section B: Biological Sciences* **81**, 85–96 (1982).
127. Vadlamani, G. *et al.* Crystal structure of Arabidopsis thaliana HPPK/DHPS, a bifunctional enzyme and target of the herbicide asulam. *Plant Communications* 100322 (2022) doi:10.1016/J.XPLC.2022.100322.
128. Kidd, B. R., Stephen, N. H. & Duncan, H. J. The effect of asulam on purine biosynthesis. *Plant Science Letters* **26**, 211–217 (1982).
129. Kaufmann, A. & Kaenzig, A. Contamination of honey by the herbicide asulam and its antibacterial active metabolite sulfanilamide. (2007) doi:10.1080/02652030410001677790.
130. Binh, C. T. T., Heuer, H., Kaupenjohann, M. & Smalla, K. Piggery manure used for soil fertilization is a reservoir for transferable antibiotic resistance plasmids. *FEMS Microbiology Ecology* **66**, 25–37 (2008).

131. Cox, G. *et al.* A Common Platform for Antibiotic Dereplication and Adjuvant Discovery. *Cell Chemical Biology* **24**, 98–109 (2017).
132. Deatherage, D. E. & Barrick, J. E. Identification of mutations in laboratory-evolved microbes from next-generation sequencing data using breseq. *Methods in Molecular Biology* **1151**, 165–188 (2014).
133. Sambrook, J. & Russell, D. W. Preparation and Transformation of Competent *E. coli* Using Calcium Chloride. *CSH Protoc* **2006**, pdb.prot3932 (2006).
134. Wiegand, I., Hilpert, K. & Hancock, R. E. W. Agar and broth dilution methods to determine the minimal inhibitory concentration (MIC) of antimicrobial substances. (2008) doi:10.1038/nprot.2007.521.
135. Lin, W. *et al.* Reduction of the fitness cost of antibiotic resistance caused by chromosomal mutations under poor nutrient conditions. *Environment International* **120**, 63–71 (2018).
136. Tran, T. T. *et al.* On-Farm Anaerobic Digestion of Dairy Manure Reduces the Abundance of Antibiotic Resistance-Associated Gene Targets and the Potential for Plasmid Transfer. *Applied and Environmental Microbiology* **87**, 1–20 (2021).
137. Venkatesan, M. *et al.* Molecular mechanism of plasmid-borne resistance to sulfonamides. *bioRxiv* 2022.06.30.498311 (2022) doi:10.1101/2022.06.30.498311.
138. Pierce, M. M., Raman, C. S. & Nall, B. T. Isothermal Titration Calorimetry of Protein–Protein Interactions. *Methods* **19**, 213–221 (1999).
139. Khan, S., Beattie, T. K., Charles, • & Knapp, W. The use of minimum selectable concentrations (MSCs) for determining the selection of antimicrobial resistant bacteria. *Ecotoxicology* **26**, 283–292 (2017).

140. Allen, G. P. & Deshpande, L. M. Determination of the mutant selection window for clindamycin, doxycycline, linezolid, moxifloxacin and trimethoprim/sulfamethoxazole against community-associated methicillin-resistant *Staphylococcus aureus* (MRSA). *International Journal of Antimicrobial Agents* **35**, 45–49 (2010).
141. Zhao, Y. *et al.* Transcriptomics and proteomics revealed the psychrotolerant and antibiotic-resistant mechanisms of strain *Pseudomonas psychrophila* RNC-1 capable of assimilatory nitrate reduction and aerobic denitrification. *Science of The Total Environment* **820**, 153169 (2022).
142. Griffith, E. C. *et al.* The structural and functional basis for recurring sulfa drug resistance mutations in *Staphylococcus aureus* dihydropteroate synthase. *Frontiers in Microbiology* **9**, 1369 (2018).
143. Singh, N. K., Desai, C. K., Rathore, B. S. & Chaudhari, B. G. Bio-efficacy of Herbicides on Performance of Mustard, *Brassica juncea* (L.) and Population Dynamics of Agriculturally Important Bacteria. *Proceedings of the National Academy of Sciences India Section B - Biological Sciences* **86**, 743–748 (2016).
144. Kurenbach, B. *et al.* Sublethal exposure to commercial formulations of the herbicides dicamba, 2,4-dichlorophenoxyacetic acid, and Glyphosate cause changes in antibiotic susceptibility in *Escherichia coli* and *Salmonella enterica* serovar Typhimurium. *mBio* **6**, (2015).
145. Zhang, H., Liu, J., Wang, L. & Zhai, Z. Glyphosate escalates horizontal transfer of conjugative plasmid harboring antibiotic resistance genes. <https://doi.org/10.1080/21655979.2020.1862995> **12**, 63–69 (2020).
146. Tiimub, B. M. *et al.* Characteristics of bacterial community and ARGs profile in engineered goldfish tanks with stresses of sulfanilamide and copper. *Environmental Science and Pollution Research* **28**, 38706–38717 (2021).

147. Lye, Y. L. *et al.* Anthropogenic impacts on sulfonamide residues and sulfonamide resistant bacteria and genes in Larut and Sangga Besar River, Perak. *Science of The Total Environment* **688**, 1335–1347 (2019).
148. Collado, N. *et al.* Effects on activated sludge bacterial community exposed to sulfamethoxazole. *Chemosphere* **93**, 99–106 (2013).
149. Occurrence and Sorption Behavior of Sulfonamides, Macrolides, and Trimethoprim in Activated Sludge Treatment. (2005) doi:10.1021/es048550a.
150. Buwembo, W., Aery, S., Rwenyonyi, C. M., Swedberg, G. & Kironde, F. Point Mutations in the folP Gene Partly Explain Sulfonamide Resistance of *Streptococcus mutans*. *International Journal of Microbiology* **2013**, (2013).
151. Khan, N., Asadullah & Bano, A. Plant Growth Promoting Rhizobacteria for Sustainable Stress Management. **12**, 362 (2019).
152. Cragg, B. A. & Fry, J. C. The use of microcosms to simulate field experiments to determine the effects of herbicides on aquatic bacteria. *Journal of General Microbiology* **130**, 2309–2316 (1984).
153. Fiebelkorn, K. R., Crawford, S. A. & Jorgensen, J. H. Mutations in folP Associated with Elevated Sulfonamide MICs for *Neisseria meningitidis* Clinical Isolates from Five Continents. *Antimicrobial Agents and Chemotherapy* **49**, 536 (2005).
154. Vedantam, G., Guay, G. G., Austria, N. E., Doktor, S. Z. & Nichols, B. P. Characterization of mutations contributing to sulfathiazole resistance in *Escherichia coli*. *Antimicrobial Agents and Chemotherapy* **42**, 88–93 (1998).
155. Duthie, S. J., Narayanan, S., Brand, G. M., Pirie, L. & Grant, G. Impact of Folate Deficiency on DNA Stability. *The Journal of Nutrition* **132**, 2444S-2449S (2002).

156. Shoeman, R. *et al.* Regulation of methionine synthesis in *Escherichia coli*: Effect of metJ gene product and S-adenosylmethionine on the expression of the metF gene. *Proceedings of the National Academy of Sciences* **82**, 3601–3605 (1985).
157. Linhart, H. G. *et al.* Folate Deficiency Induces Genomic Uracil Misincorporation and Hypomethylation But Does Not Increase DNA Point Mutations. *Gastroenterology* **136**, 227-235.e3 (2009).
158. Rao, T. V. P. & Kuzminov, A. Sources of thymidine and analogs fueling futile damage-repair cycles and ss-gap accumulation during thymine starvation in *Escherichia coli*. *DNA Repair* **75**, 1–17 (2019).
159. al Harrasi, I., Al-Yahyai, R. & Yaish, M. W. Detection of differential DNA methylation under stress conditions using bisulfite sequence analysis. *Methods in Molecular Biology* **1631**, 121–137 (2017).
160. Guo, J., Zhang, Y., Mo, J., Sun, H. & Li, Q. Sulfamethoxazole-Altered Transcriptome in Green Alga *Raphidocelis subcapitata* Suggests Inhibition of Translation and DNA Damage Repair. *Frontiers in Microbiology* **12**, (2021).
161. Jain, C. The *E. coli* *RhlE* RNA helicase regulates the function of related RNA helicases during ribosome assembly. *RNA* **14**, 381–389 (2008).
162. Ovchinnikov, Y. A. *et al.* The primary structure of *E. coli* RNA polymerase. Nucleotide sequence of the *rpoC* gene and amino acid sequence of the β' -subunit. *Nucleic Acids Research* **10**, 4035–4044 (1982).
163. Andersen-Civil, A. I. S. *et al.* The impact of inactivation of the purine biosynthesis genes, *purN* and *purT*, on growth and virulence in uropathogenic *E. coli*. *Molecular Biology Reports* **45**, 2707–2716 (2018).
164. Nagaraja, V. & Gopinathan, K. P. Involvement of DNA gyrase in the replication and transcription of mycobacteriophage 13 DNA. *FEBS Letters* **127**, 57–62 (1981).

165. Yoshida, H., Bogaki, M., Nakamura, M. & Nakamura, S. Quinolone resistance-determining region in the DNA gyrase *gyrA* gene of *Escherichia coli*. *Antimicrobial Agents and Chemotherapy* **34**, 1271–1272 (1990).
166. Ross, W., Vrentas, C. E., Sanchez-Vazquez, P., Gaal, T. & Gourse, R. L. The Magic Spot: A ppGpp Binding Site on *E. coli* RNA Polymerase Responsible for Regulation of Transcription Initiation. *Molecular Cell* **50**, 420–429 (2013).
167. Jaktaji, R. P. & Mohiti, E. Study of Mutations in the DNA gyrase *gyrA* Gene of *Escherichia coli*. *Iranian Journal of Pharmaceutical Research : IJPR* **9**, 43 (2010).
168. Laffler, T. & Gallant, J. *spoT*, a new genetic locus involved in the stringent response in *E. coli*. *Cell* **1**, 27–30 (1974).
169. Lomax, M. S. & Greenberg, G. R. Characteristics of the *deo* operon: role in thymine utilization and sensitivity to deoxyribonucleosides. *J Bacteriol* **96**, 501–514 (1968).
170. Zaritsky, A. & Zbrovitz, S. DNA synthesis in *Escherichia coli* during a nutritional shift-up. *Molecular and General Genetics MGG 1981 181:4* **181**, 564–566 (1981).
171. Thomson, J. G., Cook, M., Guttman, M., Smith, J. & Thilmony, R. Novel *sull* binary vectors enable an inexpensive foliar selection method in *Arabidopsis*. *BMC Research Notes* **4**, 1–11 (2011).
172. Jabrin, S., Ravanel, S., Gambonnet, B., Douce, R. & Rébeillé, F. One-Carbon Metabolism in Plants. Regulation of Tetrahydrofolate Synthesis during Germination and Seedling Development. *Plant Physiology* **131**, 1431–1439 (2003).
173. Surov, T. *et al.* Generation of transgenic asulam-resistant potatoes to facilitate eradication of parasitic broomrapes (*Orobancha spp.*), with the *sul*

- gene as the selectable marker. *Theoretical and Applied Genetics* 1998 96:1 **96**, 132–137 (1998).
174. Hugenholtz, P., Tyson, G. W., Webb, R. I., Wagner, A. M. & Blackall, L. L. Investigation of candidate division TM7, a recently recognized major lineage of the domain Bacteria, with no known pure-culture representatives. *Applied and Environmental Microbiology* **67**, 411–419 (2001).
175. Suyal, D. C. *et al.* Soil Metagenomics: Unculturable Microbial Diversity and Its Function. *Mycorrhizosphere and Pedogenesis* 355–362 (2019) doi:10.1007/978-981-13-6480-8_20.
176. Nichols, D. *et al.* Short peptide induces an “uncultivable” microorganism to grow in vitro. *Applied and Environmental Microbiology* **74**, 4889–4897 (2008).
177. Letten, A. D., Hall, A. R. & Levine, J. M. Using ecological coexistence theory to understand antibiotic resistance and microbial competition. doi:10.1038/s41559-020-01385-w.
178. Freilich, S. *et al.* Competitive and cooperative metabolic interactions in bacterial communities. (2011) doi:10.1038/ncomms1597.
179. de Raad, M. *et al.* A Defined Medium for Cultivation and Exometabolite Profiling of Soil Bacteria. *Frontiers in Microbiology* **0**, 1836 (2022).
180. Ripa, F. A., Nikkon, F., Zaman, S. & Khondkar, P. Optimal Conditions for Antimicrobial Metabolites Production from a New *Streptomyces* sp. RUPA-08PR Isolated from Bangladeshi Soil . *Mycobiology* **37**, 211 (2009).
181. Baunach, M., Ding, L., Willing, K. & Hertweck, C. Bacterial Synthesis of Unusual Sulfonamide and Sulfone Antibiotics by Flavoenzyme-Mediated Sulfur Dioxide Capture. *Angewandte Chemie International Edition* **54**, 13279–13283 (2015).

182. Mujumdar, P. *et al.* An Unusual Natural Product Primary Sulfonamide: Synthesis, Carbonic Anhydrase Inhibition, and Protein X-ray Structures of Psammaplin C. *Journal of Medicinal Chemistry* **59**, 5462–5470 (2016).
183. Tashiro, Y. *et al.* RelE-mediated dormancy is enhanced at high cell density in escherichia coli. *Journal of Bacteriology* **194**, 1169–1176 (2012).
184. Monk, J. M. *et al.* Genome-scale metabolic reconstructions of multiple Escherichia coli strains highlight strain-specific adaptations to nutritional environments. *Proc Natl Acad Sci U S A* **110**, 20338–20343 (2013).
185. Händel, N., Schuurmans, J. M., Brul, S. & ter Kuilea, B. H. Compensation of the metabolic costs of antibiotic resistance by physiological adaptation in escherichia coli. *Antimicrobial Agents and Chemotherapy* **57**, 3752–3762 (2013).
186. Percy, N. *et al.* Genome-Scale Metabolic Models and Machine Learning Reveal Genetic Determinants of Antibiotic Resistance in Escherichia coli and Unravel the Underlying Metabolic Adaptation Mechanisms. *mSystems* **6**, (2021).
187. Mann, R., Mediatì, D. G., Duggin, I. G., Harry, E. J. & Bottomley, A. L. Metabolic adaptations of Uropathogenic *E. coli* in the urinary tract. *Frontiers in Cellular and Infection Microbiology* **7**, 241 (2017).
188. Wood, T. K. & Song, S. Forming and waking dormant cells: The ppGpp ribosome dimerization persister model. *Biofilm* **2**, 100018 (2020).
189. Biotechnology, B., de Crécy-Lagard, V. A., Bellalou, J., Mutzel, R. & Marlière, P. *BMC Biotechnology Long term adaptation of a microbial population to a permanent metabolic constraint: overcoming thymineless death by experimental evolution of Escherichia coli.* <http://www.biomedcentral.com/1472-6750/1/10> (2001).

190. Killmer, J. L., Widholm, J. M. & Slife, F. W. Antagonistic effect of p-aminobenzoate or folate on asulam [methyl (4-aminobenzensulphonyl carbamate)] inhibition of carrot suspension cultures. *Plant Science Letters* **19**, 203–208 (1980).

Curriculum Vitae

Name: Laura Muntz

Post-secondary Education and Degrees: Acadia University
Wolfville, Nova Scotia, Canada
2015-2020 BSc Biology

The University of Western Ontario
London, Ontario, Canada
2020-2022 MSc Microbiology & Immunology

Scholarships and Awards: Atlantic Canada Society for Microbial Ecology Research
Stipend 2019